Large Variable – Conductance Heat Pipe
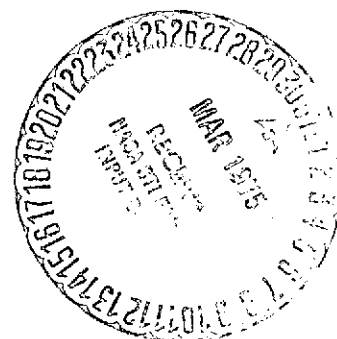
Final Report: Transverse Header

GRUMMAN

Large Variable - Conductance Heat Pipe

Final Report: Transverse Header

Prepared for

National Aeronautics and Space Administration
George C. Marshall Space Flight Center
Alabama 35812

Contract NAS 8-27793

Prepared by

Grumman Aerospace Corporation
Bethpage, New York 11714

Prepared by _____
F. Edelstein, Project Engineer

Approved by _____
R. Haslett, Program Manager

CONTENTS

FIGURES

FIGURES (Cont)

TABLES

v

FOREWORD

This report was prepared by Grumman Aerospace Corporation for the George C. Marshall Space Flight Center of the National Aeronautics and Space Administration. The work was performed under Contract NAS 8-27793-Mod 7 with Messrs. J. Loose, R. Lopez and Dr. K. McCoy serving as Technical Monitors.

The effort concerning the transverse header was performed from January 1974 to January 1975 under the direction of Mr. R. Haslett as program manager and Mr. F. Edelstein as project engineer. A major contribution was made by Mr. R. Hembach for the initial manufacturing and testing effort.

Section 1

SUMMARY

A novel variable-conductance heat-pipe approach has been developed that delivers high-capacity loads, while eliminating the problem of artery gas blockage present in conventional designs. The unit, known as a transverse header, uses ammonia as the working fluid and nitrogen as the control gas. Its overall cylindrical shape is 2 in. in diameter by 2 ft long. Under test with a fluid heat source, the maximum load achieved as a VCHP was 3,600 w. As with conventional gas-loaded pipes, good temperature control was also obtained. Two applications of this device are described - a VCHP header for a heat-pipe radiator and a self-controlled mounting plate for electronic-box thermal control.

Section 2

INTRODUCTION

The use of heat-pipe radiators was recognized early by NASA and industry as a viable tool for spacecraft thermal control. It provides several benefits for radiator systems, such as simplicity, good thermal efficiency, and insensitivity to meteoroid penetration. Moreover, it is lightweight, noiseless, has no power requirement, and provides automatic temperature control using a gas-loaded, variable-conductance heat pipe (VCHP).

Of the various radiator configurations possible for the header (fluid, heat pipe or VCHP) and the panel (heat pipe or VCHP), the most attractive with respect to manufacturing simplicity and weight is a VCHP header coupled to many single-fluid-panel heat pipes. The hardware required for the small-capacity-panel heat pipes had already been developed and flight proven. However, this was not the case for the large VCHP header. Development of this hardware was initiated at the start of the present contract, July 1971. A large-capacity VCHP was built measuring 9 ft long by 1 in. diameter and employing a spiral artery tunnel wick (Ref 1). As a single-fluid device charged only with ammonia, the pipe transported over 3,000 w (12.8 kw-ft). However, when tested as a VCHP, significant degradation in performance was observed. Entrapment of gas bubbles within the artery was determined to be the cause of the degraded capacity. The problem of removing or controlling gas bubbles within arteries is a particularly difficult one that has received considerable attention (Ref 2, 3, 4, 5, 6). While there has been some success achieved with a priming foil on a relatively low-capacity (0.8 kw-ft) methanol heat pipe (Ref 7), the solution to the bubble-control problem with respect to large capacity VCHPs remains elusive.

In this report, an entirely different approach aimed at providing large capacity VCHPs is described. It involves rearranging the evaporator and condenser surfaces so as to make them insensitive to bubble formation, while preserving the inherently simple self-controlling features of gas-loaded heat pipes. In this configuration, the liquid path is relatively short and flows across or transverse to the longer vapor path. Because of the short liquid-transport length, relatively large thermal loads can be accommodated. Furthermore, by channeling the vapor flow along the condenser, traditional VCHP control can be provided with a wicked gas reservoir.

The initial concept and early feasibility models of the transverse header were developed with in-house R & D funds. The work performed under this contract concerned the analysis, hardware modification and testing of a previously built cylindrical transverse header. This report includes results from the initial in-house test program and documents the NASA-funded modification and test program.

Section 3

DESCRIPTION OF TRANSVERSE HEADER

3.1 OPERATION

A transverse header is a heat pipe wherein the evaporator and condenser surfaces are separated by a relatively short distance, compared to a conventional axial heat pipe, and wherein the liquid flows in a direction which is transverse or perpendicular to the vapor flow. Because of the short transport length, simple wicks can be utilized to provide large heat loads (in the kilowatt range) without incurring the usually high viscous liquid pressure losses associated with arterial pipes. Temperature control can be achieved using conventional noncondensible gas techniques in a wicked or unwicked reservoir.

The transverse header concept is shown in Figure 3-1. It consists of a sealed volume, which for purposes of illustration, is rectangular in cross section. The bottom and top surfaces serve as the evaporator and condenser respectively, while the side walls are adiabatic surfaces. The inside walls are wicked along their entire length with either screen mesh, circumferential (as opposed to axial) wall grooves, etc. A thin, solid baffle is positioned between the evaporator and condenser surfaces dividing the vapor space in two. It directs or channels vapor flow along the evaporator vapor space toward the left side where an opening in the baffle permits the vapor to turn 180 deg and enter the condenser vapor space. The baffle runs the length of the unit, and except for the opening at the left, is sealed against the walls to prevent vapor from short circuiting directly to the condenser surface. However, the seal is not so tight as to prevent condensed liquid from being wicked directly from the condenser to the evaporator down the side walls. The liquid, whose pressure losses are usually high in conventional heat pipes, thus takes the shortest path from condenser to evaporator while the vapor, whose losses are usually low, travels the longer route. This results in large-load carrying capacities even with relatively simple, nonarterial wicks.

Temperature control is provided by a customary, noncondensible wicked gas reservoir which communicates with the heat pipe through the condenser vapor space (between the baffle and condenser surface). Blockage of the condenser proceeds from right to left, with complete condenser blockage occurring when the fluid/gas interface travels across the entire condenser length. In the shutoff mode, residual losses will consist of conduction along both wick and side walls, as well as vapor diffusion through the blocked condenser vapor space.

WORKING FLUID/GAS INTERFACE

ACTIVE CONDENSER

BLOCKED CONDENSER

RESERVOIR

VAPOR PATH AROUND BAFFLE

HEAT LOAD

EVAPORATOR SURFACE

BAFFLE

HEAT LOAD

CONDENSER SURFACE

WICK (LINING WALLS)

CONDENSED LIQUID RETURN TO EVAPORATOR

ADIABATIC SURFACE

EVAPORATOR SURFACE

HEAT LOAD

A—A
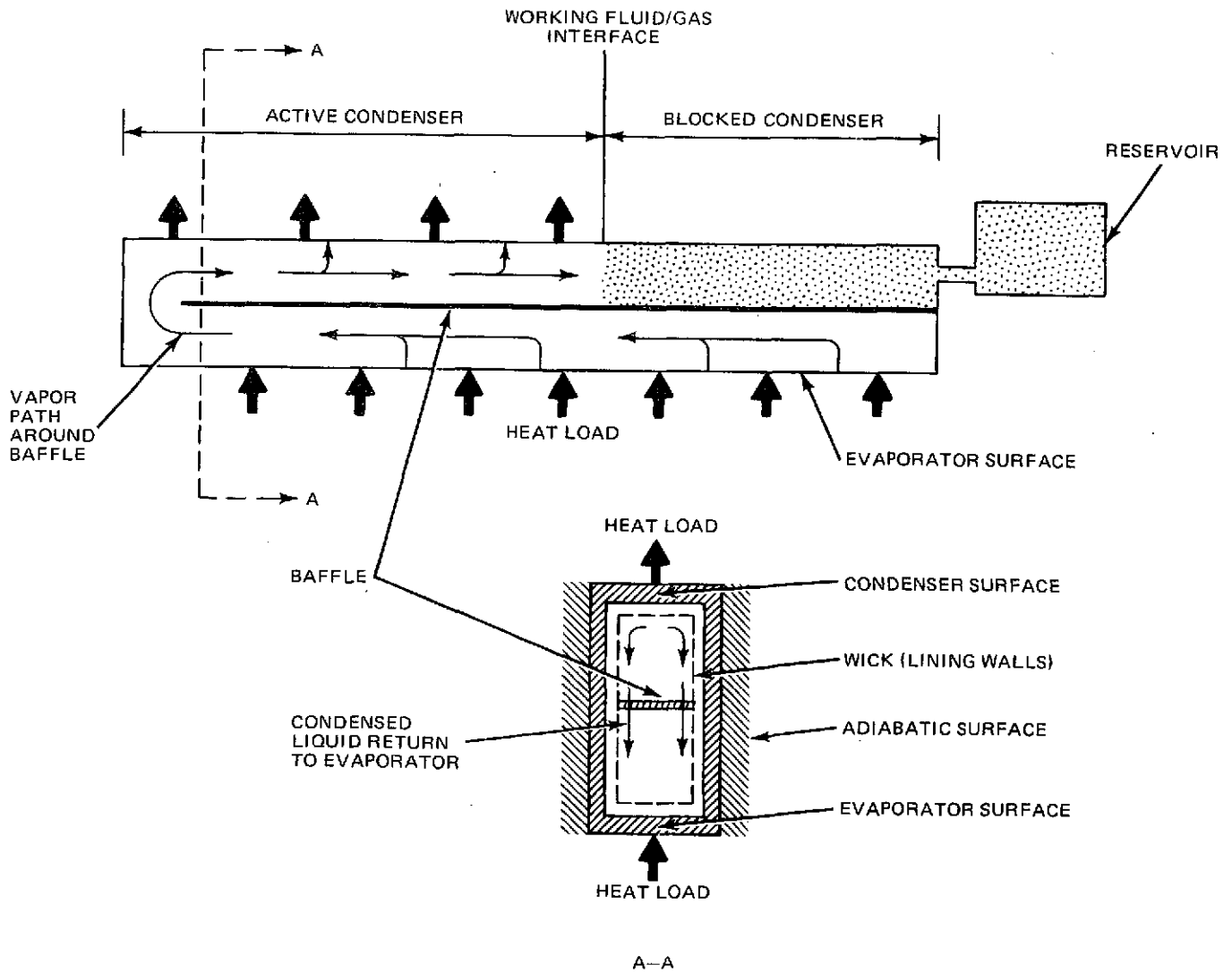
Figure 3-1. Transverse Header Concept

These losses, which also occur in conventional, variable-conductance heat pipes (VCHP), tend to be higher in the transverse header VCHP because of the proximity of the evaporator and condenser. Depending on the means of controlling the reservoir temperature, active feedback or passive control can be achieved.

During part-load operation, the fluid/gas interface will automatically adjust to changing environments and load in an attempt to maintain constant vapor temperature. Because of the simplified wicking system, movement of the gas across the wick is not expected to impair wick performance. This is perhaps the most significant benefit of the device. It can transfer high loads as a variable-conductance heat pipe without the need of an arterial wick, which up to now, has had limited success because of gas-bubble entrapment problems.

3.2 DESIGN

The rectangular configuration shown in Figure 3-1 was actually built and tested. Its purpose was to demonstrate the feasibility of the transverse header approach, which it successfully did. Next, it was decided to build a second unit whose use could be demonstrated for specific spacecraft thermal-control applications. Recent studies that evaluated heat-pipe applications for Space Station and Space Shuttle (Ref 8, 9) indicated that simple heat-pipe radiators coupled to a VCHP as a temperature controller are viable candidates for large spacecraft heat-rejection systems. Typically, such systems employ a pumped fluid loop that circulates within the spacecraft, picking up waste heat which it would then supply to the radiator for disposal. The VCHP is used to transfer the load to the radiator and to control the exit temperature of the fluid, thereby eliminating the need for bypass loops and valves. Fluid temperature control is required for a number of reasons, such as to prevent fluid from freezing under low-load conditions, to meet equipment temperature requirements, etc. (Additional discussion regarding radiator application can be found in Section 6 of this report.) Thus, it was decided to design a transverse header for a spacecraft heat-rejection system that would have a large thermal capacity, use a pumped fluid as its heat source, and be capable of controlling the exit fluid temperatures under varying loads.

It should be noted that this application is particularly suited to a transverse header under part-load conditions, when only part of the evaporator surface is required to extract heat from the circulating loop. The high-load portion of the evaporator will naturally correspond to the active part of the condenser, imposing no requirement for longitudinal liquid flow.

A second consideration was to build a device that would serve as a laboratory tool in that it would be easily modified and retested to evaluate the effect of different wicks, materials, etc. Of necessity, this resulted in a nonflight-weight development model incorporating removable mechanical components rather than an all-welded design.

Figure 3-2 shows a sketch of the second unit designed in a cylindrical configuration. It consists of two concentric cylinders whose annulus contains the working fluid, ultra-high-purity ammonia. The outer surface of the inside tube is the evaporator, while the inside surface of the outer tube is the condenser. Both surfaces have radial threads cut into them to provide wicking and heat-transfer area. A thin, cylindrical steel baffle with a Teflon coating on the outer surface is positioned midway between the evaporator and condenser. The baffle, which runs the length of the unit, is open at the left end to permit vapor to enter the condenser vapor space (the space between the baffle and the condenser), but is sealed at the right end to prevent vapor from short-circuiting directly to the condenser surface. Six equally spaced screen webs, extending the entire length of the pipe, pass through tight-fitting slots cut into the baffle, and provide the fluid return path from the condenser to the evaporator. Each web is constructed of a combination of 100 and 170 mesh screen.

The unit is designed to use a hot, flowing fluid as the heat source. Entering at the left, the fluid, water, flows through a finned annulus formed between the inner surface of the evaporator tube (i.d. = 0.870 in.) and the outer surface of a 0.75-in. diameter, solid, cylindrical flow plug. With this arrangement, heat is conducted from the fluid directly to the evaporator surface across the 0.070-in. aluminum tube wall with minimum temperature drop.

In this experiment, removal of heat on the outside condenser tube is accomplished with a water spray. In a space application, a radiator coupled to the condenser would serve as a means of rejecting heat.

Temperature control is provided by a wicked, noncondensible gas reservoir which communicates with the condenser vapor space via three tubes. Insulators placed between the pipe and reservoir provide thermal isolation for the normally cooler reservoir.

It was decided to set the vapor temperature control range at 75-78°F with the reservoir at 55°F. This corresponds to a nitrogen gas charge of 0.01756 lb. Table 3-1 lists pertinent design details of the unit. A photograph of the header is shown in Figure 3-3.

The unit described above represents the modified or final configuration on which most of the testing was performed. The original or unmodified version, which was only briefly tested, is identical except for the Teflon-coated baffle and the finning within the flow annulus. Test results of both configurations are presented in the Test Section of this report.
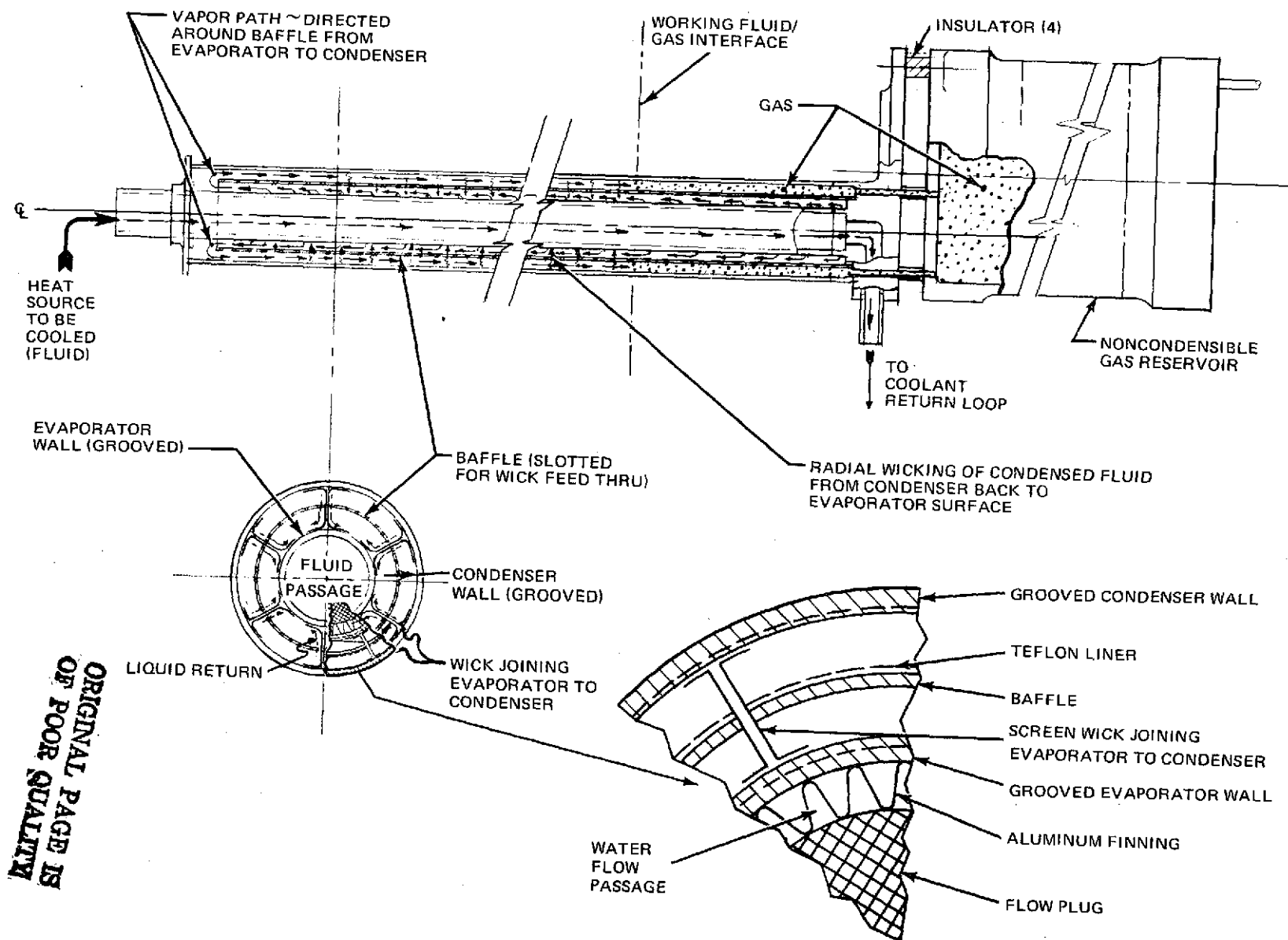
Figure 3-2. Cylindrical Transverse Header Variable-Conductance Heat Pipe

Table 3-1. Transverse Header Design Details

Item	Parameter
Heat-Pipe Fluid	Ammonia
Condenser Surface (Outer Tube)	
• Inside Diameter	1.865 In.
• Outside Diameter	2.00 In.
• Material	Aluminum
• No. of Threads/In.	150
• Length	22.3 In.
Evaporator Surface (Inner Tube)	
• Inside Diameter	0.870 In.
• Outside Diameter	1.00 In.
• Material	Aluminum
• No. of Threads/In.	150
• Length	22.3 In.
Baffle	
• Material	Stainless Steel
• Nominal Diameter	1.5 In.
• Length	22.3 In.
Wick	
• Material	Stainless Steel Mesh, 100 and 170
• No. of Webs	6
• Length	22.3 In.
Heat Source	
• Type	Circulating Heated Tap Water
• Flow Channel	Annulus
	• Inner Tube I.D. = 0.870 In.
	• Flow Plug O.D. = 0.75 In.
• Flow Length	25 In.
• Finning	Aluminum Offset Rectangular Strip Fin 12/In., 0.006-In. Thick
Reservoir	
• Material	Aluminum
• Size	7.48 In. Long X 4.5 In.-Diameter
• Noncondensible Gas	0.01756 Lb Nitrogen (When Operated As A VCHP)
• $V_R V_C$	5.4
• Type	Wicked

RESERVOIR

CONDENSER SURFACE
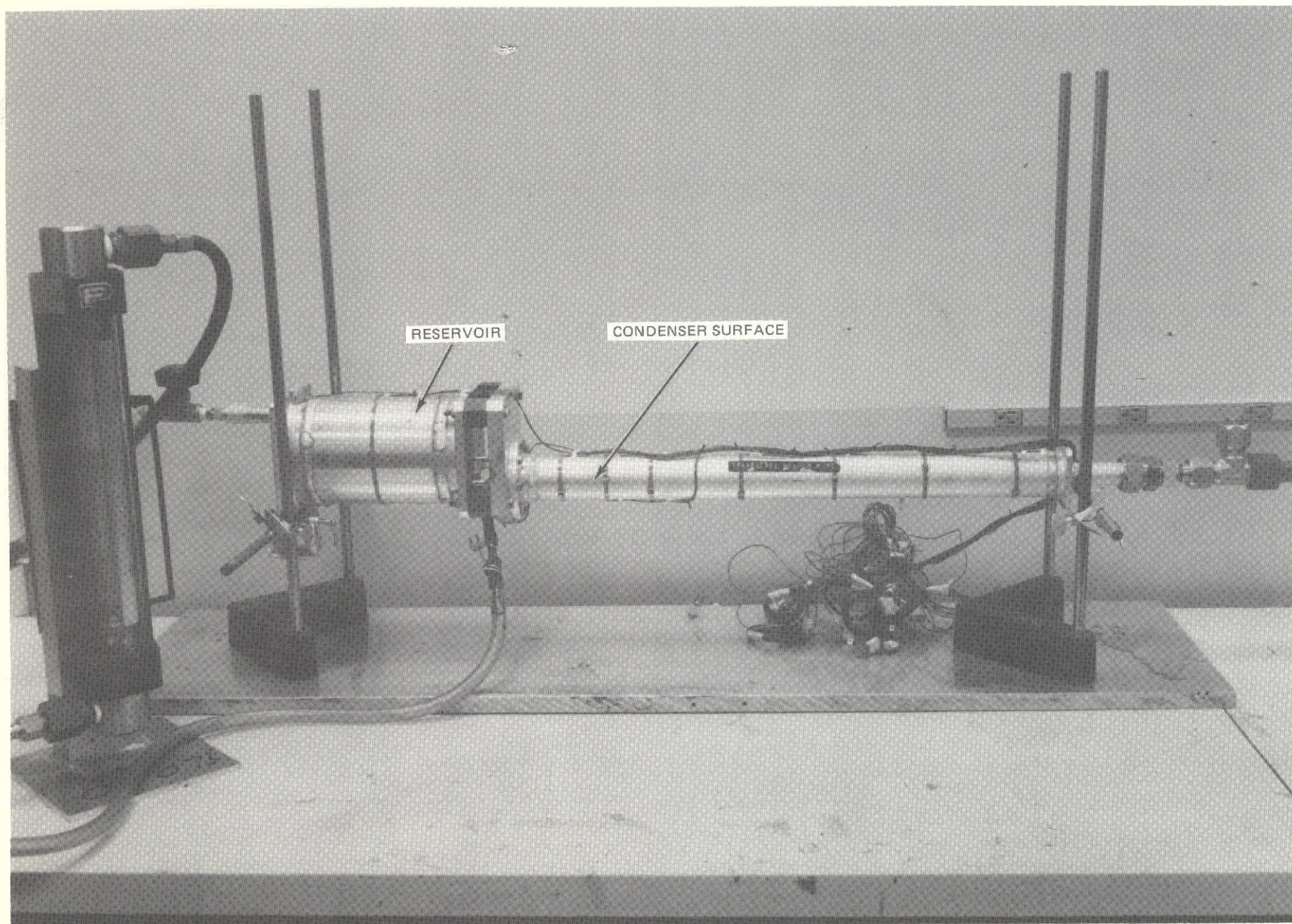
Figure 3-3. Cylindrical Transverse Header

Section 4

ANALYSIS

4.1 CAPACITY PREDICTIONS

The theoretical capacity of the cylindrical transverse header was estimated by summing the pressure losses of the liquid and vapor flow paths. Equations defining these losses were programmed to study how changes in design variables affect heat-pipe capacity. For example, Figure 4-1 shows how the heat-pipe capacity varies with the number of webs contacting the evaporator and condensor tubes, for two different fluids, ammonia and acetone. The maximum capacity occurs at about 6 and 7 webs for acetone and ammonia, respectively. Below this number of webs, liquid pressure losses in the evaporator and condenser grooves dominate, while above this number, vapor losses become significant. Six webs were selected for the ammonia working fluid, yielding a capacity of approximately 3,800 w.

Because of its superior wicking and transport qualities, ammonia yields the higher-capacity heat pipe. However, the capacity of approximately 1.0 kw achieved with the acetone is still relatively high compared to conventional pipes of comparable size. This is important in applications where a low-pressure, nontoxic working fluid is required.

The above analysis assumes a uniform heat input into the evaporator. This would be obtained, for example, with an electrical heat source. However, with a flowing-fluid heat source, evaporator heat input is nonuniform, being proportional to the temperature difference between the fluid (water) and heat-pipe vapor (ammonia). As illustrated below, this temperature differential, or heat input, is highest at the inlet, and decreases along the heat-pipe length. The net effect is that the heat-pipe capacity will usually be lower for non-uniform heat input compared to the uniform heat input case. An estimate of the reduced capacity is presented below.
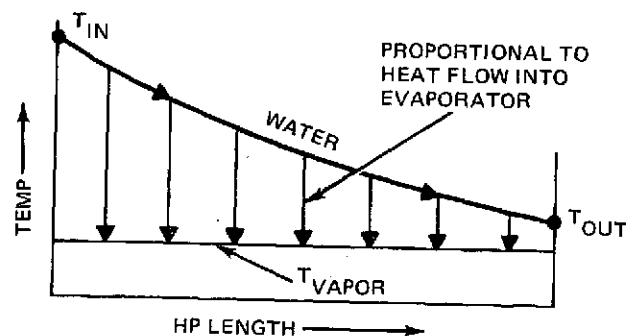
- EVAPORATOR DIAMETER = 1.0 IN.
- CONDENSER DIAMETER = 1.86 IN.
- LENGTH = 22.3 IN.
- UNIFORM EVAPORATOR HEAT INPUT
- TEMPERATURE = $80°F$
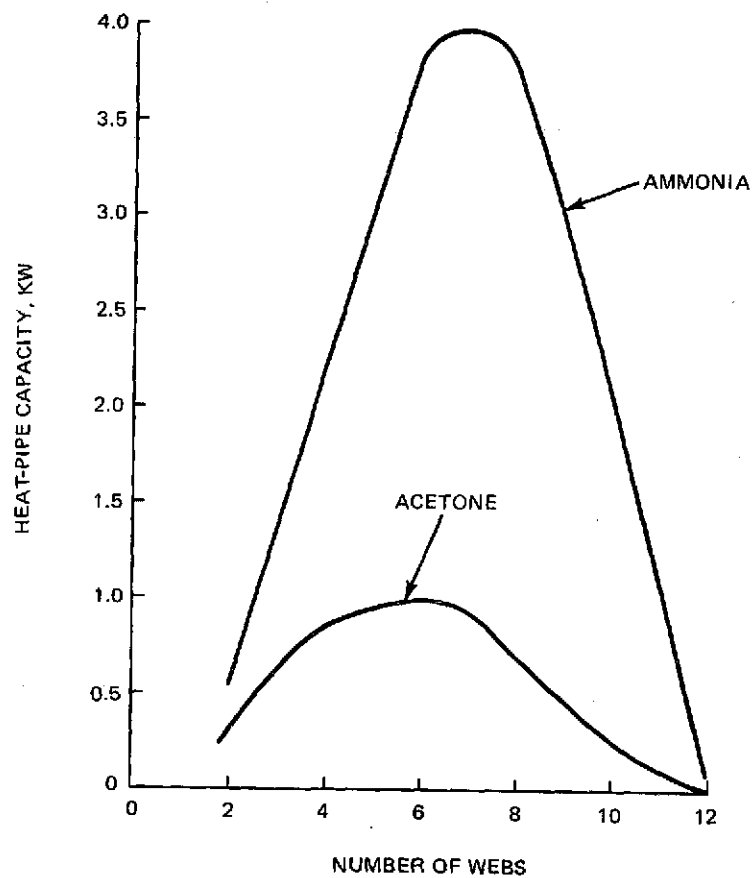
Figure 4-1. Capacity Prediction of Cylindrical Transverse Header

The maximum heat flux at the inlet is given by

$$q''_{max} = U_e(T_{in} - T_{vap})$$

where

q''_{max} = maximum heat flux per unit area of evaporator surface, Btu/hr – ft^2

U_e = overall thermal conductance between water and vapor, based on evaporator area, Btu/hr – ft^2

T_{in} = water inlet temperature, $^\circ$F

T_{vap} = ammonia vapor temperature, $^\circ$F

The average flux over the entire heat-pipe length is given by

$$q''_{avg} = \frac{WC_p(T_{in} - T_{out})}{A_e}$$

where

q''_{avg} = average heat flux per unit area of evaporator surface, Btu/hr – ft^2

W = water flow rate, lb/hr

C_p = water heat capacity, Btu/lb – F$^\circ$

A_e = evaporator area, Ft^2

The ratio of maximum to average heat flux is thus

$$\frac{q''_{max}}{q''_{avg}} = \frac{U_e A_e(T_{in} - T_{vap})}{WC_p(T_{in} - T_{out})} \tag{4-1}$$

As with conventional heat exchangers, the heat-transfer effectiveness, ξ, can be defined between the water and ammonia vapor:

$$\xi = \frac{(T_{in} - T_{out})}{(T_{in} - T_{vap})} \tag{4-2}$$

It can be shown (Ref 10) that if one of the fluids has a constant temperature, the effectiveness can be expressed as

$$\xi = 1 - e^{-U_e A_e / WC_p} \tag{4-3}$$

Solving for the exponent yields

$$\frac{U_e A_e}{WC_p} = \ln \frac{1}{(1 - \xi)} \tag{4-4}$$

Substitution of equations 4-2 and 4-4 in 4-1 expresses the flux ratio in terms of the heat transfer effectiveness:

$$\frac{q''_{max}}{q''_{avg}} = (1/\xi) \ln \frac{1}{(1 - \xi)}$$

This relation is plotted in Figure 4-2. At high effectivenesses, where the heat transfer between the water and ammonia is most efficient, the flux ratio is the largest. This implies that the ammonia evaporation rate and liquid condensate return rate will be greatest at the entrance, and consequently, the wicking system must be designed to accommodate this rate to avoid partial entrance dryout. This can result in complicated, axially-varying or over-designed wicking systems. Alternatively, if the simple wicking system cannot handle the high-entrance loads, the pipe will be forced to operate at a reduced power level, such that the lower entrance load matches wick capability.

The reduced load for the six-web, cylindrical transverse header has been estimated and is shown in Figure 4-3 as a function of effectiveness. For example, at an ξ of 0.70, the capacity is estimated at 3300 w. At low effectivenesses, the capacity approaches the "uniform heat input" load of 3,800 w.

4.2 SYSTEMS THERMAL MODEL

4.2.1 Description

An overall systems thermal model of the transverse header was generated to study how the device responds to changes in design variables and to predict steady state system performance during subsequent testing. It was used to identify operating characteristics of the pipe and suggest hardware changes that would improve its performance.
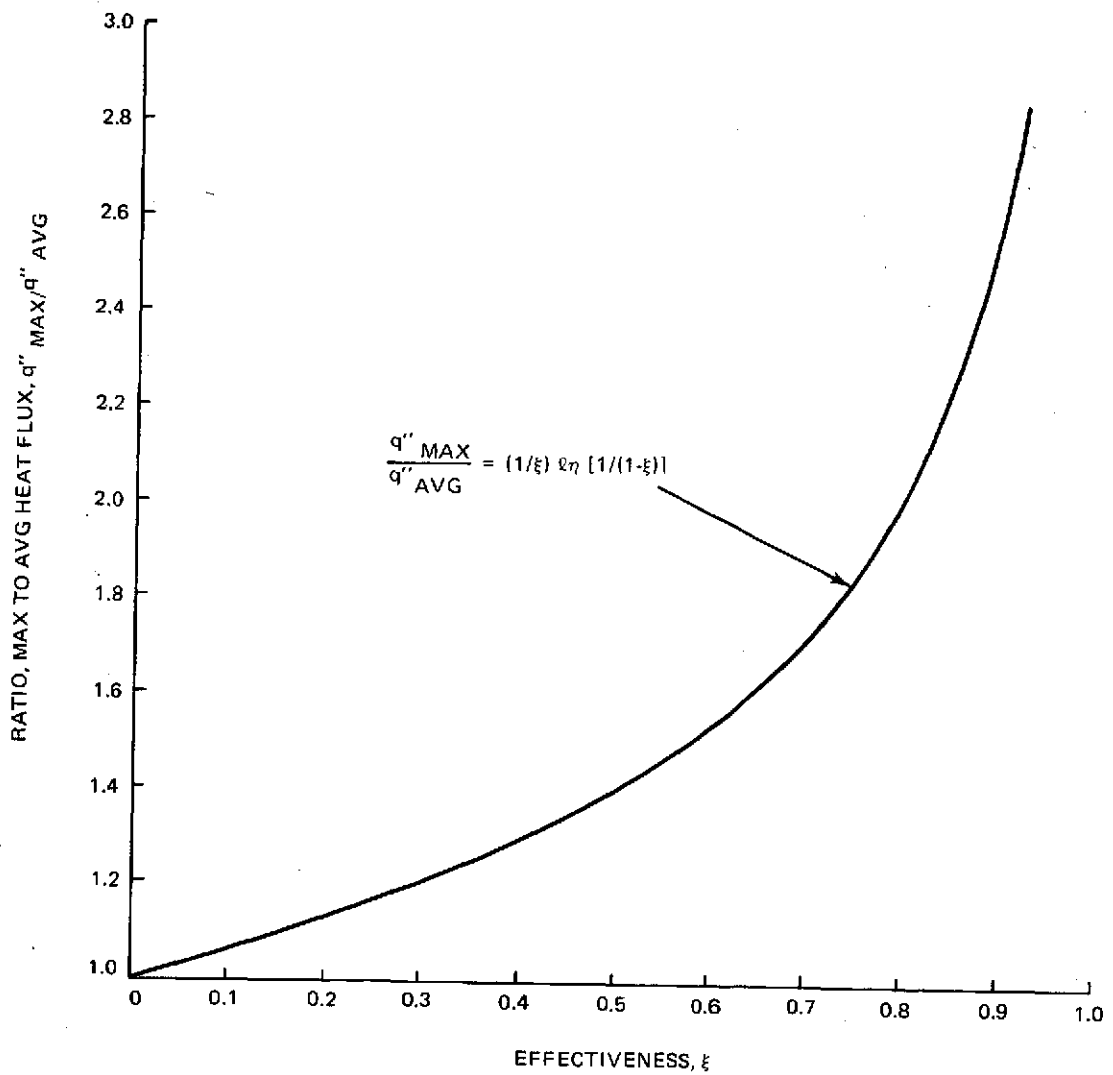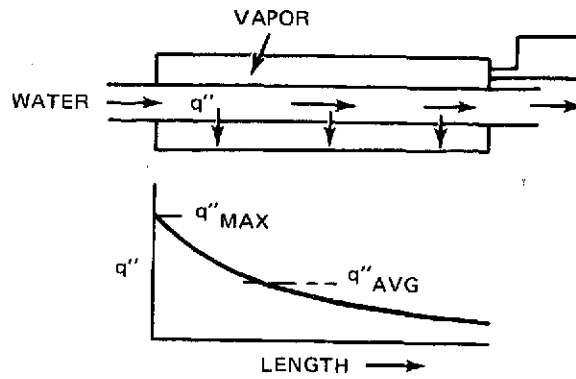
Figure 4-2. Nonuniform Heat Input From Fluid Source

$$\frac{q''_{MAX}}{q''_{AVG}} = (1/\xi)\, \ell n\, [1/(1-\xi)]$$
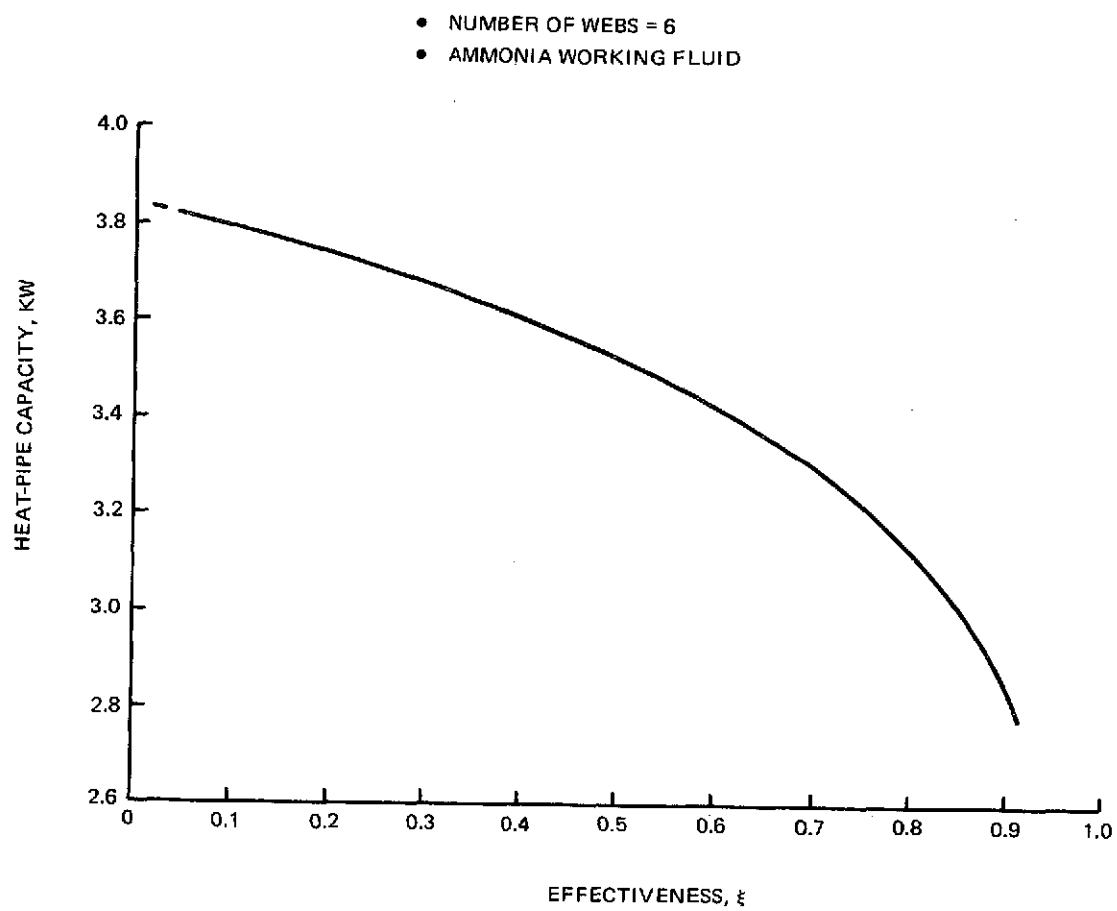
Figure 4-3. Influence of Heat-Transfer Effectiveness of a Fluid Heat Source on Pipe Capacity

A simplified systems schematic of the header is shown in Figure 4-4. The model assumes an incoming water heat source at a given temperature flowing through either a finned or unfinned annulus in the heat exchanger. The heat is removed with a separate, fixed-temperature water spray over the condenser surface. Water and ammonia heat-transfer coefficients were determined from test data or calculated from standard empirical relations to determine evaporator and condenser temperature drops. The location of the gas/vapor interface or active condenser length is calculated using the simplified flat-front theory. It is a function of a number of variables, including vapor and reservoir temperatures, reservoir-to-condenser volume ratio (V_R/V_c), nitrogen control-gas charge, etc. A summary of the various input and output parameters of the program are shown in Figure 4-5. A listing of the program is presented in Appendix A, along with a sample printout sheet.

4.2.2 Effect of Variables on Performance

Figure 4-6 shows the predicted performance of the cylindrical transverse header with water flowing at 500 lb/hr through an unfinned heat exchanger. Up to a load of about 2,850 w, the interface is located within the 22.3-in. condenser length, resulting in the traditionally constant vapor-temperature profile. Its value of 77°F is the result of the nitrogen gas charge, reservoir volume, and temperature. However, beyond the load of 2,850 w, the pipe is fully open (condenser is fully operative) and the vapor temperature now increases linearly with load.

More important than vapor-temperature control is the ability to control or restrain variations in outlet water temperature with changes in load and environment. This is a basic requirement of a spacecraft's pumped-loop heat-rejection system. Within the controllable load range, it is seen that the outlet temperature varies from 77 to 110°F.

The amount of control of outlet water temperature is a strong function of the effectiveness, ξ, of heat transfer between the water and ammonia vapor. This effectiveness was defined earlier by equation 4-2. It can be rewritten in the form

$$T_{out} = (1 - \xi)T_{in} + \xi T_{vap} \qquad (4-5)$$

Ideally, a unit that has an effectiveness of 100% provides an outlet water temperature equal to the vapor temperature. Figure 4-7 shows the outlet water-temperature variation with load as a function of heat exchanger effectiveness. It is apparent that if the VCHP has a high effectiveness, the outlet temperature will closely track the vapor temperature. This is desirable since a VCHP inherently provides a near-constant vapor temperature with load. Conversely, a VCHP with a low effectiveness provides less regulation of outlet temperature.

SINK SPRAY

SINK FILM COEFFICIENT

CONDENSER FILM COEFFICIENT

RESERVOIR

SINK SPRAY

VAPOR

CONDENSER

WATER IN → HEAT EXCHANGER → WATER OUT

EVAPORATOR

BAFFLE

NONCONDENSIBLE GAS

ACTIVE CONDENSER LENGTH

WATER →

FLOW →

FINNED OR PLAIN TUBE SURFACE

HX FILM COEFFICIENT

EVAPORATOR FILM COEFFICIENT
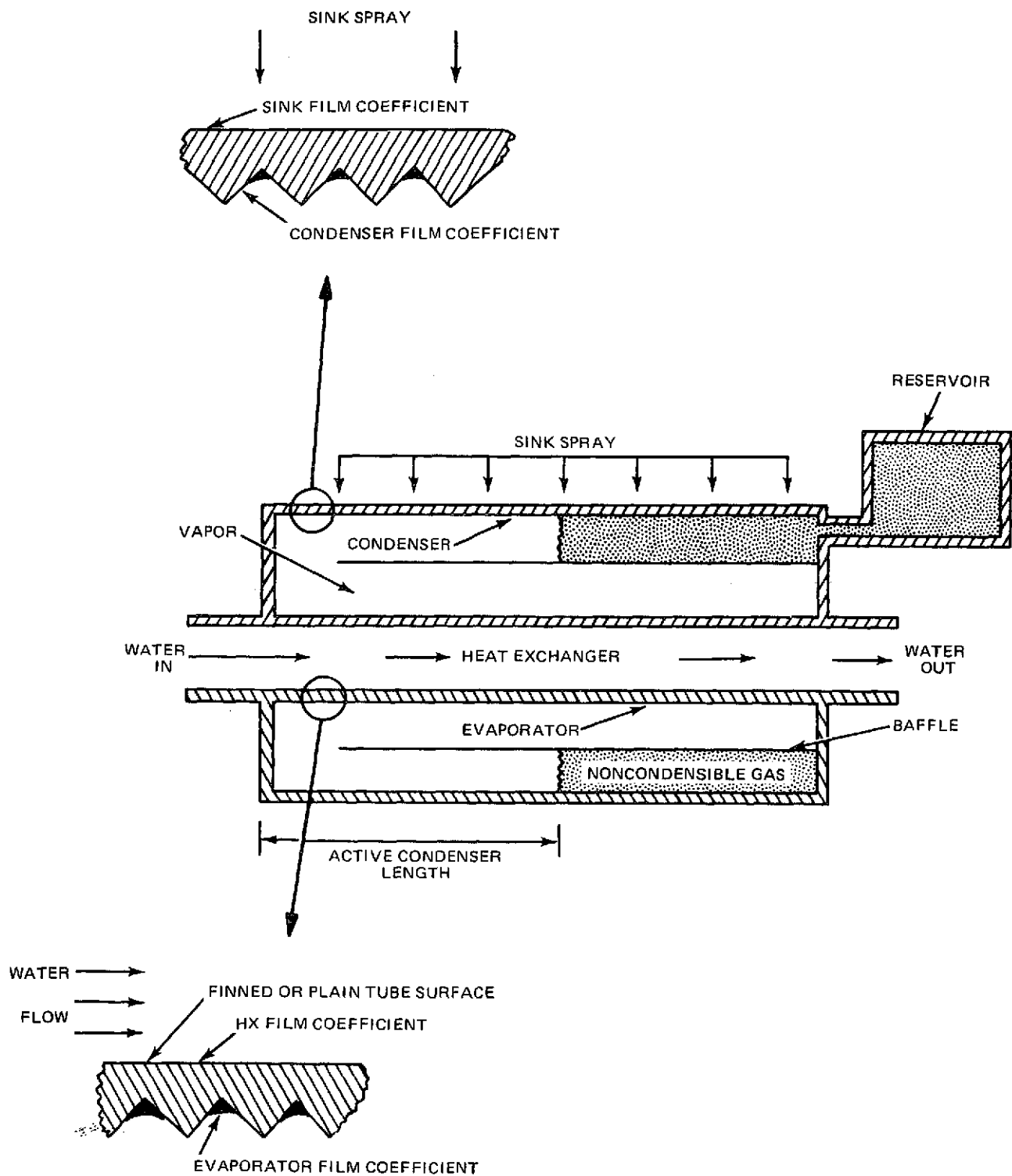
Figure 4-4. Schematic of Mathematical Thermal Model of Transverse Header

INPUT PARAMETERS

- GEOMETRY
  - SURFACE DIMENSIONS: EVAPORATOR, CONDENSER
    HEAT EXCHANGER (HX)
  - RESERVOIR VOLUME
- HEAT-TRANSFER DATA
  - FILM COEFFICIENTS: EVAPORATOR, CONDENSER
    SINK, HX
  - HX FLUID: FLOW RATE, HEAT CAPACITY,
    VISCOSITY, ETC
  - HX SURFACE: PLAIN TUBE OR FINNED
- CONTROL GAS
  - TYPE (NITROGEN)
  - QUANTITY
- BOUNDRY TEMPERATURES
  - INLET HX FLUID (WATER)
  - SINK SPRAY
  - RESERVOIR

MATH MODEL
PROGRAM

OUTPUT

- OUTLET HX FLUID TEMPERATURE
- VAPOR TEMPERATURE
- HEAT LOAD
- INTERFACE LOCATION
- HX EFFECTIVENESS

4-9

Figure 4-5. Basic Input/Output Parameters of Transverse Header Mathematical Thermal Model

- W = 500 LB/HR
- UNFINNED HX
- NITROGEN CHARGE = 0.01756 LB
- V_R/V_C = 5.4

HX EFFECTIVENESS = 0.37

INLET

OUTLET

VAPOR

CONDENSER WALL (ACTIVE)

SINK/RESERVOIR

TEMP, °F

LOAD, KW
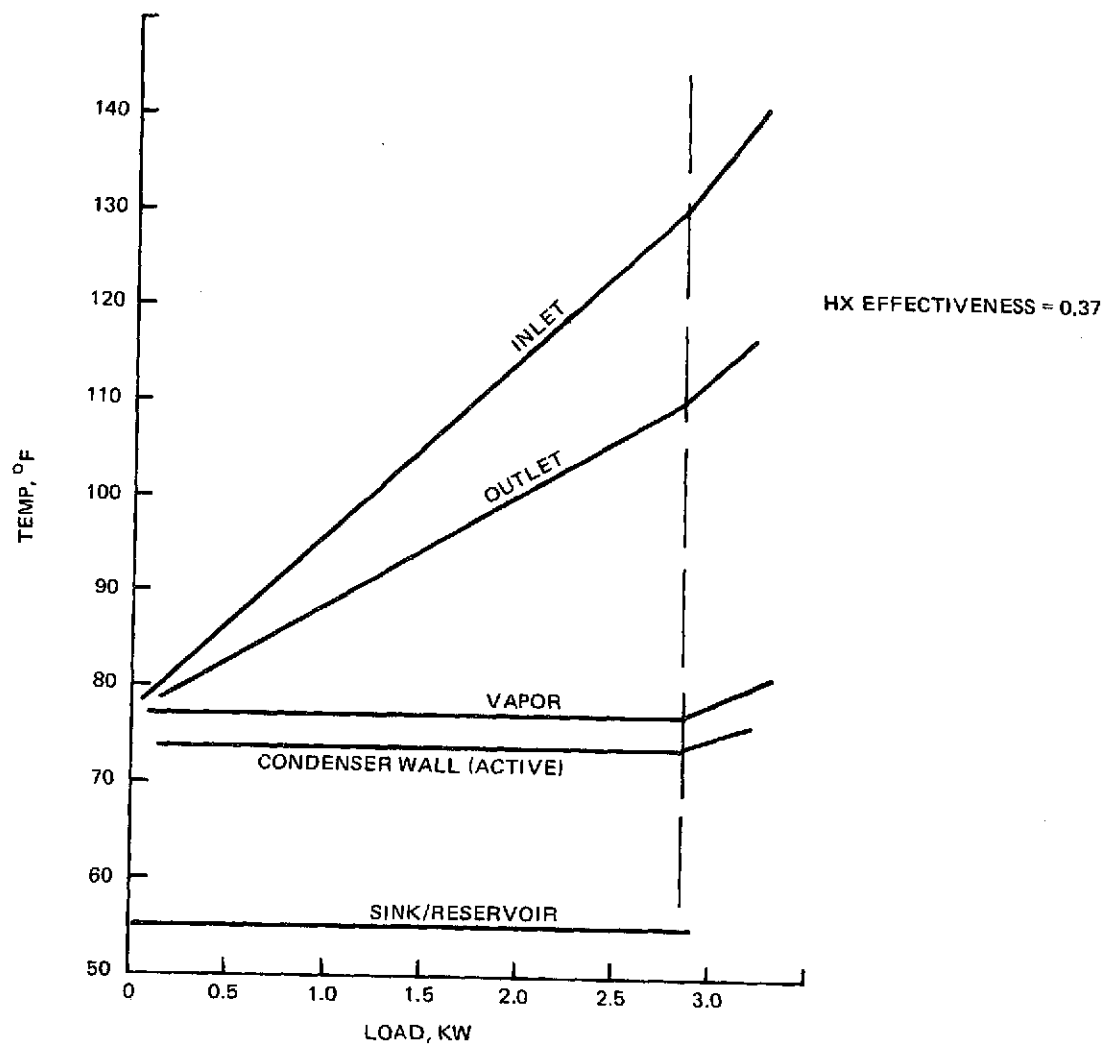
Figure 4-6. Performance Prediction of Transverse Header

- W = 500 LB/HR
- NITROGEN CHARGE = 0.01756 LB
- $V_R/V_C = 5.4$
- LOCATION OF INTERFACE WITHIN CONDENSER
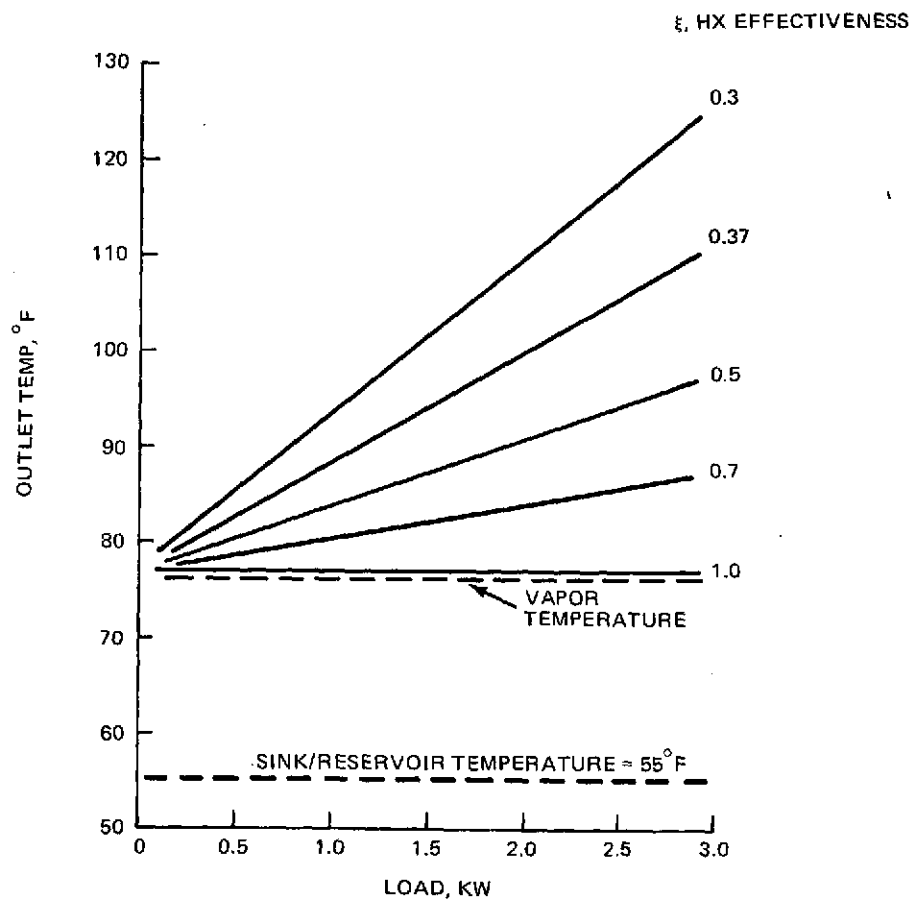
ξ, HX EFFECTIVENESS

Figure 4-7. Influence of HX Effectiveness on Outlet Temperature Control

Equation (4-3) indicates that the effectiveness can be improved by either increasing the overall conductance, UA, or decreasing the flow rate. Overall conductance is directly proportional to the water and evaporator film coefficients, as well as to their corresponding heat-transfer surfaces. The heat-transfer area can be increased easily by either providing extended heat-transfer surface in the form of finning or by increasing the length of the unit. Both effects will, however, cause a higher pressure drop across the heat exchanger. Lowering the flow rate influences the effectiveness in opposite ways. From the above equation, a lower flow rate will increase ξ; however, a lower flow rate will also result in a lower water film coefficient, which decreases ξ. Generally, when the flow is in a single regime, e.g., turbulent or laminar, the first effect is more pronounced and the effectiveness will improve with decreasing flow.

This effect is seen in Figure 4-8, which shows the change in effectiveness predicted by the model as a function of flow rate for both a finned and unfinned heat exchanger. For the unfinned case, ξ increases with decreasing flow rate, except in the transition region where it drops off sharply due to a large decrease in water side-film coefficient. For example, between the flow rates of 500 and 350 lb/hr (a 30% decrease), the calculated water film coefficient decreases from 707 to 243 Btu/hr-ft^2-°F (a 67% decrease). An identical decrease in flow in the turbulent region of the unfinned case produces a decrease in film coefficient of only 25%.

The addition of finning in the flow annulus significantly improves effectiveness from a value of 0.37 (unfinned) to a value of 0.67 (finned), at the same 500 lb/hr flow rate. The finning used in the analysis and subsequently installed in the unit was manufactured by Hughes-Treitler (Garden City, New York) and is specified in Table 3-1. Water-film coefficient data used in the analysis were obtained from Kayes and London, Figure 10-63 (Ref 10) for the finned annulus and from Krieth, equation 8-20 and Figure 8-15 (Ref 11) for the unfinned annulus.

To summarize, the performance of the transverse header, as measured in outlet temperature control, can be improved by increasing the heat exchanger effectiveness between the flowing-water side and ammonia vapor side. The effectiveness can be significantly increased by adding additional heat-transfer surface in the flow annulus of the heat exchanger. In general, lowering the flow rate also improves effectiveness in a particular flow region.

4.2.3 Performance Predictions

Performance of the unfinned unit has already been given in Figure 4-6 at a 500 lb/hr flow rate. The performance of the finned unit at the same flow rate is shown in Figure 4-9.
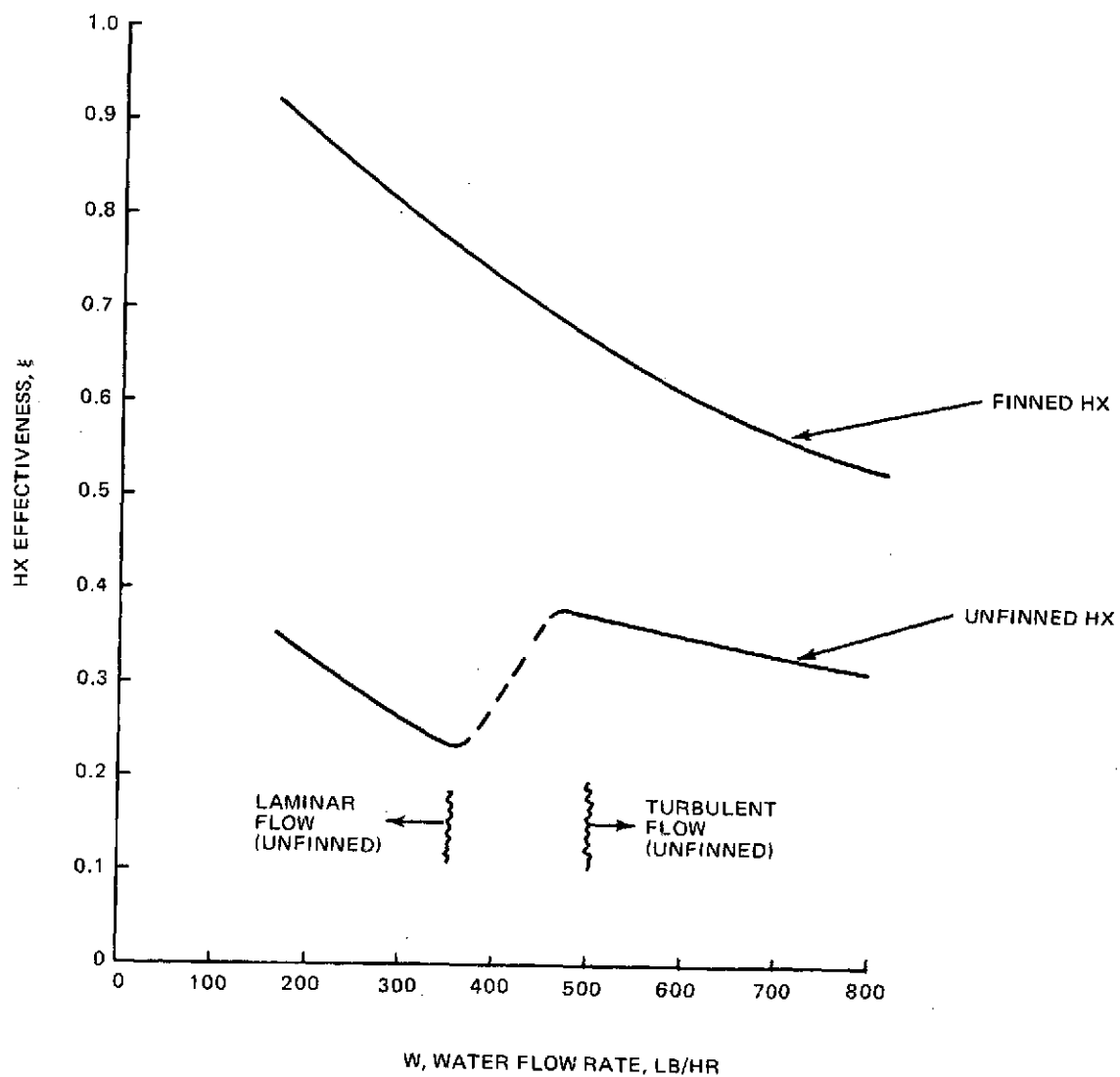
Figure 4-8. Influence of Flow Rate and Finning on Heat Exchanger Effectiveness
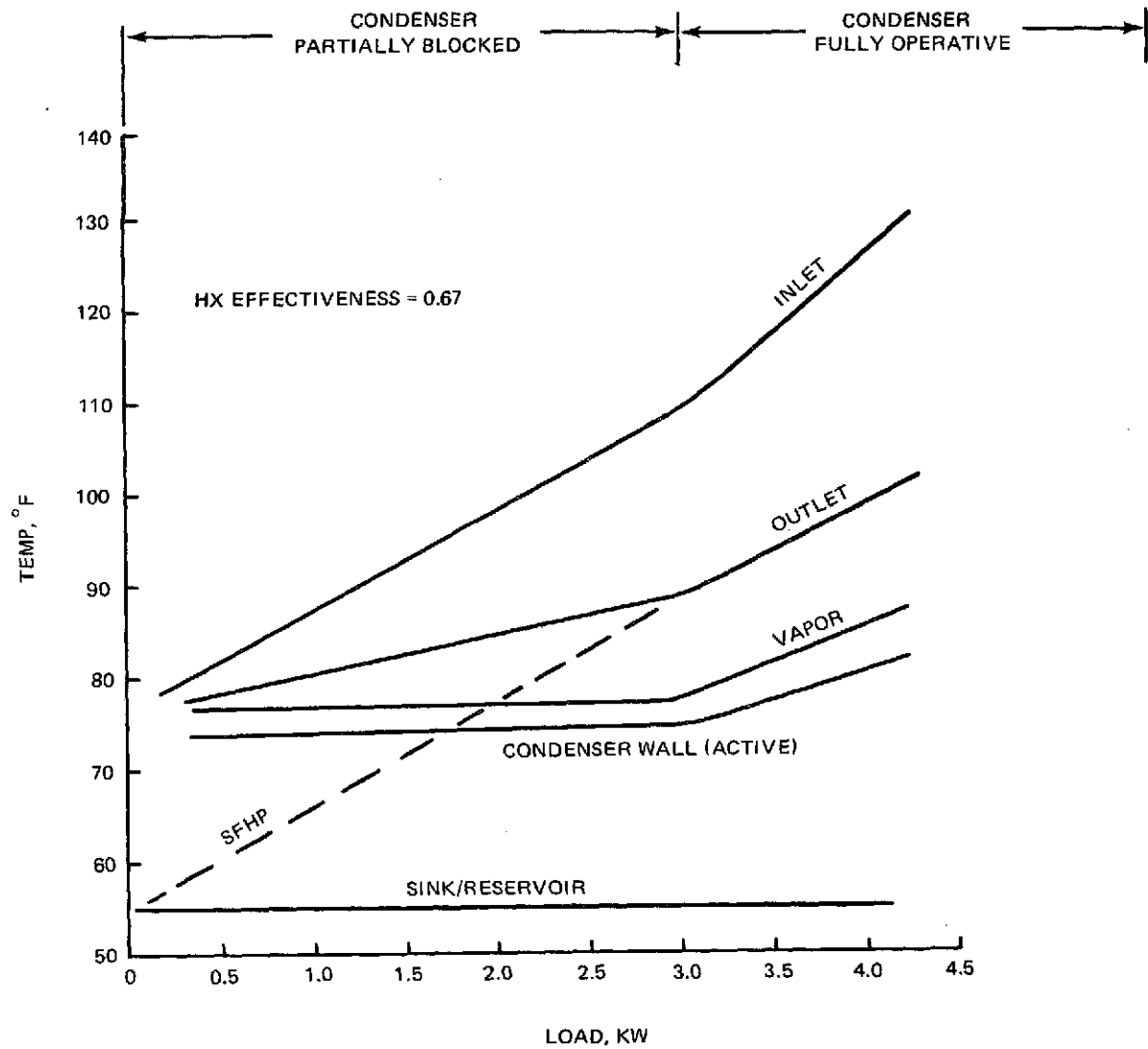
Figure 4-9. Performance Prediction of Transverse Header

4-14

As expected, the addition of finning increases the effectiveness, producing a flatter outlet-water temperature response. Within the controllable range of the pipe (up to about 3.0 kw) its temperature varies from 77 to 89°F, compared to a variation of 77 to 110°F for the unfinned case. The corresponding lower inlet temperatures of the finned case is a further benefit in minimizing fluid-loop temperature extremes. Like the vapor, the active condenser wall temperature remains constant up to 3.0 kw, since changes in load across the condenser wall are handled by readjustment of the active condenser area. The location of the interface that determines the active condenser is plotted in Figure 4-10. For loads lower than 3.0 kw, the interface is located within the 22.3-in. length of the condenser.

It is interesting to note how the unit behaves as a single-fluid heat pipe (SFHP) without the control afforded by the nitrogen gas. For this condition the outlet temperature responds linearly, as shown by the dashed line in Figure 4-9. Its temperature varies from 55 to 89°F or 34°F over a 3.0-kw load range. This is approximately three times the 12°F variation (77 to 89°F) over the same load range achieved with VCHP control.

The response of the finned unit at other flow rates is shown in Figure 4-11. There is a surprisingly small variation in outlet temperature response over the range of flow rates from 167 to 800 lb/hr. This is because there is a high effectiveness, i.e. $\xi = 0.92$ at the low flow rate, while at the high flow rate, where the effectiveness is lower, the relatively flat outlet temperature results from the smaller required variation in inlet temperature. As was mentioned before, this smaller variation in inlet temperature is advantageous in minimizing fluid-loop temperature extremes. Thus, except for possible pressure drop penalties, high flow-rate designs can also provide acceptable performance in spite of their lower effectiveness.

Figure 4-12 depicts the theoretical temperature profiles of the water and condenser wall at three different power levels. For example, at a power of 350 w, the condenser wall is constant at 73°F up to a point about 3 in. from the left end. This corresponds to the location of the vapor/gas interface. The remainder of the condenser from 3 to 22.3 in. is blocked by the control gas, and its temperature is that of the sink, namely 55°F. At higher loads the interface moves toward the right, decreasing the blocked length.
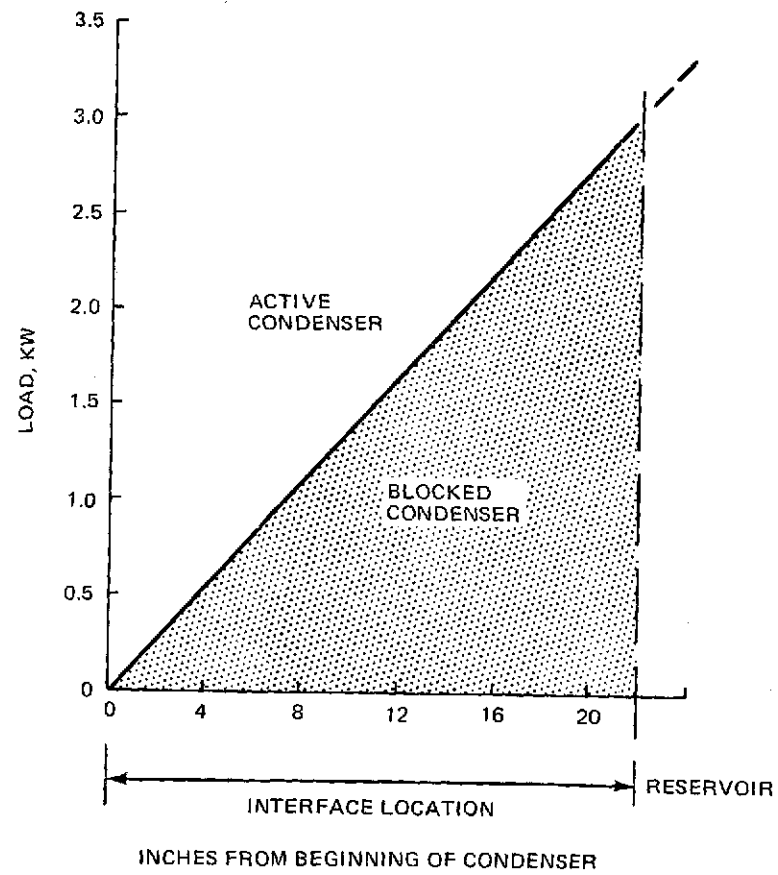
Figure 4-10. Predicted Interface Location

4-16

- FINNED HX
- NITROGEN CHARGE = 0.01756 LB
- V_R/V_C = 5.4

WATER FLOW RATE, LB/HR

W, LB/HR	ξ
167	0.92
500	0.67
800	0.53
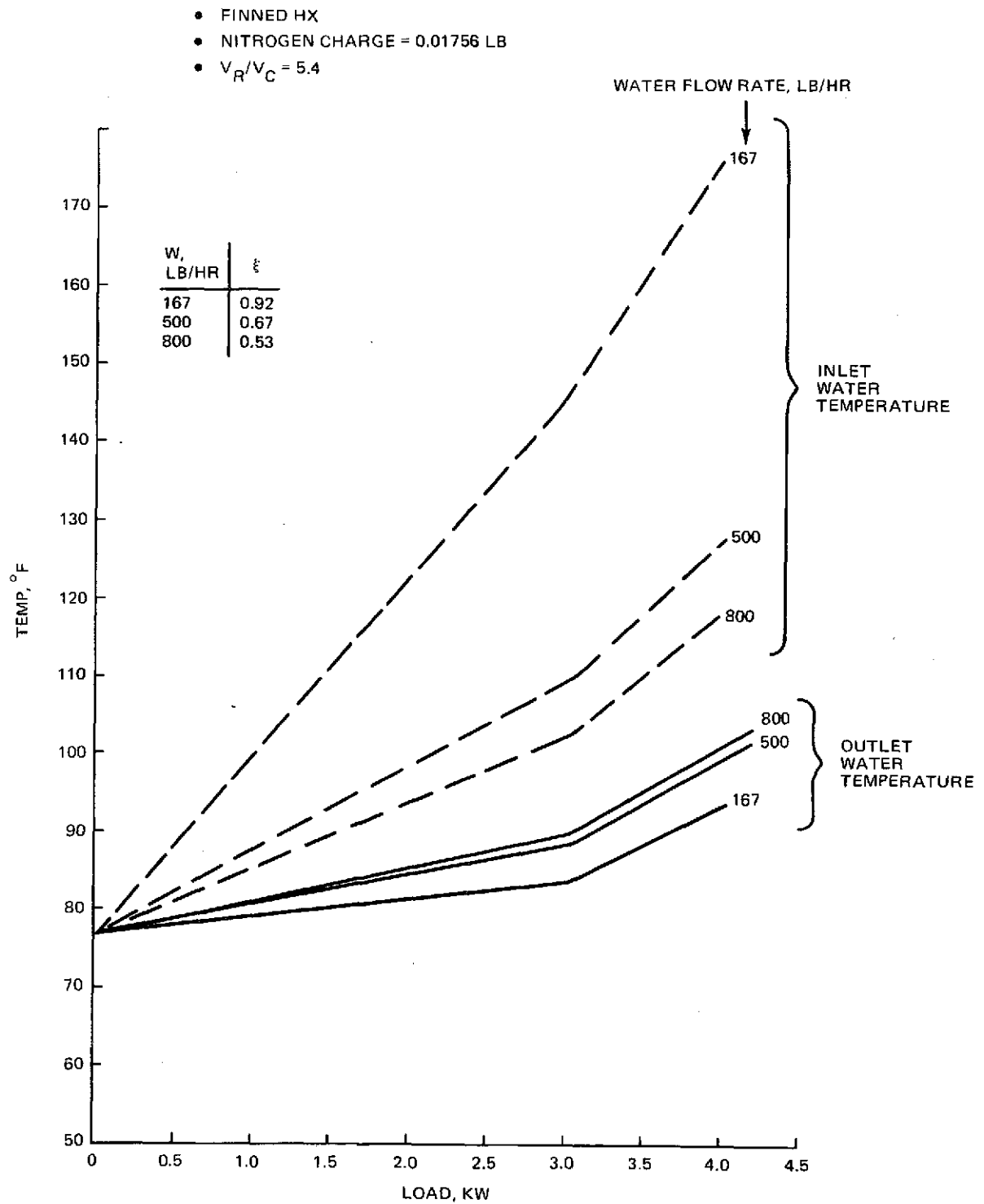
Figure 4-11. Transverse Header Performance Prediction at Different Flow Rates

- W = 500 LB/HR
- FINNED HX
- SINK/RESERVOIR TEMPERATURE = 55°F
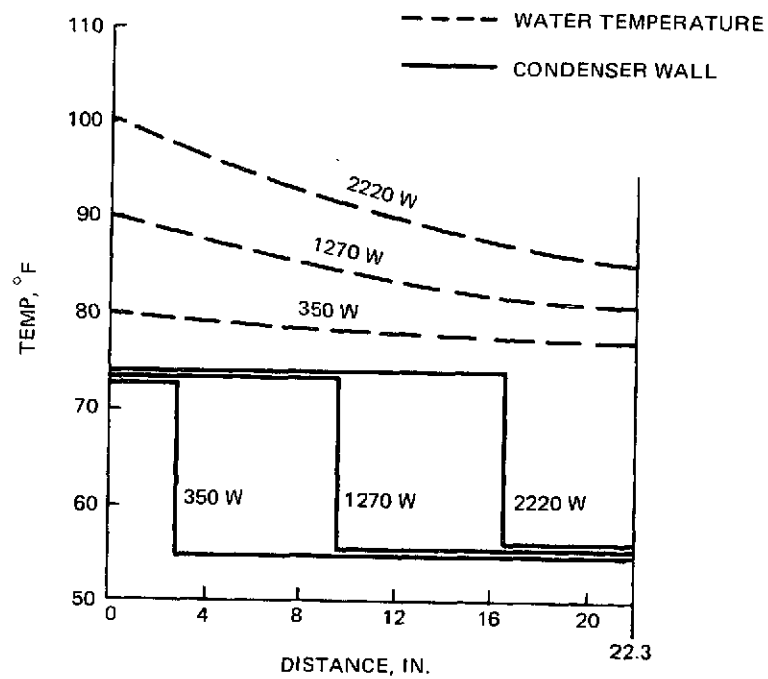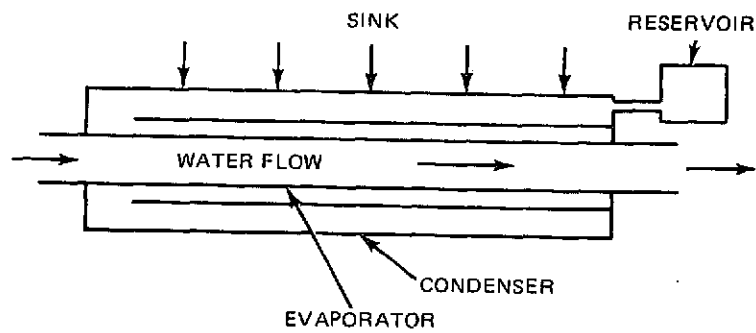
Figure 4-12. Predicted Temperature Profile at Different Loads

Section 5

TESTING

Tests were performed on both configurations of the cylindrical transverse header. The first involved the original design, which did not have finning in the heat exchanger or the Teflon-lined baffle. The second or modified design incorporated both features. Although the bulk of the test effort involved the modified design, data from both tests are included, along with a discussion of result. This follows a description of the test setup which was similar for both the original and modified configurations.

5.1 DESCRIPTION OF TEST SETUP

The pipe was instrumented with 24 thermocouples, as shown in Figure 5-1. Ten condenser measurements were taken, seven on top at 12 o'clock, (T/C 1-7), two on the bottom at 6 o'clock (T/C 8, 9) and one at the side (T/C 10). These thermocouples were held tightly in place with mechanical tie-wraps. Seven evaporator thermocouples were placed on the inside surface (12 o'clock) of the inner tube (water side) to record the evaporator wall temperature. Although they were mechanically held against the surface, their contact with the wall could not always be guaranteed. This was because the thermocouple locations in the inner tube were generally inaccessible and complicated by the requirement that they provide minimum interference with the water flow in the annular passage.

The heat source was a regulated tap-water supply whose temperature could be increased with an in-line electric heater. The flow rate was measured with a rotometer, which along with inlet and outlet immersion thermocouples (T/C 21, 22), was used to determine the thermal load, i.e., $Q = WC_p (T_{in} - T_{out})$. Figure 5-2 plots thermal load for different flows and ΔT's.

Cooling was provided by a water spray over the entire length and circumference of the condenser. When the pipe was used as a VCHP, a separate water spray was used to control the reservoir temperature. However, when operated as a single-fluid device (charged only with ammonia), reservoir cooling was discontinued and the reservoir was insulated. Its temperature measurements served as an indication of vapor temperature. When the pipe was operated as a VCHP, a pressure gauge was attached to the reservoir to determine vapor temperature. This gauge was not installed until after the first series of tests.

THERMOCOUPLE

①	TO	⑩	CONDENSER SURFACE, OUTSIDE DIAMETER
[11]	TO	[13]	RESERVOIR
⟨14⟩	TO	⟨20⟩	EVAPORATOR SURFACE, INSIDE DIAMETER
⟨21⟩	AND	⟨22⟩	WATER INLET, OUTLET
23			CONDENSER SPRAY, WATER
24			RESERVOIR SPRAY, WATER

NOTE

*DURING SINGLE-FLUID RUNS
RESERVOIR IS INSULATED
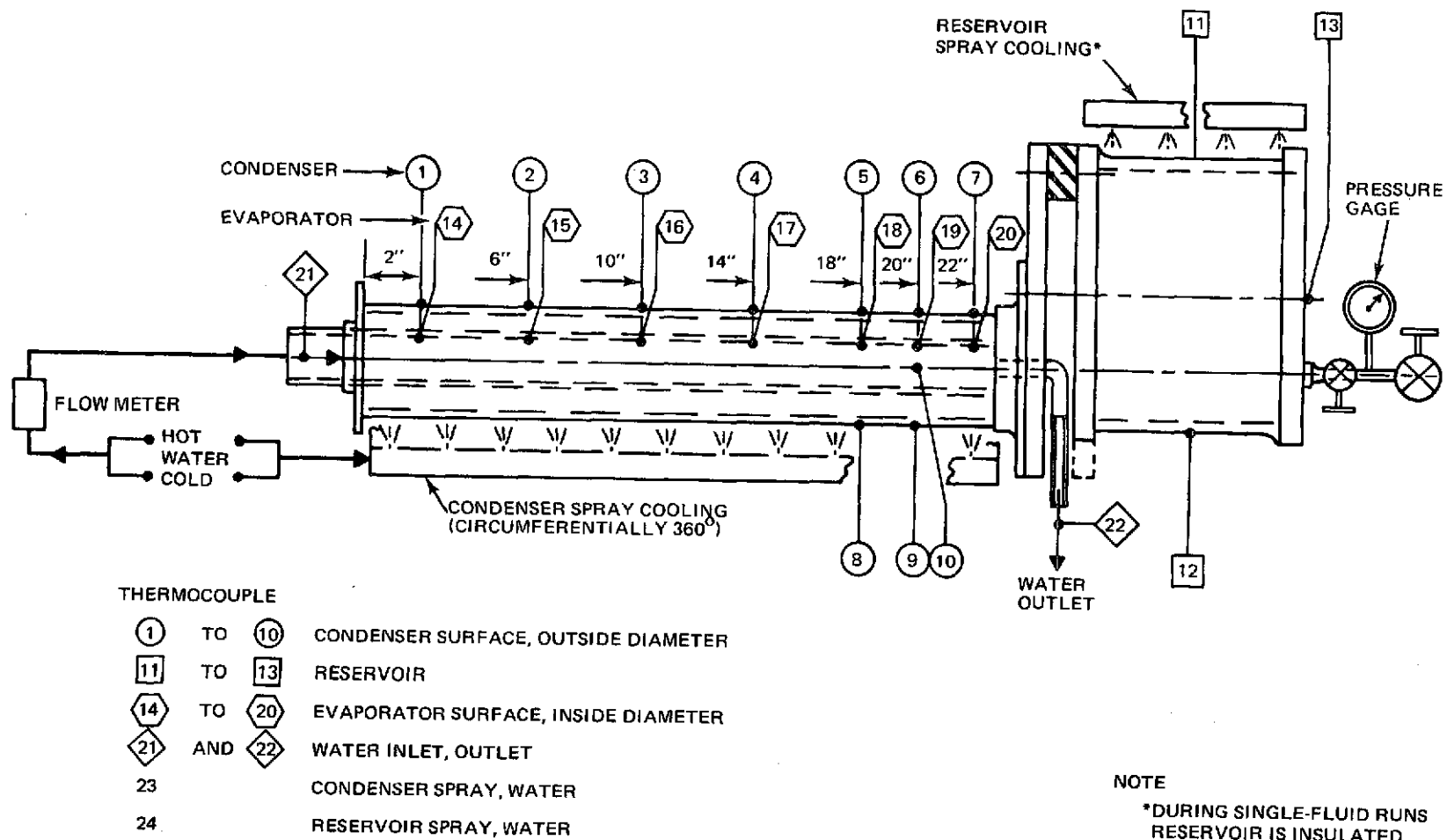
Figure 5-1. Transverse Header Instrumentation
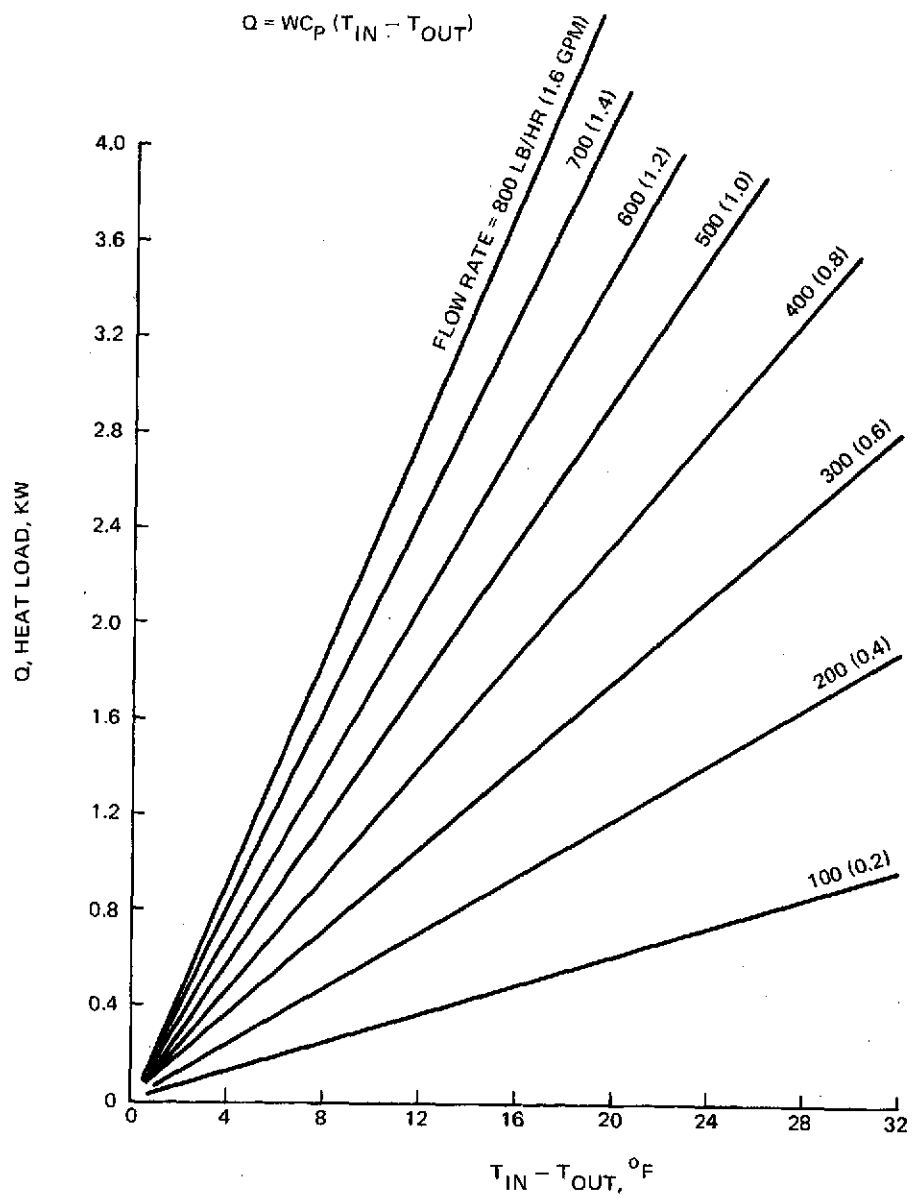
Figure 5-2. Thermal Load From Flowing Water Heat Source

5.2 TEST RESULTS - ORIGINAL CYLINDRICAL DESIGN

The purpose of the first series of tests on the original cylindrical configuration was to evaluate how the unit performed and to suggest possible improvements in header design for additional test evaluation. Testing was initially done with the header as a single-fluid heat pipe (SFHP) to establish a baseline case that could be compared to the subsequent variable-conductance heat-pipe (VCHP) runs. SFHP tests are also useful to determine evaporator and condenser film coefficients. The test effort with the original cylindrical design was performed under in-house funding.

5.2.1 Single-Fluid Heat-Pipe (SFHP) Tests

The pipe was charged with approximately 85 g of ammonia for the SFHP tests. For these runs the reservoir was insulated. In general, a test point consisted of fixing the pipe orientation to the desired tilt, turning on the spray cooling for the condenser sink, and finally adjusting the inlet water temperature and flow rate to the desired values. After a few minutes steady state was achieved, and the data from the instrumentation was recorded. Table 5-1 lists the pertinent steady state test points that were taken.

Runs were made at different tilts, flow rates, inlet water temperatures, and sink temperatures. However, to allow subsequent comparison with VCHP data, most of the test points were taken with the pipe level, a flow rate of 500 lb/hr (1.0 gpm) and a condenser sink temperature available from the tap at 55° F. The performance of the pipe under these conditions is shown in Figure 5-3. As expected, water inlet, outlet, and vapor temperatures were linear with load. The highest capacity obtained during these runs was 2,670 w.

Although no attempt was made to determine dryout, the linearity of the parameters in Figure 5-3 suggests that dryout was not reached. (When dryout occurs, it would be expected that the water temperature and the evaporator/vapor ΔT would increase at a progressively higher rate with load, as the wetted evaporator surface continues to decrease).

At a steady state operating condition the evaporator wall temperature is not constant, but decreases along its length, tracking the decrease in water temperature. This is shown in Figure 5-4, where the temperature distribution is plotted as a function of pipe length for the water, evaporator, vapor and condenser. Two distributions are shown, one at 2,670 w and the other at 1,500 w. In both cases, the flow rate and sink temperature were the same, namely, 500 lb/hr and 55° F, respectively.

5-4

Table 5-1. Single-Fluid Performance Test Points — Original Design

Test Points	Tilt, In.	W = Lb/Hr	Water Temp, °F In	Water Temp, °F Out	Sink Temp, °F*	Vapor Temp, °F	$Q = WC_{p\Delta T}$, Watts	h_e **	h_c **
1S	Level	200	80.2	69.2	57.0	50.3	620	734	1390
2S	Level	500	63.7	61.0	54.7	57.4	400	1090	1270
3S	Level	500	75.7	69.7	56.0	61.3	900	980	2290
4S	Level	500	77.7	70.7	56.5	61.7	1025	1140	1860
5S	Level	500	85.8	76.0	57.0	64.3	1500	1040	3810
6S	Level	500	94.3	82.0	48.0	67.3	1800	1050	3810
7S	Level	200	105.0	88.5	59.5	70.7	2420	1080	4600
8S	Level	500	109.7	91.5	60.0	70.9	2670	990	—
9S	Level	800	88.8	80.2	59.0	68.3	2024	1230	3860
10S	Level	800	86.5	78.5	59.0	65.9	1920	1160	4060
11S	Level	200	91.0	81.0	72.0	74.2	590	873	4500
12S	Level	400	91.3	71.3	75.0	75.0	950	1020	3620
13S	Level	600	92.0	84.7	71.0	76.0	1285	1140	4080
14S	+0.46	200	78.5	68.0	56.2	59.3	600	—	—
15S	−0.46	200	81.0	69.5	56.5	59.8	640	—	—
16S	+1.05	825	87.2	78.7	58.0	66.2	2060	—	—

*The sink thermocouple (T/C No. 23) reflects a mixed inlet and outlet water spray temperature. Except for points 11S, 12S and 13S, the inlet temperature was constant at approximately 55°F. For runs 11S, 12S, and 13S, the inlet temperature was a few degrees lower than shown

**Film Coefficients, Btu/Hr-Ft^2–°F
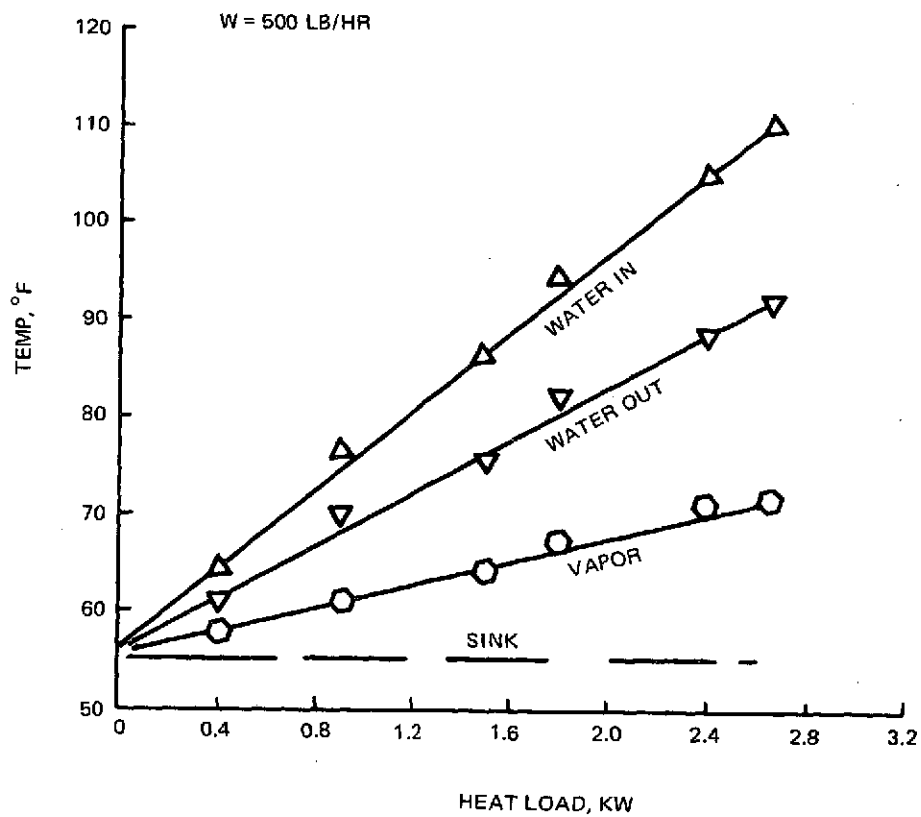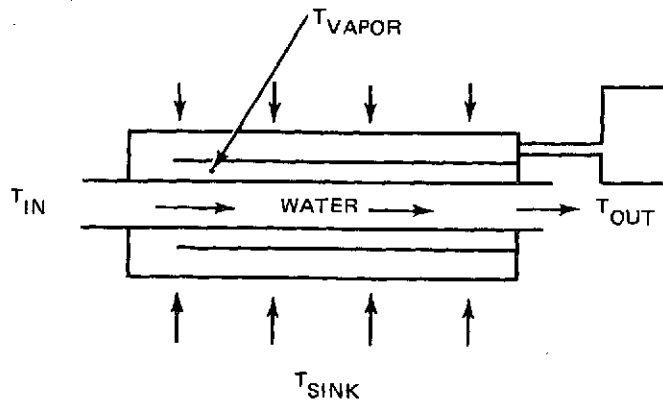
Figure 5-3. Single-Fluid Performance — Original Design
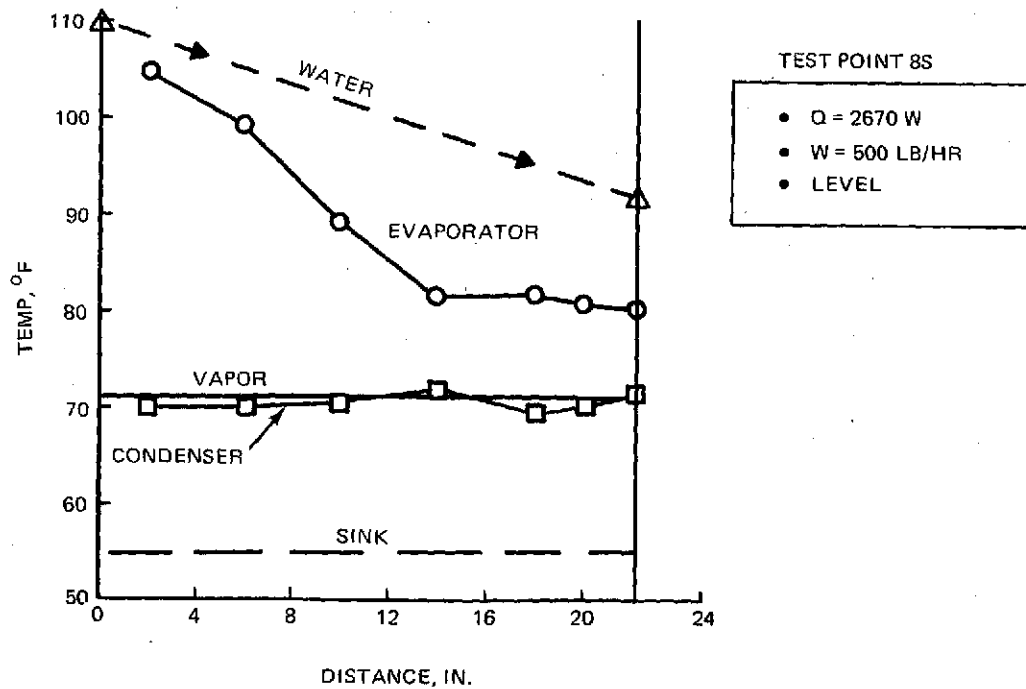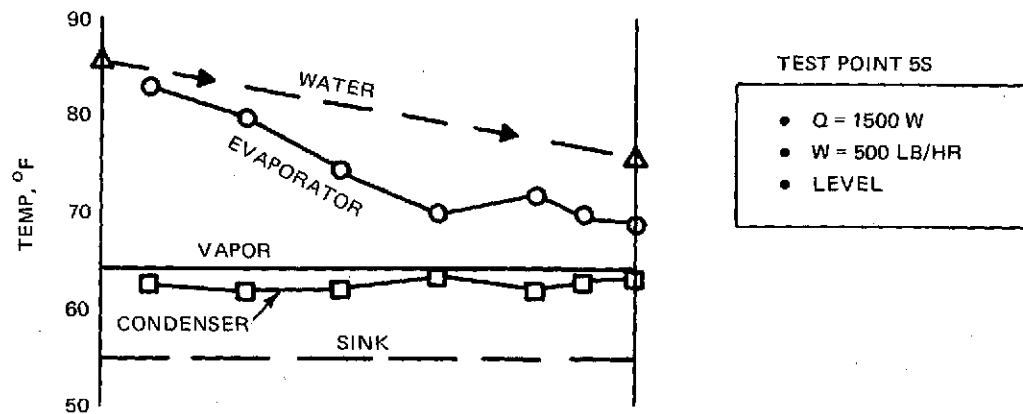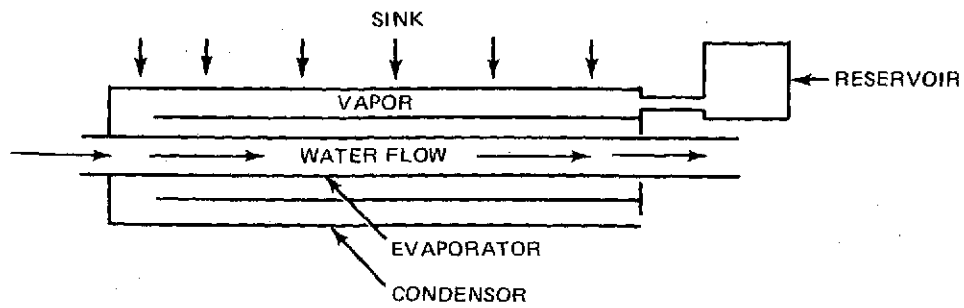
Figure 5-4. Single-Fluid Temperature Distribution — Original Design

At the water flow entrance, the temperature difference between the water and evaporator is surprisingly smaller than at points further down stream, indicating a higher heat load at the exit rather than the entrance. However, it is possible that the evaporator wall is actually lower than indicated by its thermocouples which, because of poor contact, are reading values somewhere between local water and wall temperature. It is also possible that local topside evaporator grooves situated near the water entrance are partially dried out, since this is the region that is subject to the highest heat flux and gravity head. In any event, progressive dryout with load is not indicated from the linearity of the data in Figure 5-3.

The temperature drop between the vapor and condenser surface is much smaller than the drop between the evaporator and vapor. This is partially due to the fact that the condenser area is approximately twice that of the evaporator. In addition, the topside condenser thermocouples reflect the small, no-puddle, film drop across the condenser, whereas the topside evaporator thermocouples (even assuming perfect contact) are in the region where partial groove-dry may occur, thereby resulting in the largest possible ΔT's.

Estimates were made of evaporator and condenser film coefficients from the test data using the following equations:

$$h_e = \frac{Q}{A_e \Delta T_{LM, e-v}} \tag{5-1}$$

$$h_c = \frac{Q}{A_c \Delta T_{v-c}} \tag{5-2}$$

where

$\Delta T_{LM, e-v}$ = the log mean-temperature difference between the evaporator wall and vapor at the pipes' entrance and exit, $^\circ F$

ΔT_{v-c} = difference between the average vapor and condenser temperatures, $^\circ F$

Q = heat load, Btu/hr

h = film coefficient, Btu/hr-ft^2-$^\circ F$

The log mean ΔT was used for the evaporator film coefficient because the varying temperature difference between the evaporator and vapor is similar to that found in conventional fluid heat exchangers. The total evaporator and condenser areas used were

$$A_e = \pi (1.0)(22.3) = 70 \text{ in.}^2$$

$$A_c = \pi (1.865)(22.3) = 131 \text{ in.}^2$$

Table 5-1 lists the calculated values of film coefficient for each of the level test points. It is seen that the evaporator film coefficients are fairly consistent over all the test points, with the arithmetic average being 1,050 Btu/hr-ft^2-$^\circ$F. However, due to the suspected poor thermocouple contact, it is estimated that the film coefficient is higher, probably around 2,000 Btu/ht-ft^2-$^\circ$F, based on test data from similar groove dimensions (Ref 4).

The condenser film coefficients are higher and are somewhat more erratic than those of the evaporator, with the average value being 3,260 Btu/hr-ft^2-$^\circ$F. The scatter is partially due to the inaccuracies of the small temperature difference between the condenser wall and vapor, as seen in Figure 5-4.

A few points were taken to determine the effect of tilt on pipe performance (test points 14S, 15S and 16S). Tilt was applied by elevating the water inlet side above the outlet side (positive tilt values) or elevating the outlet above the inlet side (negative tilt values). The effect on temperature distribution was hardly noticeable, as seen in Figure 5-5, which compares 16S (tilt = +1.0 in.) with point 13S (level) at approximately the same power level of 2,000 w. Similarly, no change was observable between the positive and negative tilts of test points 14S and 15S.

The heat exchanger effectiveness, ξ, as defined by equation 4-2, was calculated from the data in Figure 5-3 to be 0.46 at a flow of 500 lb/hr. This is 25% higher than the analytical value of 0.37 obtained from Figure 4-5. It is felt that the presence of evaporator-wall thermocouples in the flow passage result in flow disturbances that enhance the film coefficient predicted by the analysis.

5.2.2 Variable-Conductance Heat-Pipe (VCHP) Tests

Following the single-fluid tests, nitrogen was injected into the pipe to provide thermal control. Tests were conducted with the insulation removed from the reservoir and cooled with 55°F tap water. A summary of the tests is given in Table 5-2. All test points were conducted in a level orientation at a water flow rate of 500 lb/hr, except test point 9V, which was run at 800 lb/hr. For this higher flow rate, a load of 3,060 w was achieved.

Figure 5-6 shows the VCHP performance as a function of load at a flow rate of 500 lb/hr. Comparing its behavior under the same conditions to that of the single-fluid data in Figure 5-3, the VCHP mode produces modulated vapor and outlet water temperature. Vapor temperature was controlled from 77 to 80°F over a load variation of 400 to 2,610 w. Over the same range, the single-fluid test yielded a vapor temperature range of 57 to 71°F. Thus, the vapor temperature was controlled to a 3°F range in the VCHP mode, compared to 14°F in the SFHP mode over a load of variation exceeding 2 kw.
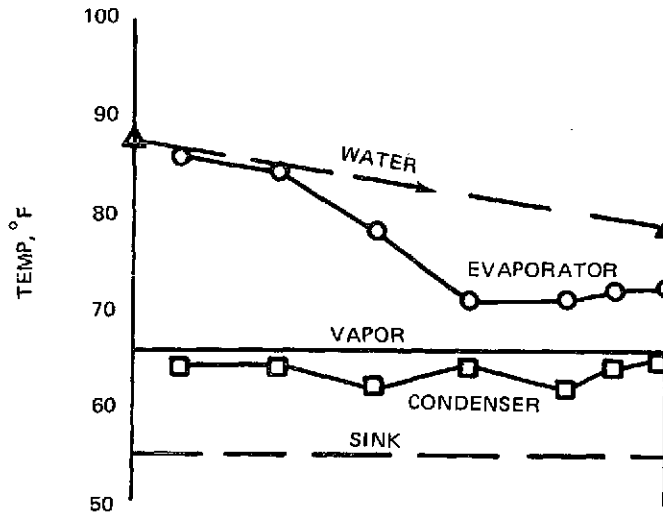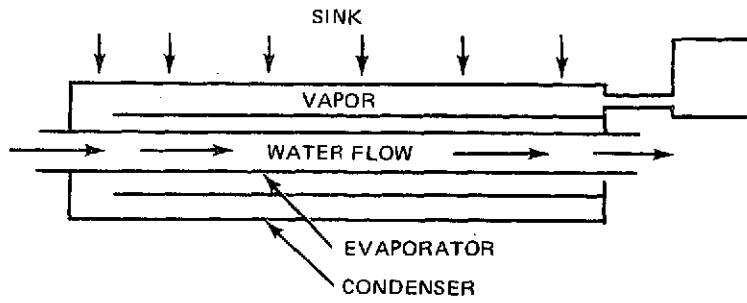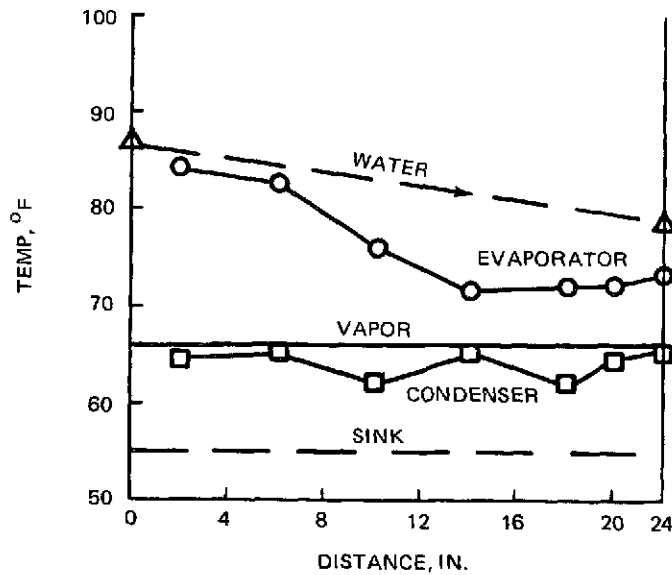
Figure 5-5. Effect of Tilt on Performance, Single-Fluid Data — Original Design

Table 5-2. VCHP Performance Test Points — Original Design

Test Point	Tilt, In.	W, Lb/Hr	Water Temp, $^\circ$F		Sink Temp, $^\circ$F	$Q = WCp\Delta T$, Watts	T_v, $^\circ$F (Calc)
			In	Out			
1V	Level	500	67.7	66.5	54.5	178	65
2V	Level	500	76.5	74.5	54.5	305	73
3V	Level	500	83.7	80.5	55.3	470	77
4V	Level	500	85.3	81.5	55.5	545	78
5V	Level	500	98.0	89.8	57.0	1225	77
6V	Level	500	102.3	92.0	59.0	1550	80
7V	Level	500	115.0	98.5	63.3	2450	80
8V	Level	500	116.5	99.3	63.5	2610	80
9V	Level	800	112.0	99.0	64.3	3060	79
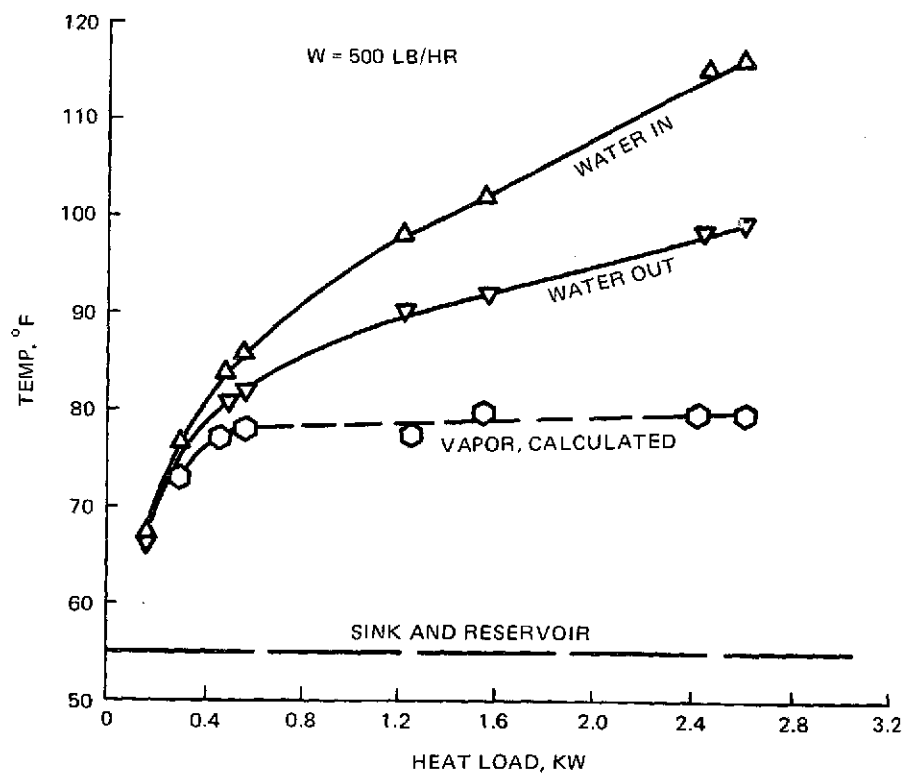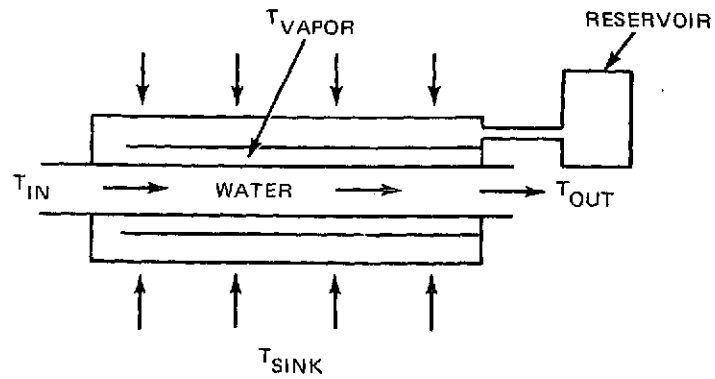
Figure 5-6. VCHP Performance — Original Design

The vapor temperature for the VCHP mode was not measured but calculated from equation (5-1). An average evaporator film coefficient of $1,050$ Btu/hr-ft$^{2\circ}$F was assumed, based on the single-fluid data. This should be valid for the VCHP mode since the evaporator region, like the single-fluid mode, is entirely within an ammonia vapor environment, i.e., no noncondensibles. In addition, the evaporator temperature profiles are similar, as will be seen later.

It is seen from Figure 5-6, that the outlet water temperature, the desired control parameter, is also modulated with load. Its response in the VCHP mode is compared in Figure 5-7 with that of the single-fluid mode. Over the load range of 400 to 2600 w, the variation was $31°$F in the SFHP mode, compared to $21°$F in the VCHP Mode, or a reduction in outlet temperature variation of 32%. Greater regulation of outlet water temperature can be obtained, as discussed in Section 4, with higher heat-transfer effectivenesses between the water heat source and ammonia vapor. For this unfinned configuration, the effectiveness was calculated to be 0.46 for both the SFHP and VCHP modes.

The highest load tested at 500 lb/hr was 2,610 w at a water inlet temperature of $116.5°$F. Furthermore, the linearity of the parameters in Figure 5-6 beyond the load of $1,200$ w suggests that dryout or partial dryout had not been reached.

Temperature profiles in the VCHP mode are shown in Figure 5-8 for loads of $1,550$ and 2610 w at 500 lb/hr and level orientation. A comparison between the single-fluid profiles in Figure 5-4 and the VCHP profiles in Figure 5-8 at comparable power levels reveals that the evaporator temperature distributions are about the same. However, a significantly larger overall ΔT exists between the condenser and vapor in the VCHP mode. This is due to the action of the control gas which, as vividly illustrated in test point 6V of Figure 5-8, has blocked off a significant portion of the right side of the condenser. In the high-load condition of test point 8V, most of the gas has been driven from the condenser, leaving a small blocked region at the beginning and end. The blocked region at the beginning (or left side) of the condenser is unexpected and may be due to a trapped pocket of gas that is isolated from the sweeping action of the vapor as it turns around the baffle and enters the condenser. The results in Figure 5-8 clearly show that the vapor temperature is relatively constant over the load range, while the blockage in the condenser decreases with increasing load.

The low end of the control range appears to be about 400 w (Figure 5-6). Below this value the vapor temperature is no longer constant, and it is presumed that the control gas completely fills the condenser vapor space. Under these conditions, the losses between the
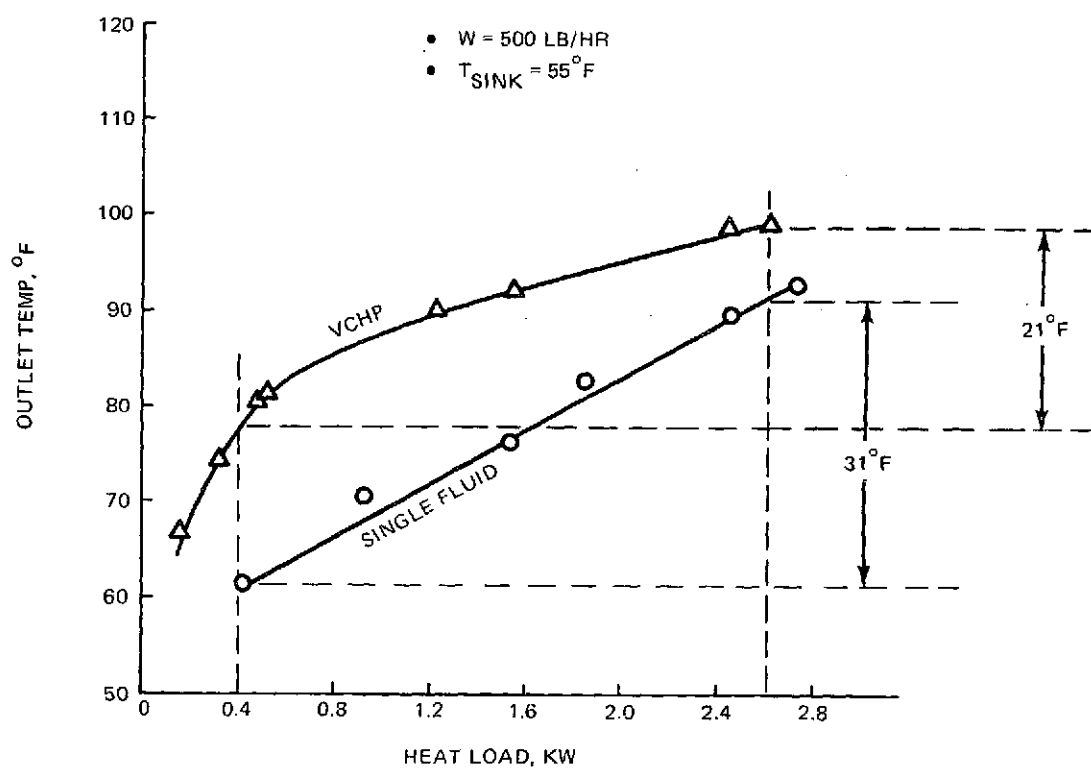
Figure 5-7. Outlet Temperature Control — Original Design
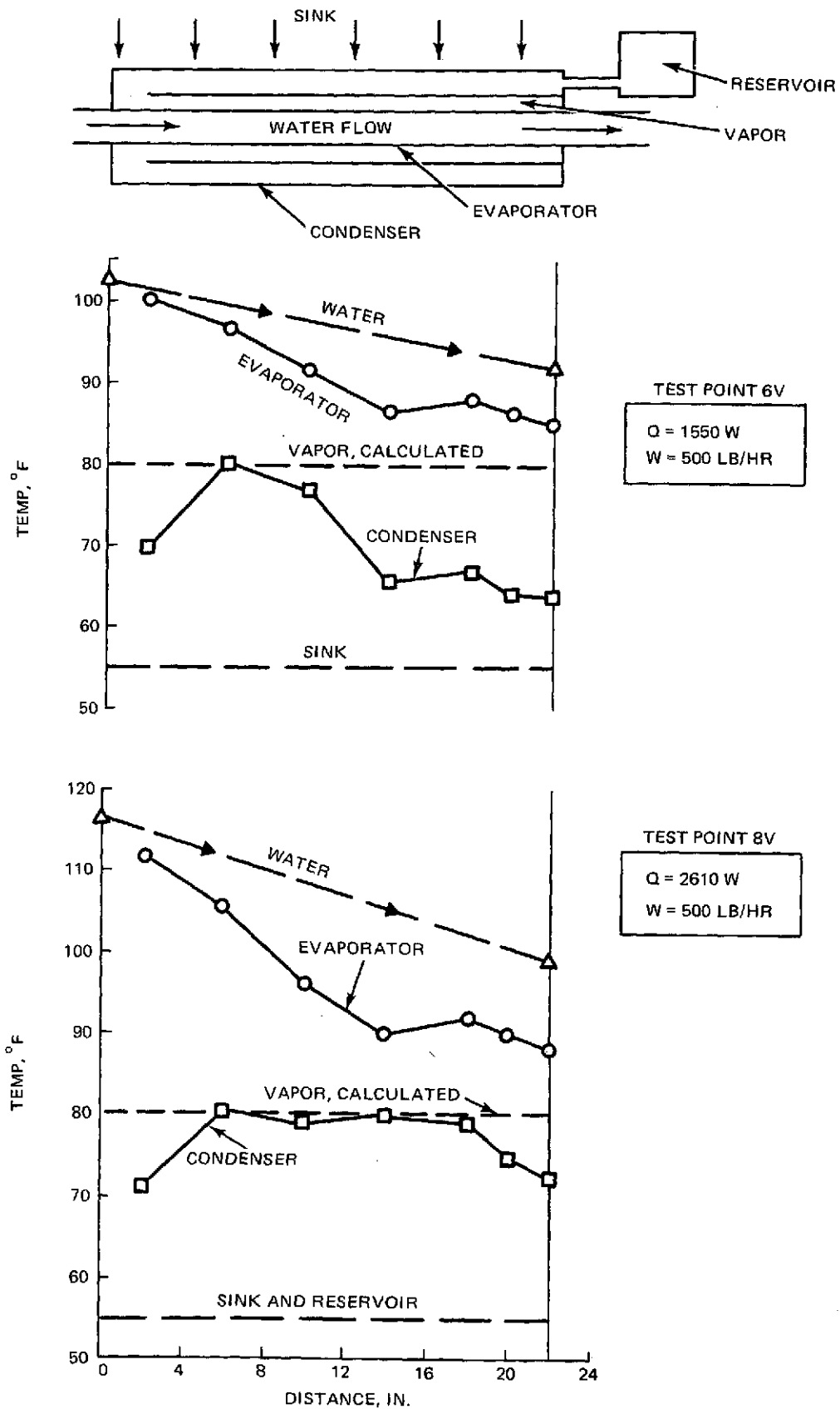
Figure 5-8. VCHP Temperature Distribution — Original Design

water stream and condenser consist of conduction through both end walls, conduction through the ammonia-saturated wick and vapor diffusion of ammonia through the nitrogen control gas. An analysis of these losses, presented in Appendix B, concludes that vapor diffusion is the major contributor of losses in the shutoff mode. Methods of reducing these losses, if required for a particular application, are suggested in Appendix B. The ratio of maximum to minimum power, some times called the turndown ratio, is calculated to be 3060/400 or 7.7 to 1.

5.2.3 Conclusions and Recommendations

Test results regarding the original cylindrical transverse header design can be summed up as follows:

1. A high-capacity, gas-controlled VCHP has been built and tested that can handle at least 2,600 w in the VCHP mode without any noticeable degradation.

2. Vapor and outlet-fluid temperature control has been demonstrated via the blocking action of the control gas. The vapor temperature variation was $3°F$ in the VCHP mode, compared to $14°F$ in the SFHP mode, over a load range of 400 - 2600 w. The corresponding variation of outlet water temperature was $21°F$ (VCHP), compared to $31°F$ (SFHP).

3. Losses in the shutdown mode were approximately 400 w. These are mainly due to ammonia diffusion through the nitrogen control gas.

Recommendations for subsequent hardware modifications and testing are:

1. Improve outlet-water temperature control by increasing the effectiveness between the water heat source and ammonia vapor using finning in the flow annulus.

2. Investigate means of reducing losses in the shutoff mode, for example, by shielding the baffle and webs to minimize wetting with ammonia.

3. Determine vapor temperature in the VCHP mode by using a vapor thermocouple or pressure gauge.

4. Determine dryout limit in both single-fluid and VCHP modes.

5.3 TEST RESULT - MODIFIED CYLINDRICAL DESIGN

After the first series of tests the unit was modified in accordance with the recommendations cited earlier. The following changes were made:

1. Installation of a nonwetting Teflon tape to the outer surface of the steel baffle to reduce mass diffusion losses when header is shut down

2. Installation of aluminum finning to the water flow annulus to increase the heat exchanger effectiveness and temperature control of the device

3. Installation of a pressure gauge to determine the vapor temperature when the unit is operated in the variable-conductance mode

The scope of the test effort was also expanded to study parameters not previously evaluated. These included: testing over a wider range of water flow rates (150 to 800 lb/hr) and inlet temperatures (55 to 140°F); two sink/reservoir temperatures (55°F and 75°F); and two water flow directions in the evaporator tube – normal (toward reservoir) and reverse.

Evaporator wall thermocouples were reinstalled, but because of the limited access imposed by the finned annulus, good wall contact could not be assured. As was previously done, the first test sequence was with a single fluid, i.e., ammonia. This was followed by nitrogen gas-injection and testing in the VCHP mode.

5.3.1 Single-Fluid Heat-Pipe (SFHP) Tests

The pipe was again charged with 85 g of ammonia and configured for single-fluid testing by insulating the reservoir. Table 5-3 lists the steady state runs that were made. In this table a test run, such as 3S, means a series of steady state test points at different inlet water temperatures from 60 to 140°F, with constant flow rate, tilt, sink temperature and flow direction.

Figures 5-9, 5-10 an d 5-11 show the response of the inlet, outlet and vapor temperatures with load for water flow rates of 150, 500 and 800 lb/hr, respectively. All the temperature data is linear with load; the slope, as expected, is inversely proportional to flow rate. Similar responses were obtained for the intermediate flow rates of 350 and 650 lb/hr. The highest load achieved was 3.9 kw for run 3S. No indication of dryout was observed for these or subsequent single-fluid runs.

For the flow rate of 500 lb/hr, a heat exchanger effectiveness of 0.63 was obtained from the test date of Figure 5-10. As expected, this is higher than the 0.45 value obtained for the unfinned heat exchanger. The effectiveness, computed from test data at different flow rates, is shown in Figure 5-12 for the finned (modified) transverse header. The predicted behavior from Figure 4-8 is also shown. It is seen that test values agree reasonably well with predicted values, particularly at higher flow rates. The improvement in effectiveness over the unfinned transverse header is also shown. The effectiveness for the unfinned configuration at different flow rates was obtained from the test data in Table 5-1.

Table 5-3. Modified Transverse Header — Single-Fluid Runs

Run No.	W, Water Flow Rate, Lb/Hr	T Inlet, °F	Tilt	Sink Temp,* °F	Flow Direction
1S	150	60	Level	55	Normal
2S	350	80	Level	55	Normal
3S	500	100	Level	55	Normal
4S	650	120	Level	55	Normal
5S	800	140	Level	55	Normal
6S	150	80	Level	75	Normal
7S	500	100	Level	75	Normal
8S	800	120	Level	75	Normal
		140			
9S	500	60-140	−1/2 In.	55	Normal
10S	500	60-140	+1/2 In.	55	Normal
11S	150		Level	55	Reverse
12S	500	60-140	Level	55	Reverse
13S	800		Level	55	Reverse

*Sink spray flow rate to be approximately 3.2 gpm water for all runs

- SINGLE FLUID
- LEVEL
- NORMAL FLOW DIRECTION
- W = 150 LB/HR
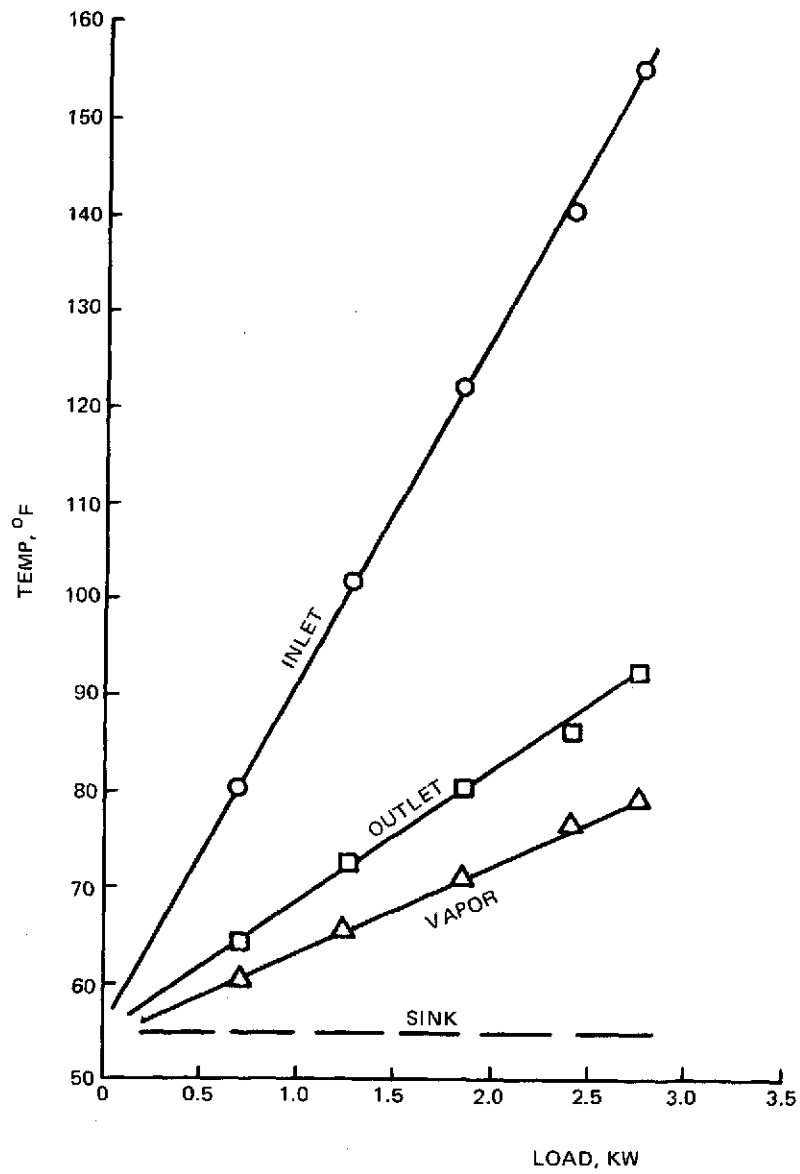
Figure 5-9. Performance — Modified Design, Run 1S

5-19

- SINGLE FLUID
- LEVEL
- NORMAL FLOW DIRECTION
- W = 500 LB/HR
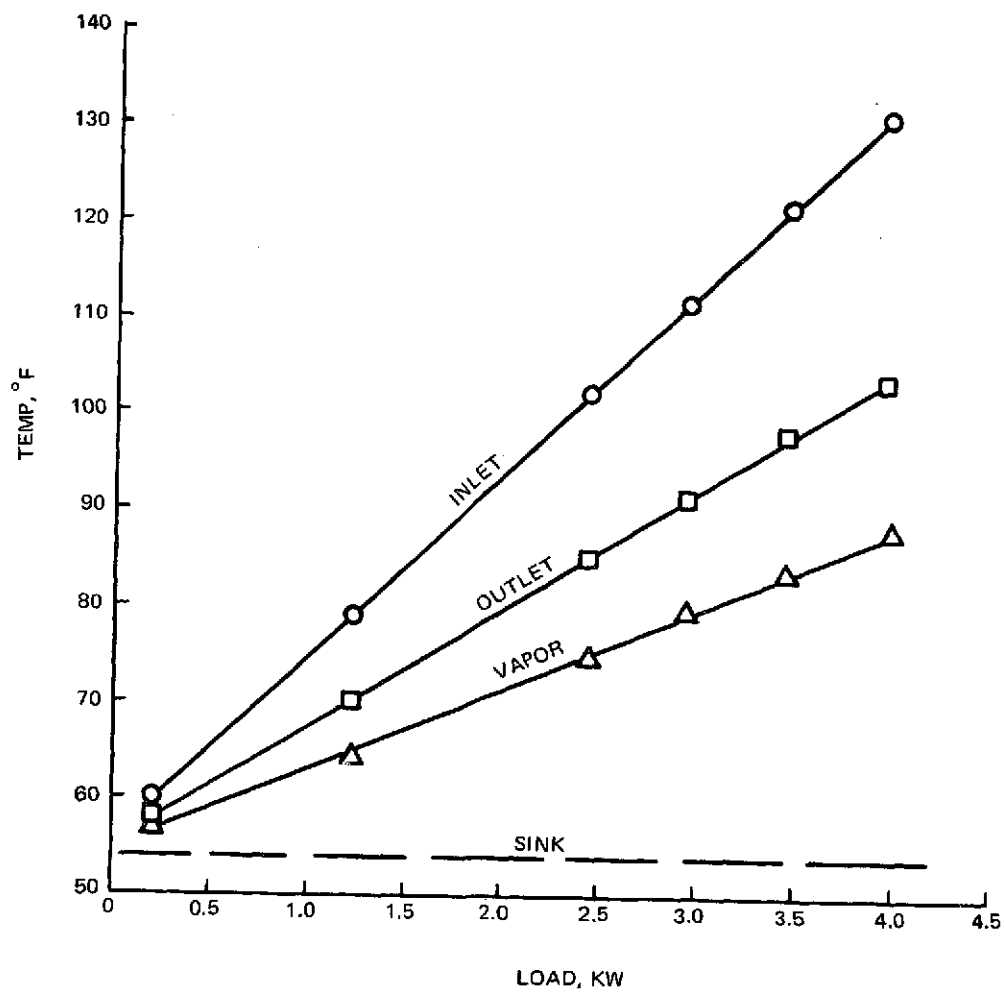
Figure 5-10. Performance — Modified Design, Run 3S
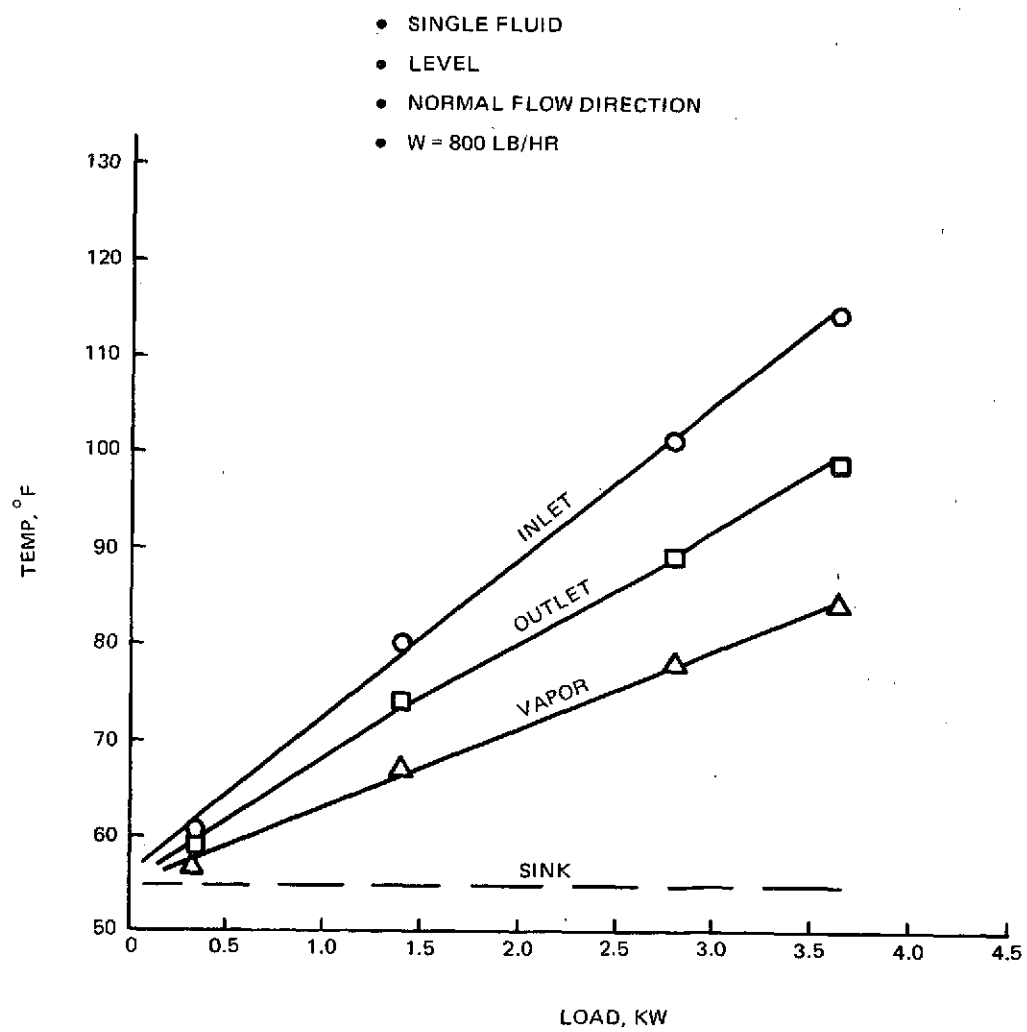
Figure 5-11. Performance — Modified Design, Run 5S

- SINGLE-FLUID DATA
- SINK = 55°F
- DATA POINTS
  - O & □ NORMAL FLOW DIRECTION
  - C REVERSE FLOW (FINNED HX)
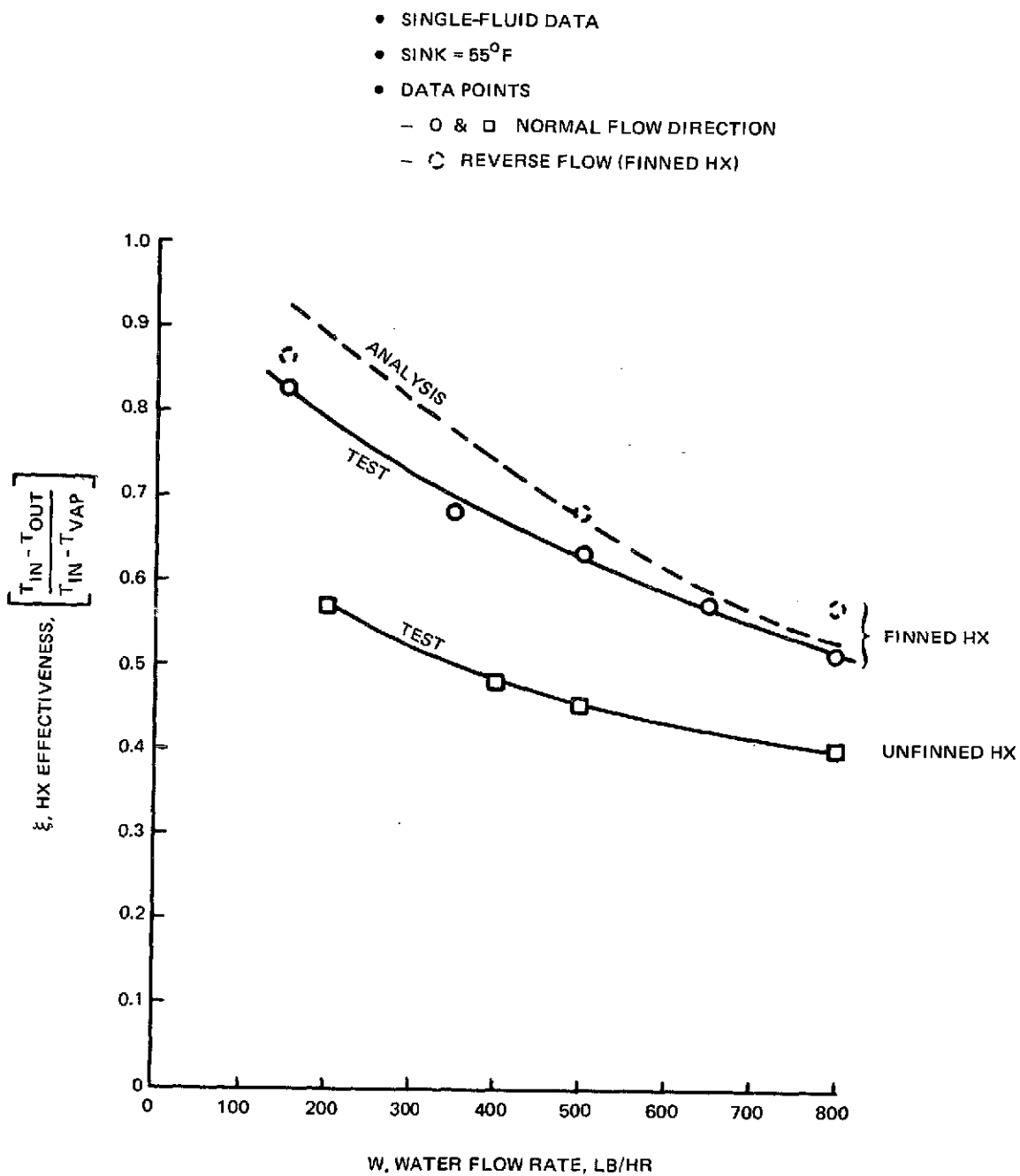
Figure 5-12. Influence of HX Finning on Header Effectiveness

A typical temperature profile for a flow rate of 500 lb/hr at a load of 1245 w is presented in Figure 5-13. It is seen that the evaporator wall temperatures are apparently the same as the water temperatures. This is attributed to improved effectiveness between the water and evaporator, as well as to poor thermocouple contact with the evaporator wall. It is estimated that the average water-to-evaporator wall temperature drop should be about $2°$ F for the load and flow conditions depicted in Figure 5-13.

The effect of different sink temperatures for a flow of 500 lb/hr, and typical for the other flow rates is shown in Figure 5-14. Water outlet temperature is plotted against load for sink temperature of 55 and $75°$ F, respectively. As expected, the outlet temperature is $20°$ F higher for the higher sink temperature run.

The typical effect of tilt on performance for a flow of 500 lb/hr is shown in Figure 5-15. Like the unfinned configuration, no change in performance was noted at + 1/2 or - 1/2-in. tilts.

The effect of reverse water flow on performance for a flow rate of 500 lb/hr is shown in Figure 5-16. It is interesting to see that there is a slightly lower outlet temperature at high loads during reverse flow. This was not as noticeable in the other two reverse flow rates tested, i.e., 150 and 800 lb/hr. However, all reverse flow runs showed a slightly higher effectiveness over their normal flow counter parts, as shown by the ⊙ data points in Figure 5-12.

This may be due to nonsymetrical flow effects caused by the seven evaporator-thermocouple lead wires which exit the flow passage at the left end, furthest from the reservoir. Partial blockage or adverse disruption of flow could result. There are no instrumentation wires in the flow entrance at the right end closest to the reservoir. Now, for any flow direction, the highest heat-transfer rates occur at the entrance of the flow passage. (See Figure 4-2.) Consequently, for water entering at the left (normal direction), the effectiveness will be impacted more strongly than water entering at the right (reverse direction).

5.3.2 Variable-Conductance Heat-Pipe (VCHP) Tests

Following the single-fluid tests, nitrogen was again injected into the pipe to provide the same $75-78°$ F vapor temperature-control range. Table 5-4 lists the steady state runs that were tested. Except for the letters S (for single fluid) and V (for VCHP) the runs in Table 5-4 correspond exactly to those in Table 5-3. In the discussion of the results below, the performance of the modified versus unmodified configurations will first be compared. This will be followed by data which examines the effect of the following parameters on performance: water flow rate, sink/reservoir temperature, tilt, and reverse flow.

- SINGLE FLUID
- W = 500 LB/HR
- NORMAL FLOW DIRECTION
- LEVEL
- Q = 1245 W
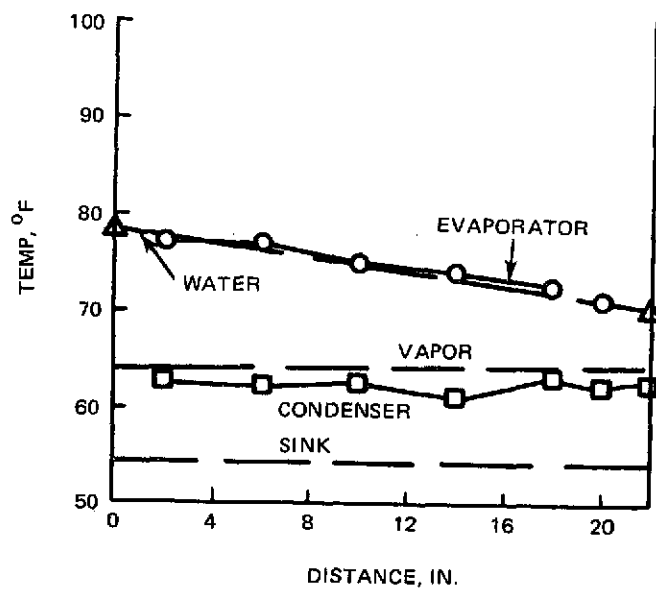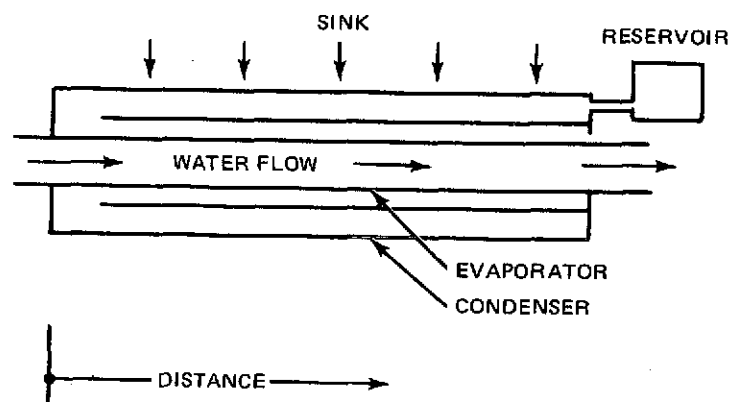
Figure 5-13. Temperature Distribution — Modified Design, Run 3S

- SINGLE FLUID
- NORMAL FLOW DIRECTION
- LEVEL
- W = 500 LB/HR

○ SINK TEMPERATURE = 75°F, RUN 7S
□ SINK TEMPERATURE = 55°F, RUN 3S
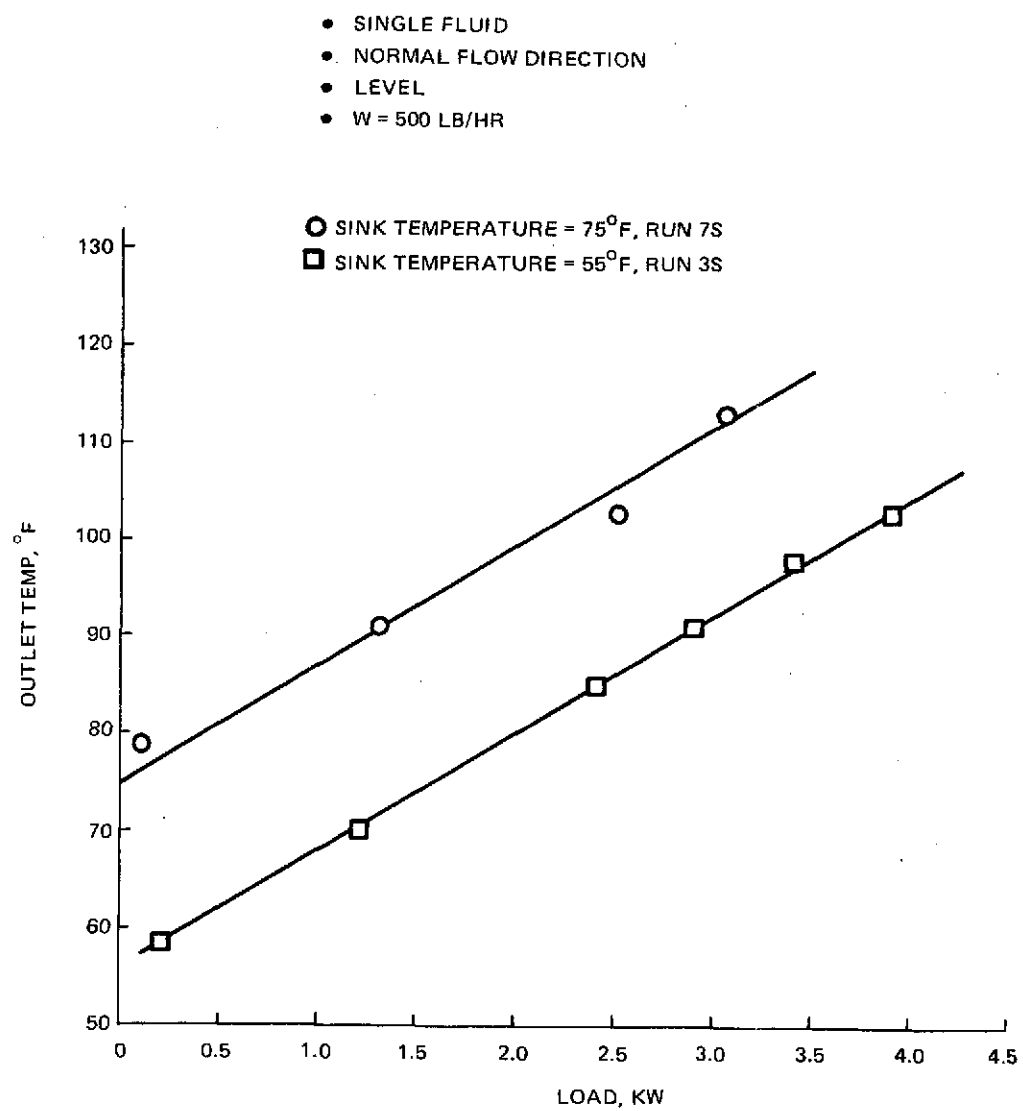
Figure 5-14. Effect of Sink Temperature on Performance
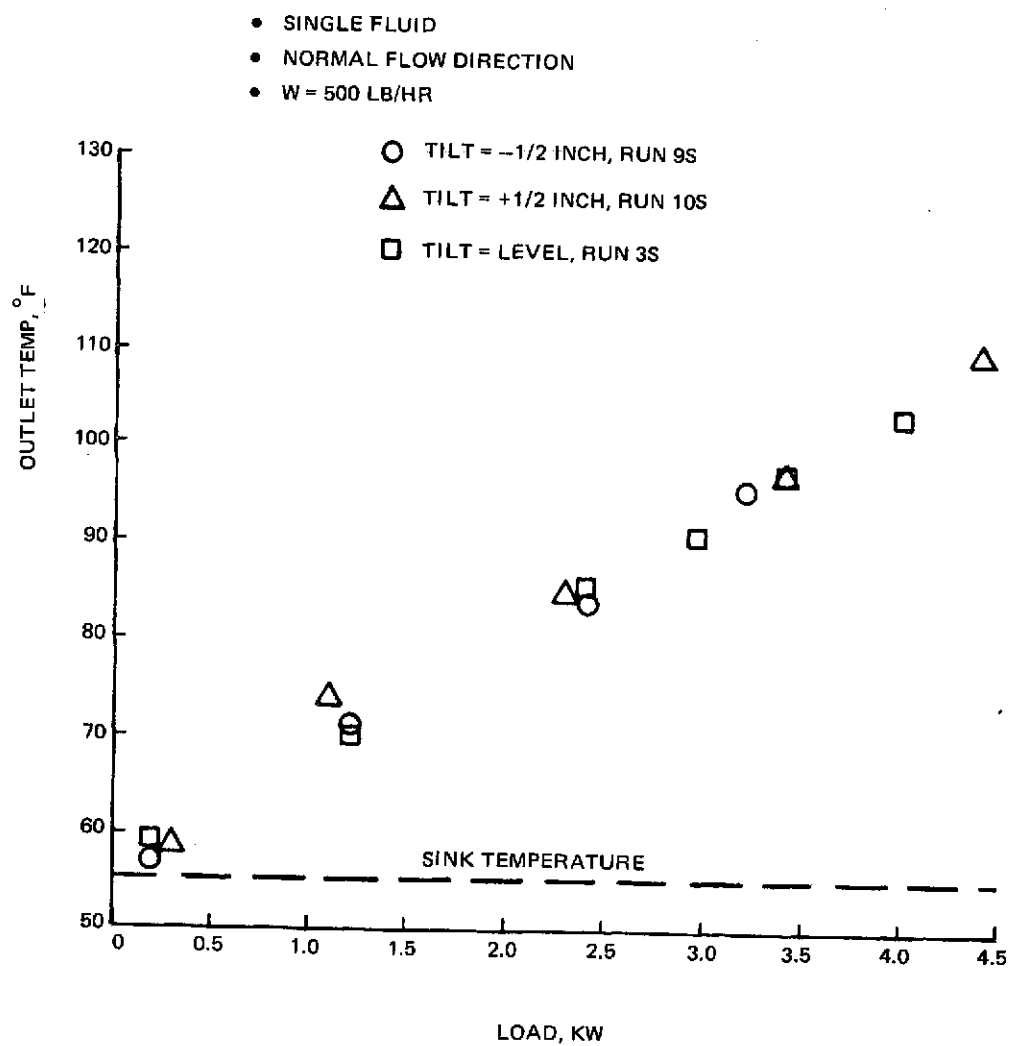
Figure 5-15. Effect of Tilt on Performance
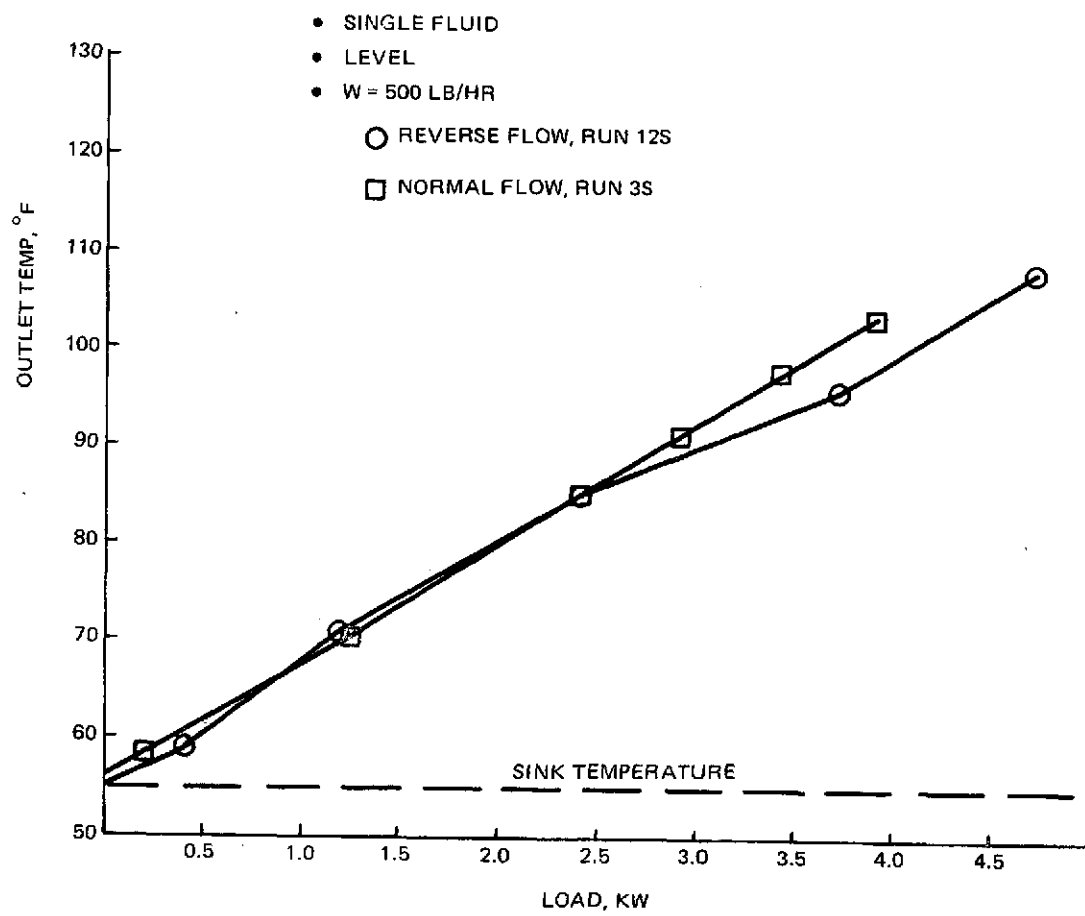
Figure 5-16. Effect of Reverse Flow on Performance

Table 5-4. Modified Transverse Header — Variable-Conductance Runs

Run No.	Water Flow Rate, Lb/Hr	T Inlet, °F	Tilt	Sink* Temp, °F	Reservoir Temp, °F	Flow Direction
1V	150	55 to 70	Level	55	55	Normal
2V	350	in 5°F Δ's	Level	55	55	Normal
3V	500		Level	55	55	Normal
4V	650	70 to 140	Level	55	55	Normal
5V	800	in 10°F Δ's	Level	55	55	Normal
6V	150	75 to 90 in 5°F Δ's	Level	75	75	Normal
7V	500	90 to 140	Level	75	75	Normal
8V	800	in 10°F Δ's	Level	75	75	Normal
9V	500	Same As	−1/2 In.	55	55	Normal
10V	500	Runs 1V-5V	+1/2 In.	55	55	Normal
11V	150	Same As	Level	55	55	Reverse
12V	500	Runs 1V-5V	Level	55	55	Reverse
13V	800		Level	55	55	Reverse

*Sink spray flow rate to be approximately 3.2 gpm water for all runs

The response of the modified transverse header at a normal flow rate of 500 lb/hr is shown in Figure 5-17. The highest load tested was over 4,000 w. However, beyond about 3,600 w, the behavior of the inlet, outlet and vapor temperatures is erratic, perhaps indicating dryout, or the movement of the interface into the reservoir, or both. Note that the dryout predicted from Figure 4-3 at an effectiveness of 0.63 is about 3,400 w and that above 3,000 w the interface is estimated to be into the reservoir. (See Figure 4-10.)

A comparison of the vapor temperature response for the single-fluid and VCHP modes is shown in Figure 5-18. Over a load range of 400 to 260 w the vapor temperature is re-markably "constant", varying from 77 to only 79°F ($\Delta T = 2F$) for the VCHP mode, com-pared to a variation of 58 to 76°F ($\Delta T = 18°F$) for the single-fluid mode. Vapor temperature values, determined from the pressure gauge attached to the reservoir, agree reasonably well with the calculated values of vapor temperatures obtained for the original unmodified design in Figure 5-6.

The response of the outlet temperature for the single-fluid and VCHP modes is shown in Figure 5-19. Over a load variation of 400 to 2,600 w, the outlet temperature varied 9°F in the VCHP mode, and 26°F in the single-fluid mode. For the unfinned configuration, the corresponding values over the same load were 21°F for the VCHP and 31°F for the single-fluid mode. (See Figure 5-7.) Thus, the variation in outlet temperature decreased from 68% (21/31) for the unfinned unit to 35% (9/26) for the finned unit.

The outlet temperature response for the two transverse header configurations from Figures 5-7 and 5-19 are replotted in Figure 5-20. Test conditions for both units were identical. It is seen that the modified unit produces a more flattened outlet-temperature profile over a wider load range. This is due to the improved effectiveness caused by the finned heat-transfer surface. In addition, residual losses appear to be lower for the modified unit as a result of the Teflon-coated baffle. These losses are difficult to measure accurately, but can be arbitrarily estimated as the point where the average fluid temperature equals the extrapolated vapor temperature. From Figures 5-6 and 5-17, these values are estimated to be approximately 350 and 150 w for the unlined and Teflon-lined baffle configurations, respectively.

Temperature profiles at two power levels are shown in Figure 5-21. As mentioned before, the evaporator thermocouples are not reliable and should be ignored. Comparing the condenser profile to that of the unmodified design in Figure 5-8, it is seen that both profiles are essentially the same. The slightly lower left-end condenser wall temperatures in Figure 5-8 have apparently disappeared in Figure 5-21 due, probably, to the purging of a nitrogen gas pocket. The predicted values of the interface location are also shown in Figure 5-21.
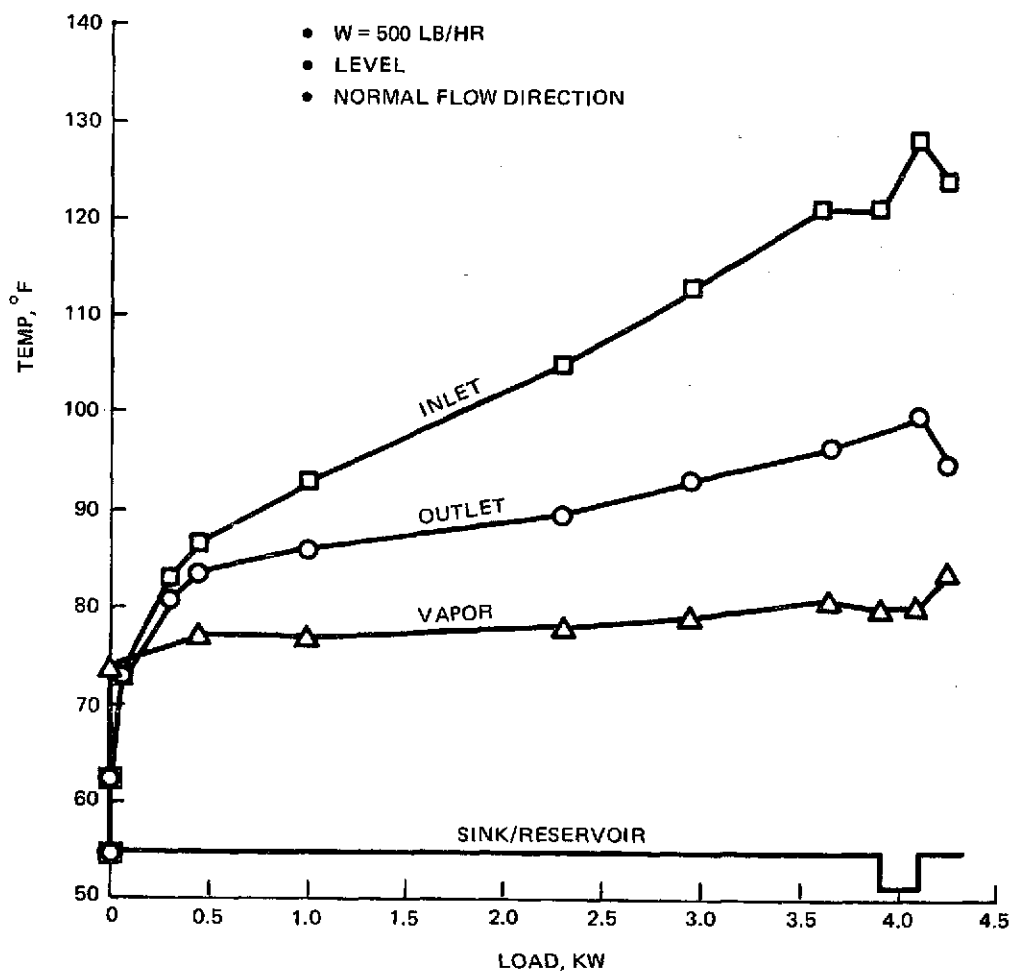
Figure 5-17. VCHP Performance — Modified Design, Run 3V
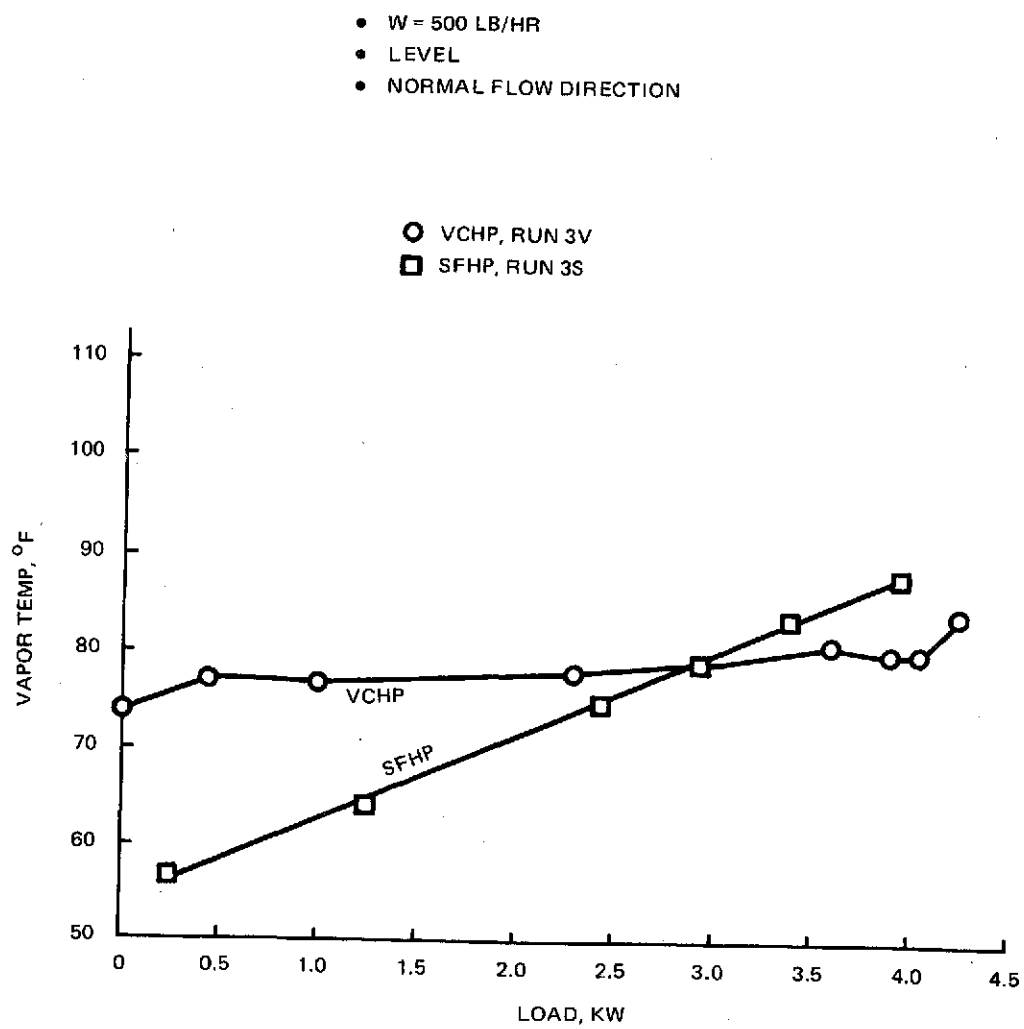
Figure 5-18. Vapor Temperature — Modified Design

- W = 500 LB/HR
- $T_{SINK/RES} = 55°F$
- LEVEL
- NORMAL FLOW DIRECTION

O VCHP, RUN 3V
□ SINGLE FLUID, RUN 3S
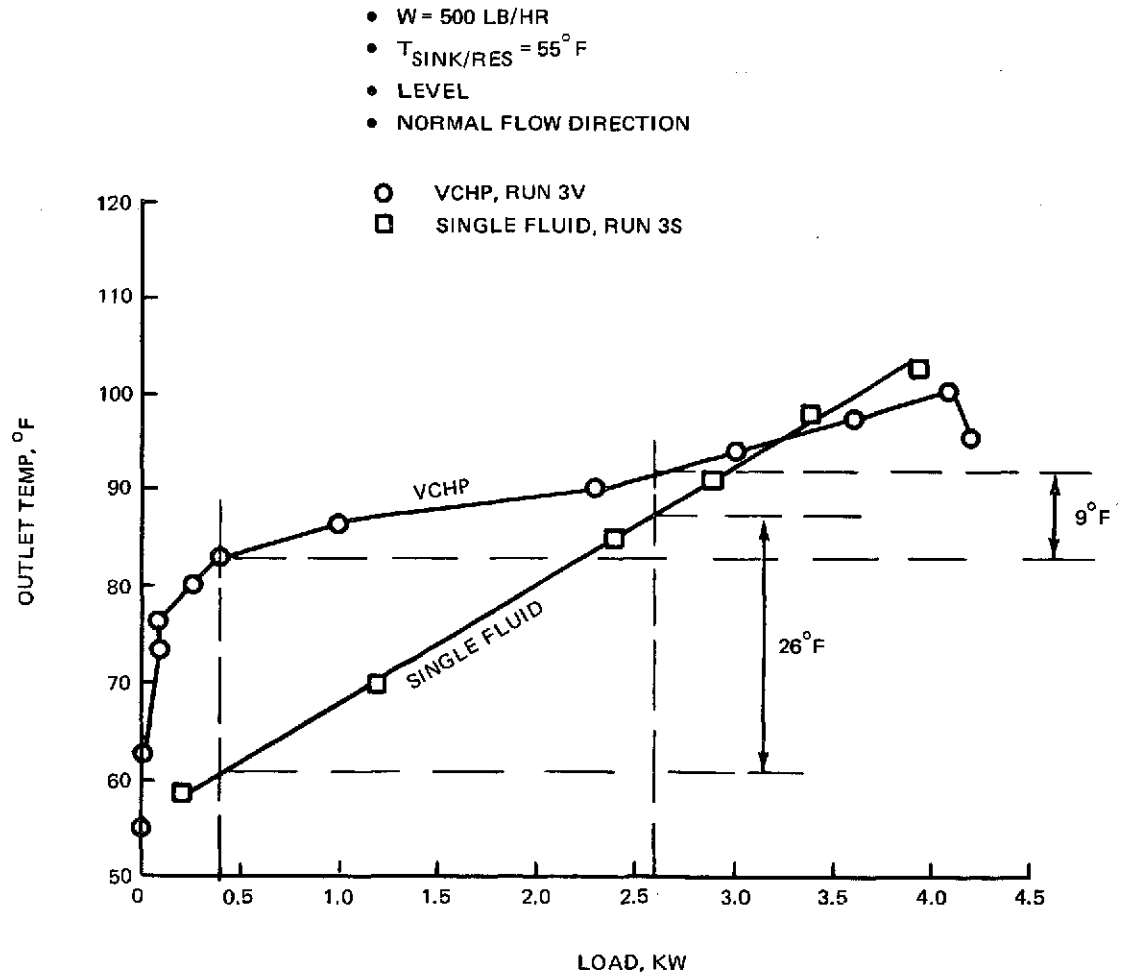
Figure 5-19. Outlet Temperature Control — Modified Design
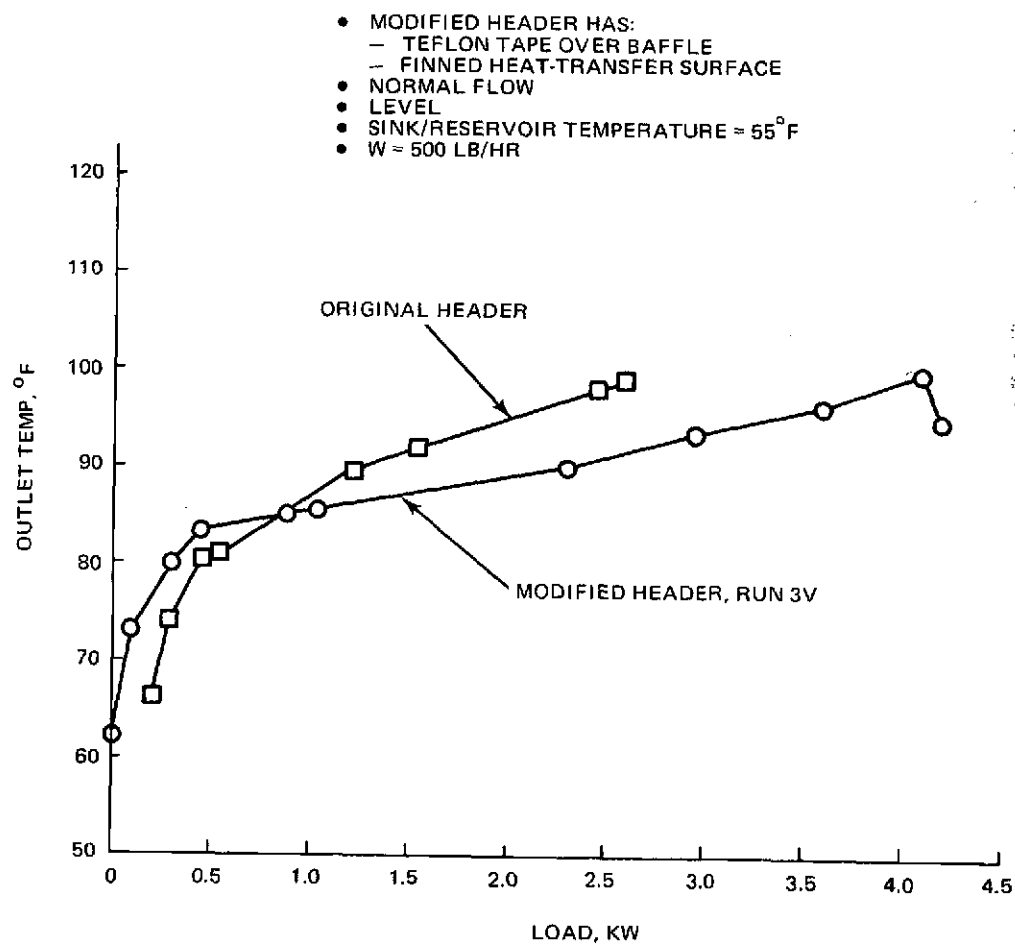
Figure 5-20. Performance Comparison Between Original and Modified Transverse Header
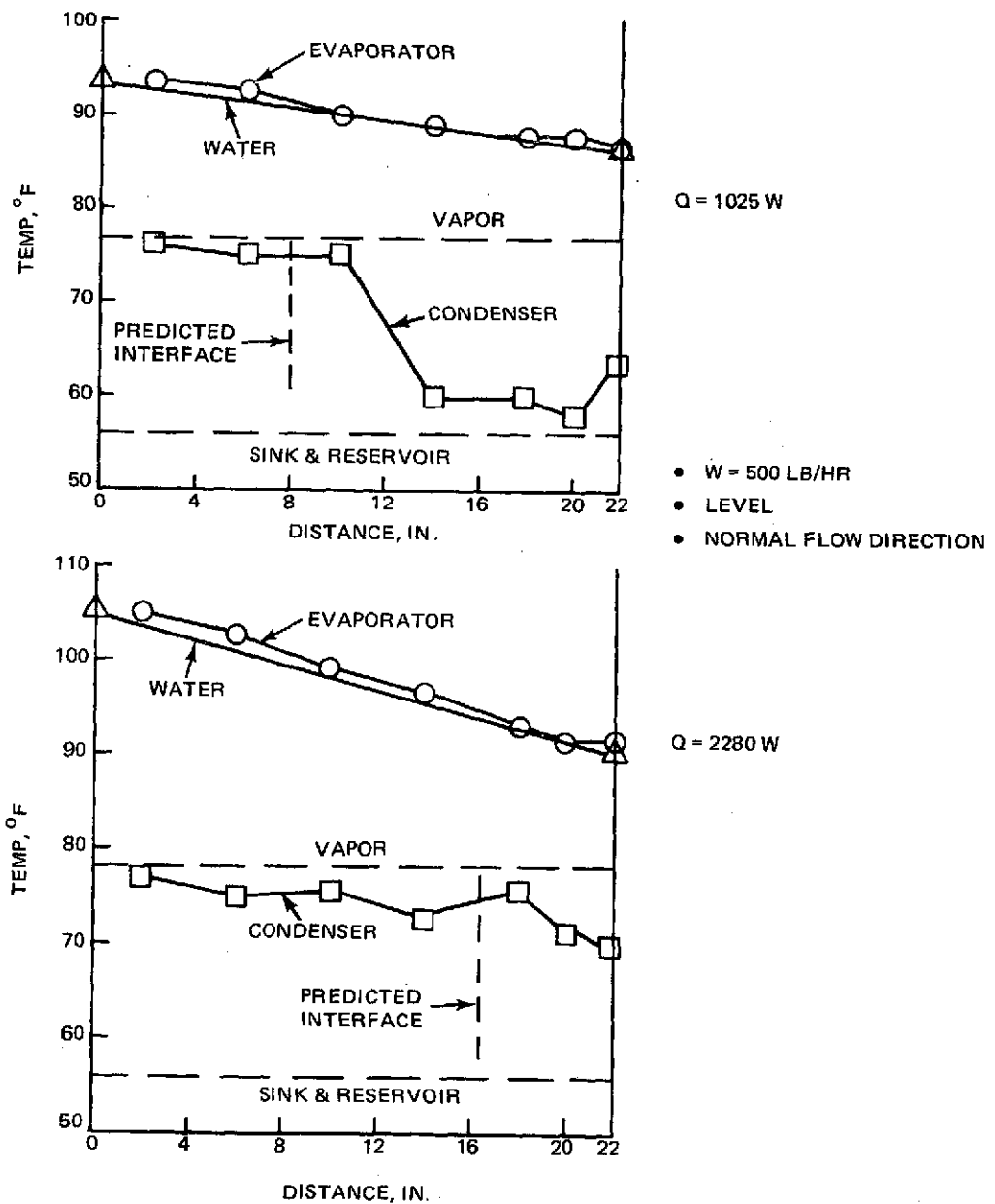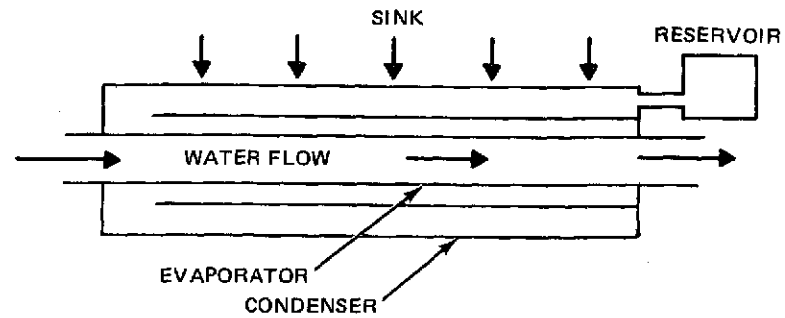
Figure 5-21. VCHP Temperature Distribution — Modified Design, Run 3V

The correlation is not precise, especially for the high power case where the interface is not clearly defined (as it is in the lower power profile) from the thermocouple data. An improved model, as well as a better understanding of how the interface varies along the condenser surface, is needed. For example, in the 1025-w profile of Figure 5-21, it may be possible that undetected pockets of nitrogen are trapped within the "active" condenser portion, thereby making the interface appear closer to the reservoir than it should.

To sum up, the modified cylindrical transverse header with the finned heat-transfer surface and Teflon-lined baffle performed measureably better, providing a flatter-fluid-temperature response and reduced shutdown losses. Table 5-5 summarizes the performance characteristics of both header configurations at a flow rate of 500 lb/hr and a sink/reservoir temperature of $55°F$.

Performance of the modified transverse header at flow rates of 150, 350, 650 and 800 lb/hr are shown in Figures 5-22 to 5-25, respectively. (Performance at 500 lb/hr was already presented in Figure 5-17). Within the working-load range, the vapor temperature is relatively constant for all flow rates. Furthermore, the outlet temperature profiles are similar, regardless of flow rate, as was predicted earlier in paragraph 4.2.3. This is shown in Table 5-6, which lists the outlet temperatures at two loads for the different flow rates tested.

The sharp sudden increase in fluid temperatures, dramatically illustrated in Figures 5-22 and 5-23, is an indication that partial dryout has occurred. The maximum VCHP dryout loads obtained for the various flow rates are shown in Table 5-6 and compared to the highest test values achieved with the single-fluid heat pipe (SFHP). Although dryout data for the single-fluid tests were not obtained, the comparison gives some idea of the decrease in load in the VCHP mode. In addition, for flow rates of 150, 350 and 800 lb/hr, the VCHP dryout values are about 0.5 kw lower than would be predicted from the analysis. This represents a degradation of about 15%, which is in general agreement with values in the table.

Figure 5-26 shows the effect of operating at a higher sink and reservoir temperature. Raising the reservoir temperature by $20°F$ results in an increase in outlet temperature of about $13°F$. This is because raising the reservoir temperature increases the pipe pressure, resulting in an upward shift in the operating temperature (vapor) of the pipe.

Figure 5-27 examines the effect of tilt on VCHP performance for a flow rate of 500 lb/hr. Unlike the single-fluid data of Figure 5-15, which showed no change, the VCHP data shows a somewhat lower dryout point at both the + 1/2 and - 1/2-in. tilts, compared to the level orientation.

Table 5-5. Performance Characteristics of Variable-Conductance Cylindrical Transverse Header

Parameters	Header Configuration			
	Unmodified		Modified***	
● Effectiveness	0.45	(0.37)*	0.63	(0.67)
● Maximum Load, W	2,600**		3,600	(3,400)
● Temperature Control Between 400 and 2600 W				
ΔT_{Vapor}, °F	3	(2)	2	(1)
ΔT_{Outlet}, °F	21	(25)	9	(9)
● Estimated Shutoff Losses, W	350		150	

*Values in parenthesis are predicted
**Dryout not reached
***Teflon-Lined Baffle, Finned Hx Surface
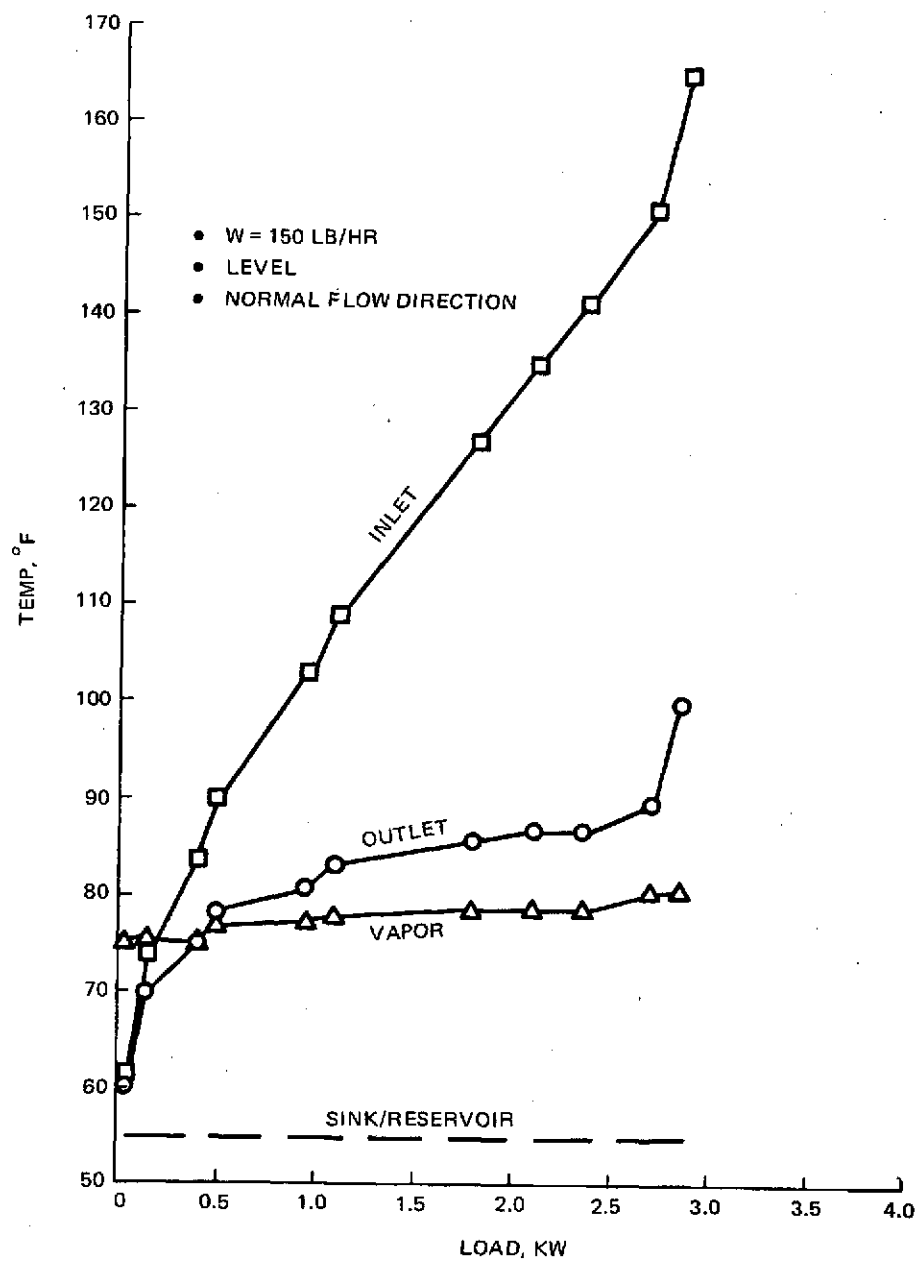
Figure 5-22. VCHP Performance — Modified Design, Run 1V
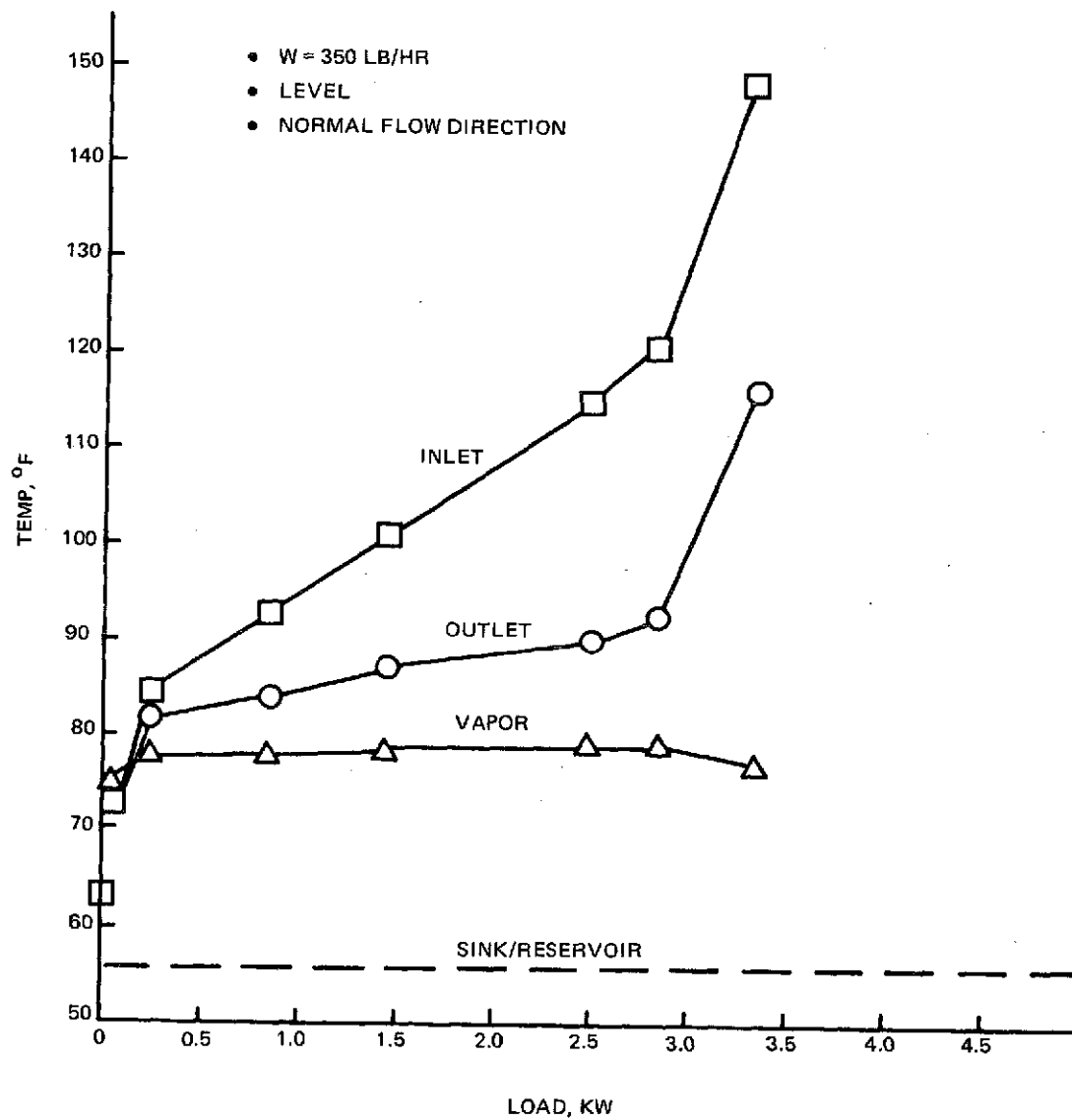
Figure 5-23. VCHP Performance — Modified Design, Run 2V
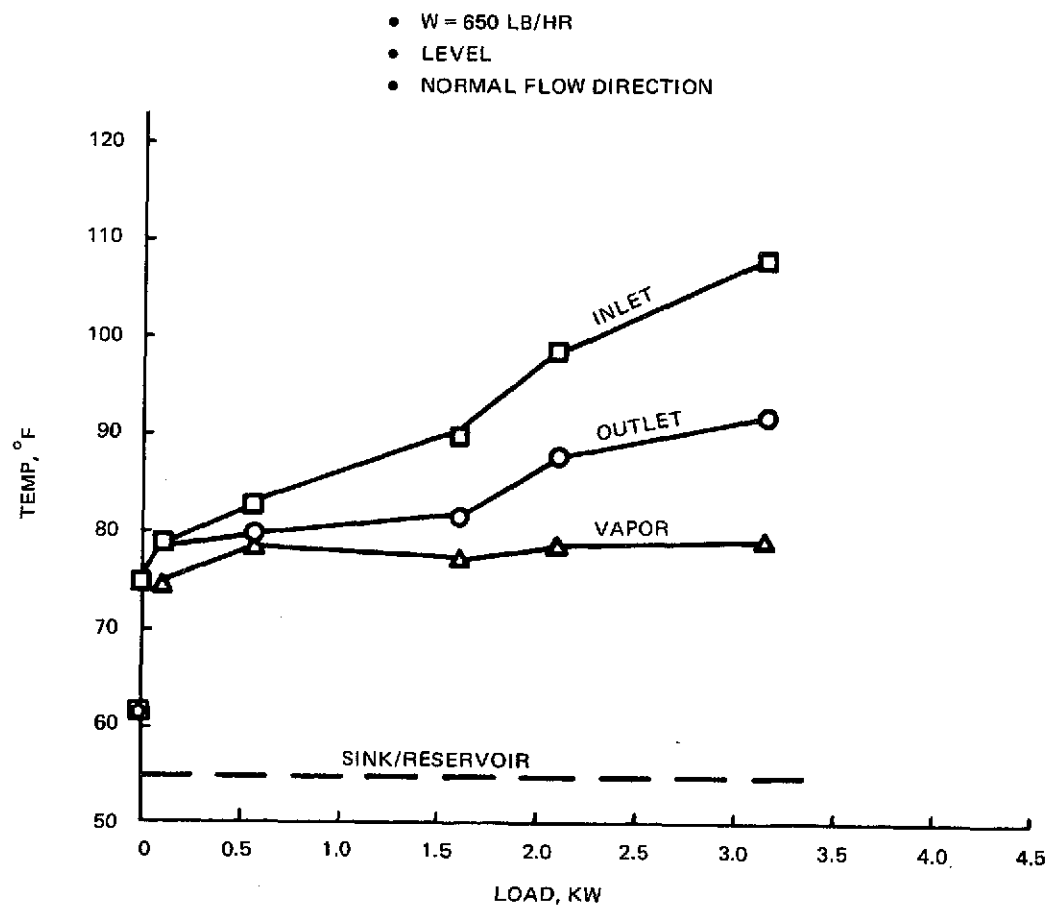
Figure 5-24. VCHP Performance — Modified Design, Run 4V
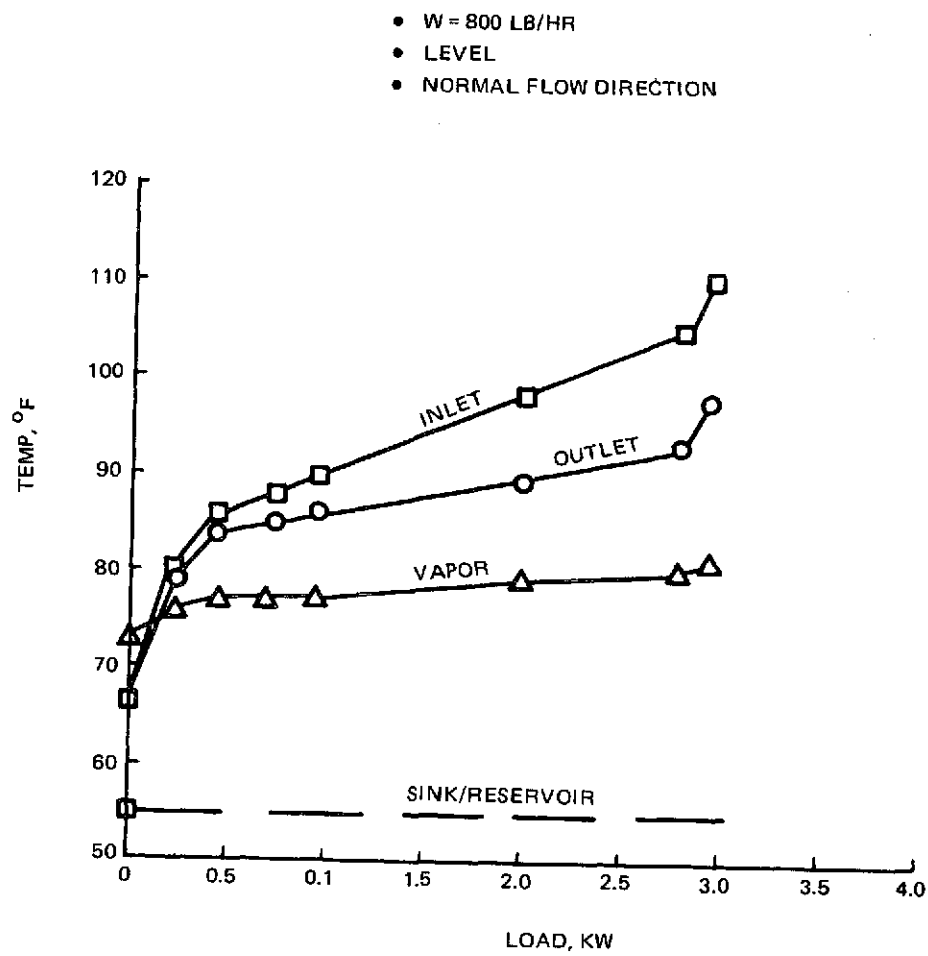
Figure 5-25. VCHP Performance — Modified Design, Run 5V

Table 5-6. Performance of Modified Transverse Header

Flow Rate, Lb/Hr	T_{out}, °F		ΔT_{out}, °F	Max VCHP Load at Dryout, Kw	Max SFHP Load Tested,* Kw	Decrease in Load, %
	2,600 W	400 W				
150	89	76	13	2.70	2.80	4
350	90	82	8	2.85	3.80	25
500	92	83	9	3.65	3.90	6
650	90	79	11	3.15*	3.40	—
800	92	83	9	2.80	3.60	22

*Dry out not reached

- LEVEL
- NORMAL FLOW DIRECTION
- W = 500 LB/HR

O SINK/RES TEMPERATURE = 75°F, RUN 7V
□ SINK/RES TEMPERATURE = 55°F, RUN 3V
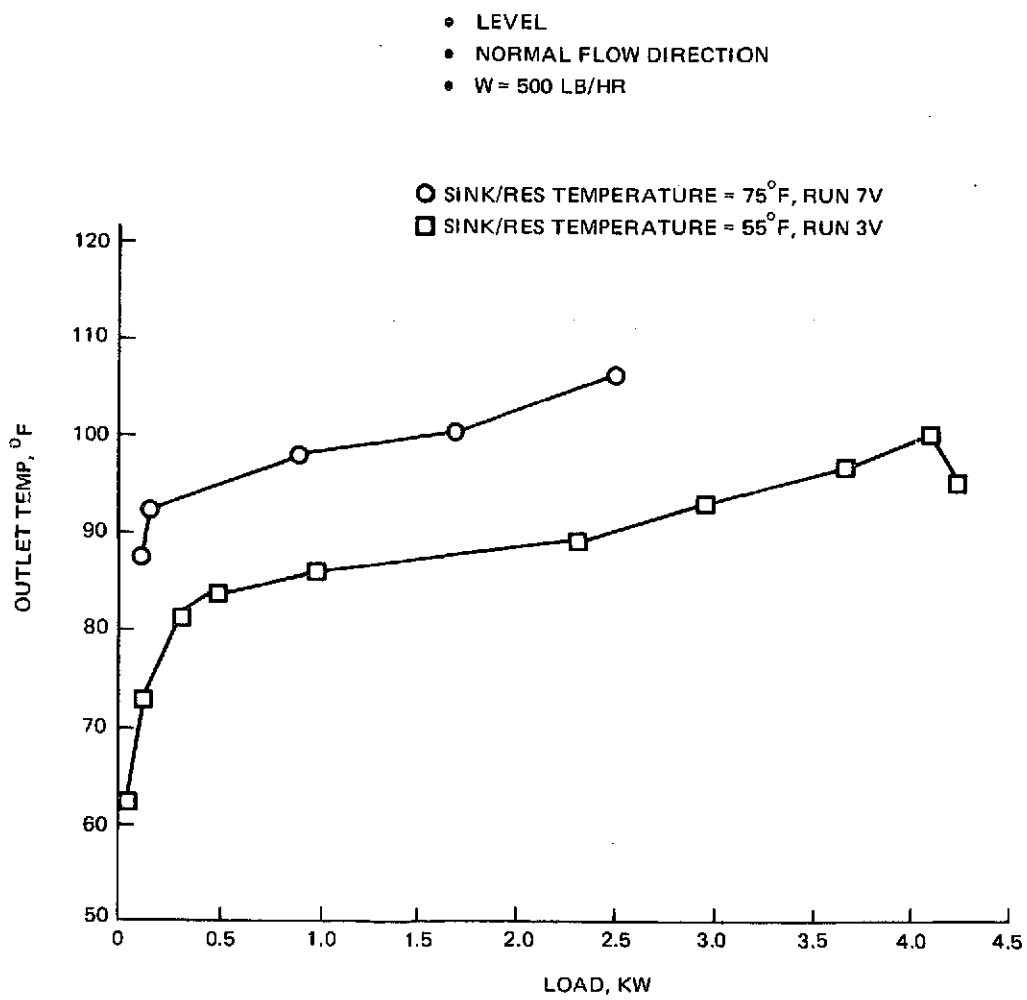
Figure 5-26. Effect of Sink/Reservoir Temperature on VCHP Performance

5-42

- NORMAL FLOW DIRECTION
- SINK/RESERVOIR = $55°F$
- W = 500 LB/HR

O	−1/2-INCH TILT, RUN 9V
△	+ 1/2-INCH TILT, RUN 10V
▢	LEVEL, RUN 3V
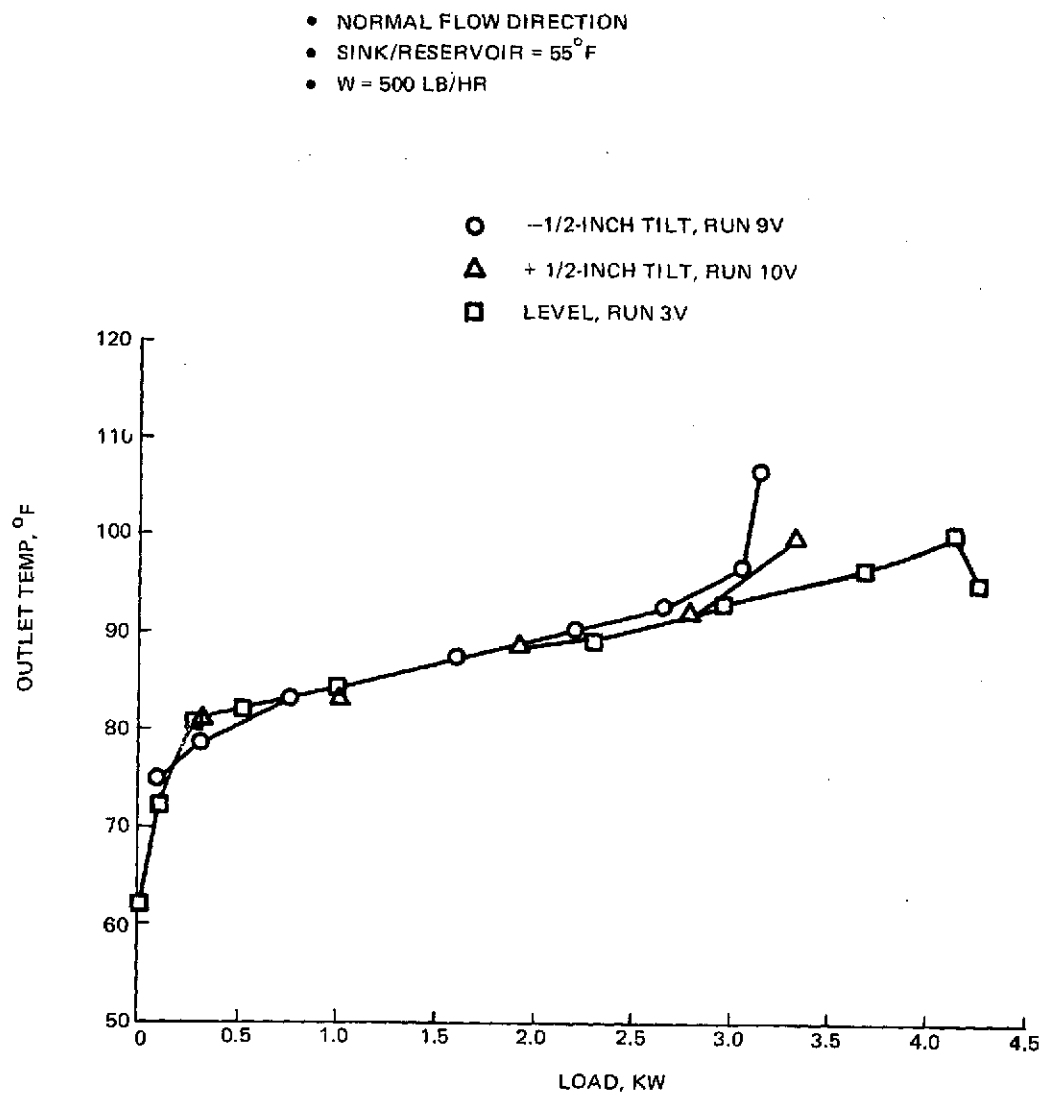
Figure 5-27. Effect of Tilt on VCHP Performance

The effect of reverse flow on VCHP performance for a flow rate 500 lb/hr is shown in Figure 5-28. The lower dryout during reverse flow exhibited here is typical of the other two reverse flow runs at 150 lb/hr (run 1V) and 800 lb/hr (run 5V). It is postulated that a greater liquid ammonia pressure drop in the axial direction is responsible. This comes about because the highest evaporation rates occur on the right side, closest to the reservoir (flow entrance), which is furthest from the condenser region on the left side. Thus, there is a longer liquid ammonia flow-path for reverse flow compared to the normal flow case.

5.4 SUMMARY OF TEST RESULTS

1. The cylindrical transverse header VCHP with the finned heat-transfer surface and Teflon-lined baffle demonstrated good vapor temperature control ($\Delta T_v = 2°$ F) and outlet fluid temperature control ($\Delta T_{out} = 9°$ F) over a wide power range (400 to 2,600 w).

2. Good temperature control was also obtained over a wide range of water flow rates from 150 to 800 lb/hr.

3. Shutoff losses were approximately 150 w, with a source temperature (80° F)-to-sink temperature (55° F) differential of 25° F.

4. The maximum load achieved without dryout as a VCHP was 3,600 w at a water flow rate of 500 lb/hr. At other flow rates between 150 and 800 lb/hr, the lowest dryout point tested was 2,700 w.

5. Approximately 15% lower capabilities were observed in the VCHP mode compared to the single-fluid mode.

6. In the VCHP mode, capabilities at ± 1/2-in. tilt were about 600 w lower than the level orientation.

7. In the VCHP mode, when the water flow direction was reversed, capacities were approximately 1,000 w lower than the normal flow direction.
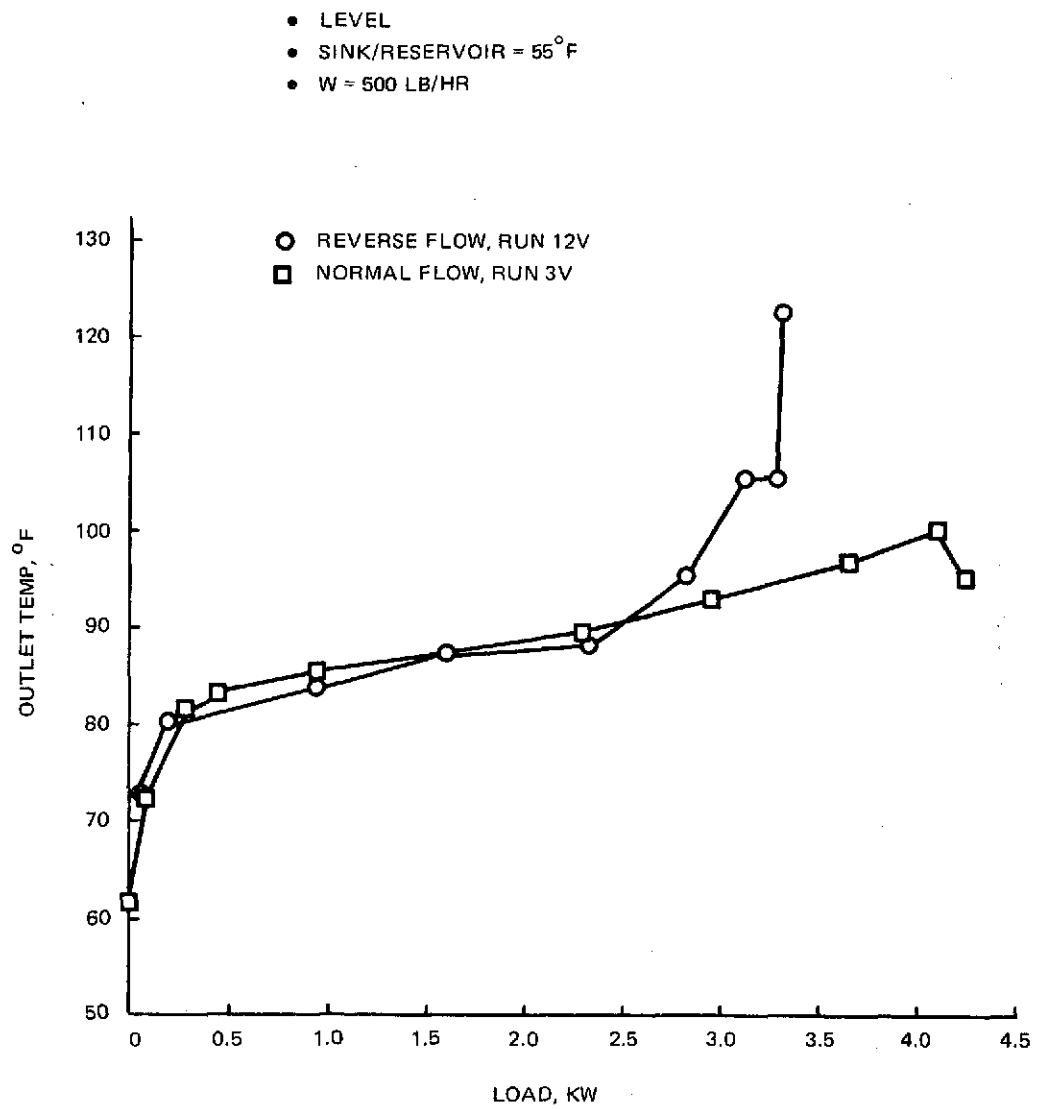
Figure 5-28. Effect of Reverse Flow on VCHP Performance

Section 6

APPLICATION STUDIES

The variable-conductance transverse header is a pipe whose primary function is to control, rather than transport, thermal energy. One such application is to use the VCHP transverse header coupled to a large-capacity heat-pipe radiator to provide a no-moving-part, self-regulating control system that does not require bypass valves, pumps, etc. A second rather unique application that features automatic temperature control, isothermalization and direct radiation of waste heat, makes use of the transverse header concept to provide a flat mounting plate for electronics.

In this section these two applications will be described. Primary emphasis has been placed on utilization of the transverse concept to meet practical spacecraft thermal-control requirements, not obtainable with more conventional thermal-control hardware.

6.1 HEAT-PIPE RADIATOR HEADER

One of the more attractive methods to achieve fluid temperature control in a heat-pipe radiator is the use of a variable-conductance heat-pipe header attached to a radiator composed of single-fluid heat pipes. This system provides competitive radiator performance for the high-kilowatt capacities that will be required in future missions. Table 6-1 lists typical system radiator requirements currently being planned for future payloads (Ref 12).

For this application, a transverse variable-conductance heat pipe could be used for the header. Figure 6-1a shows how the header would be used directly with the fluid-loop heat source which is pumped outside the spacecraft to the radiator. This panel represents one of many that would be combined in series and/or parallel to meet the necessary system capacity. If it is desired to keep the fluid within the confines of the spacecraft, a transport heat pipe can be used to couple the fluid to the transverse header as shown in Fig. 6-1b. This pipe would be a high-capacity, single-fluid arterial design which has already demonstrated large capacities.

Adaption of the cylindrical transverse header to a heat-pipe radiator is depicted in Figure 6-2. The transverse header is positioned between two heat-pipe radiator panels, rather than mounted on the edge of the panel. This results in more efficient use of the header condenser area. In addition, the mid-panel arrangement results in a lower load/unit length of feeder-evaporator surface, with a corresponding reduction in temperature drop.

Table 6-1. Typical Requirements for Large Spacecraft Systems

- Net Heat Rejection

  — Maximum Load : 22,000 W

  — Minimum Load : 2,000 W

- Absorbed Environmental Heat Flux

  — Maximum: 60 Btu/Hr-Ft^2

  — Minimum: 25 Btu/Hr-Ft^2

- Fluid Loop

  — Fluid: Freon-21

  — Flow Rate: 500 to 2,000 Lb/Hr

  — Temperature
    - Inlet (variable) : 42 to 150°F
    - Outlet : 40°F

SPACECRAFT

INTERIOR ⟵ ⟹ EXTERIOR

TRANSVERSE HEADER

OUTLET

FLUID

INLET

HEAT-PIPE
RADIATOR
PANEL

a. PUMP FLUID DIRECTLY TO RADIATOR

FLUID
OUTLET   INLET   TRANSPORT HEAT-PIPE   TRANSVERSE HEADER

FLUID/HEAT-PIPE HX

HEAT-PIPE
RADIATOR
PANEL

b. USE TRANSPORT HEAT PIPE TO CARRY LOAD TO RADIATOR
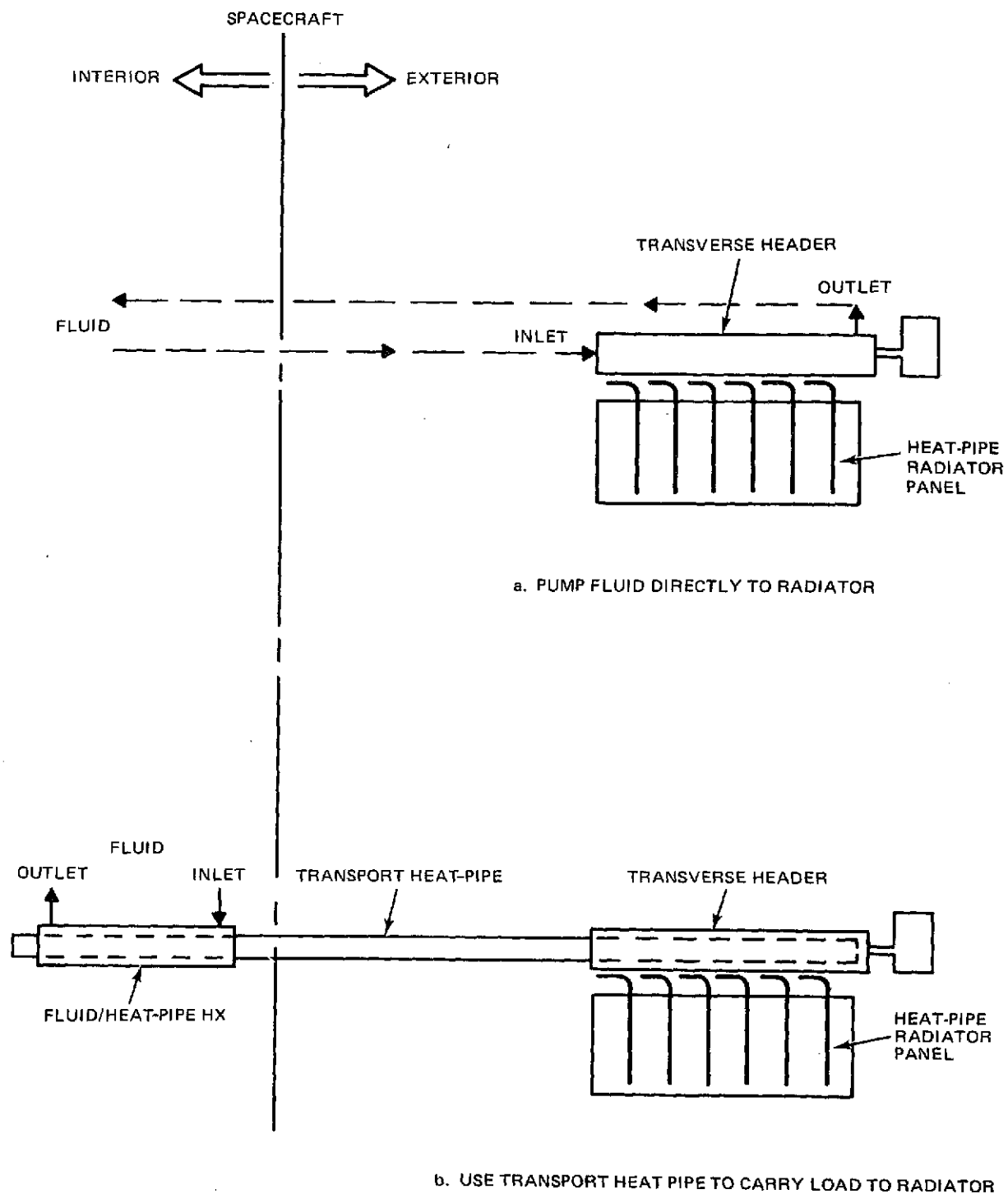
Figure 6-1. Transverse Header/Heat-Pipe Radiator

TRANSVERSE
HEADER

TRANSPORT
HEAT PIPE

COUPLE TRANSVERSE HEADER
TO A REMOTE HEAT SOURCE VIA
A TRANSPORT HEAT PIPE

FEEDER HEAT PIPE (2)
(EVAP SECT)

TRANSVERSE
HEADER
O.D.

HEADER/FEEDER CLAMPING
INTERFACE TECHNIQUE

RADIATOR PANEL (2)

FEEDER HEAT PIPES

NONCONDENSIBLE
GAS RESERVOIR

TO RETURN
COOLANT LOOP

COUPLE TRANSVERSE HEADER
TO FLUID HEAT SOURCE

INLET ~ FLUID
HEAT SOURCE
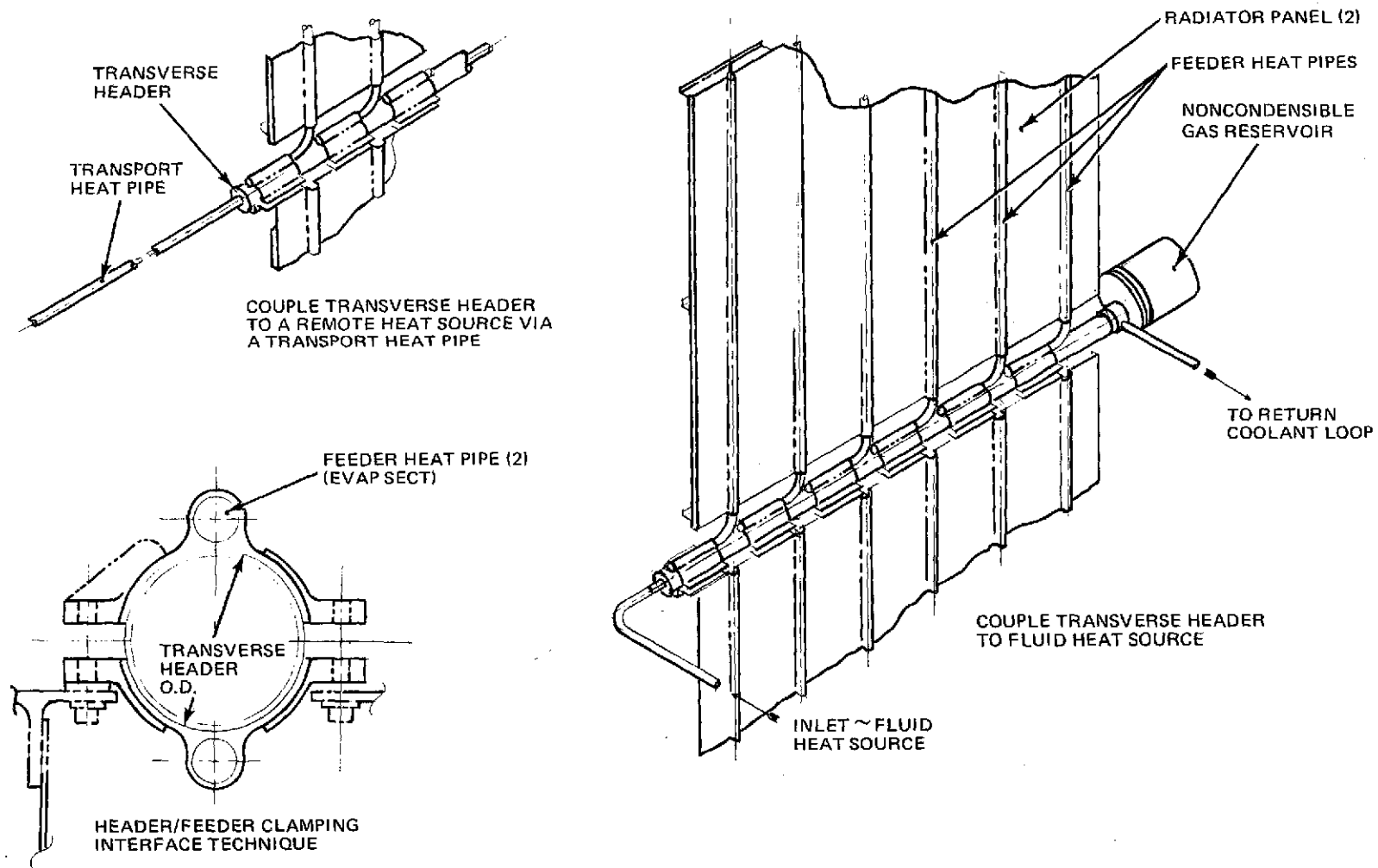
Figure 6-2. Transverse Header/Heat-Pipe Radiator

Preliminary estimates, based on the requirements in Table 6-1, indicate the maximum heat-rejection capability of the radiator would be approximately 23 w/ft^2 for a 0.020-in. thick aluminum radiator with 10.6-in. heat-pipe spacing. Its weight is estimated to be about 0.7 lb/ft^2, resulting in a specific power of 33 w/lb. The overall area of a unit radiator is typically 75 ft^2. As shown in Figure 6-2, a transport heat pipe could also be used to provide the load to the radiator.

6.2 VARIABLE-CONDUCTANCE PLATE

Up to now the majority of thermal control techniques used for heat-dissipating electronic boxes have been one of the following:

1. Convection-cooled: equipment mounted in pressurized cabin area

2. Cold Plate-cooled: equipment mounted on cold plates cooled by a circulating coolant

3. Radiation-cooled: equipment mounted on a heat-sink plate which radiates either through a louver (see Figure 6-3a) or to a reradiating skin (see Figure 6-3b)

In addition, recently developed heat-pipe hardware has been used on an experimental basis to provide equipment temperature control. These include variable-conductance and diode heat pipes (flown on OAO-C, and ATS-F Spacecrafts) and a heat-pipe plate or conditioning panel. The last item, developed by MSFC, is a 30-in. by 30-in. isothermalizing panel on which electronic equipment is mounted. Waste heat is conducted into the panel, removed either by a coolant loop, sublimator, heat pipe, etc., and ultimately rejected to space. (See Figure 6-3c.)

Using the transverse header principle, an improvement to the heat-pipe panel can also be obtained by providing built-in temperature control for the electronics and direct radiation of waste heat to space. This is shown schematically in Figure 6-4. The mounting plate, called a variable-conductance plate (VCP), permits equipment to be mounted to only one side. Waste heat is heat-piped to the other side, where it is radiated directly to space. This surface is provided with conventional radiator coatings, silver-backed Teflon, OSR's, etc. Unlike the thermal conditioning panel, the VCP uses gas-controlled, transverse-type heat pipes to regulate the temperature of the electronics. Thus, the VCP not only provides the advantages of a heat-pipe conditioning panel (central mounting location, load sharing, uniform temperature, etc.), but provides temperature control of electronics and can dissipate waste heat directly to space.

EQUIPMENT

SPACE

LOUVER

INSULATED
AREA
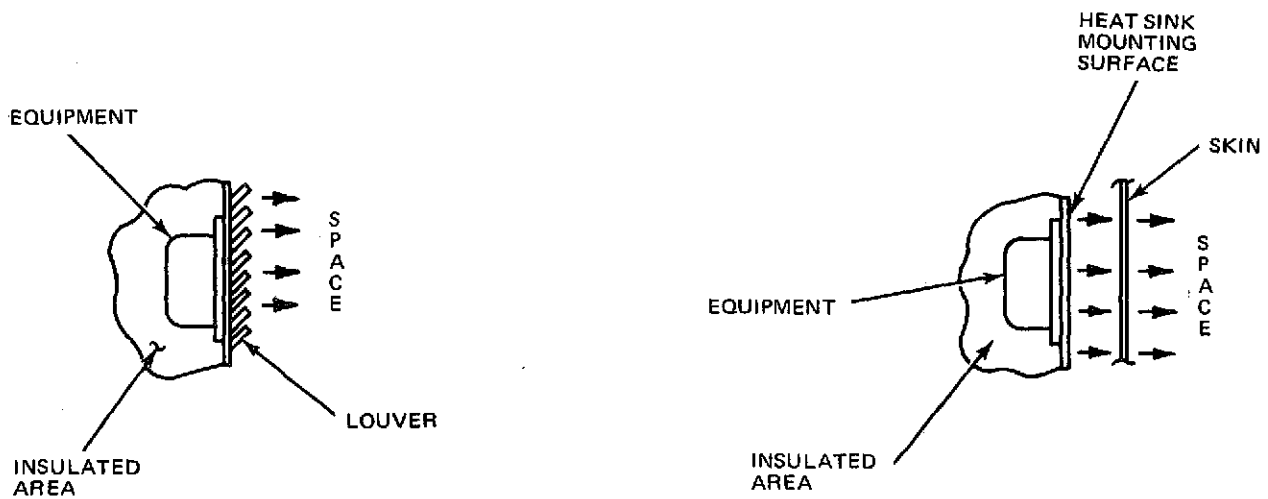
a. Louvers, Direct Radiation to Space

HEAT SINK
MOUNTING
SURFACE

SKIN

EQUIPMENT

SPACE

INSULATED
AREA

b. Radiation Coupling

EQUIPMENT

HEAT-PIPE
PLATE

TRANSPORT
• HEAT PIPE
• VCHP
• COOLANT

HEAT REJECTION
• VCHP RADIATOR
• HEAT-PIPE RADIATOR
• PUMPED RADIATOR
• BOILER SUBLIMATOR
• LOUVER
• SKIN
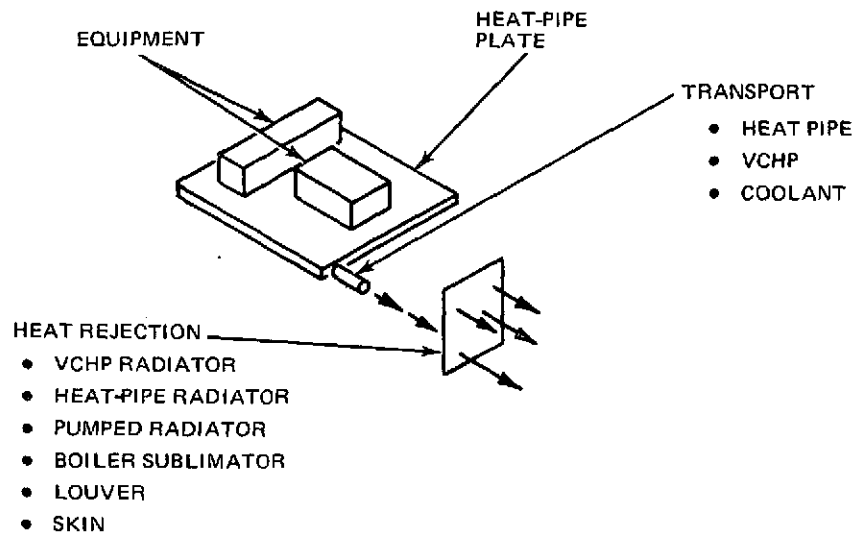
c. Thermal Conditioning Panel

Figure 6-3. Equipment Thermal Control Techniques

6-6

VEHICLE
STRUCTURE

VARIABLE-
CONDUCTANCE
PLATE

DIRECT
RADIATION
TO
SPACE

ELECTRONICS
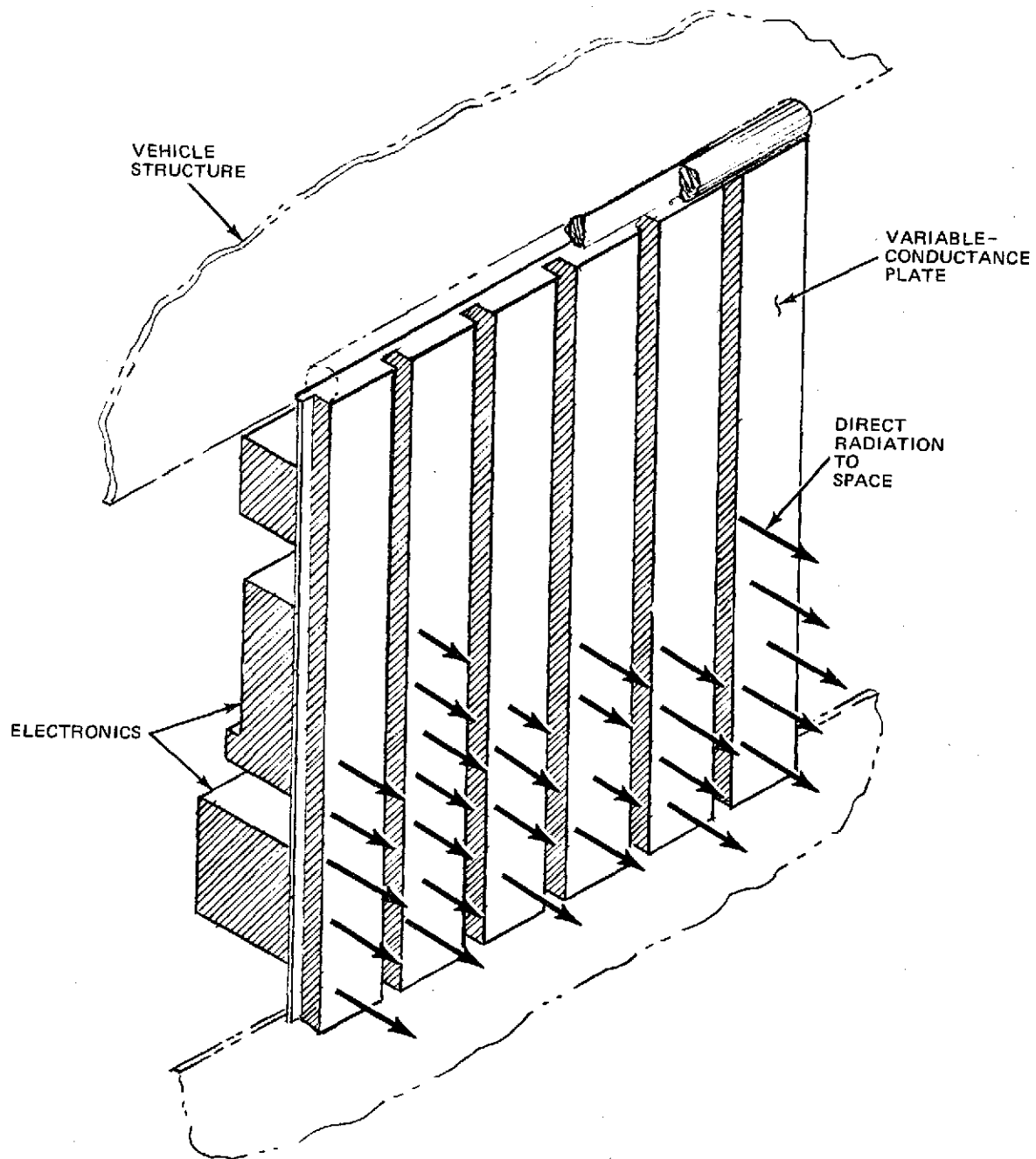
Figure 6-4. Variable-Conductance Plate

Functionally, the variable-conductance plate acts in much the same way as a conventional louver. However, it has the potential of being cheaper, lighter, and more reliable (no moving parts) than the louver. Unlike the VCP, the louver is sensitive to direct solar impingement and may require a secondary radiator (used, for example on OAO) or impose orientation constraints on the vehicle. Other benefits of the VCP in terms of its potential application to upcoming NASA programs include:

1. The VCP can be made in modular size units, e.g., 4 ft by 4 ft, which can be coupled together to form larger panels, 4 ft by 8 ft, 8 ft by 8 ft, etc., for central location of common avionics subsystems.

2. Because of its heat-pipe construction, the VCP provides an isothermal mounting surface.

3. Standardized equipment mounting points can be provided, e.g., 4-in. centers.

4. Both the shutoff capability and the load-sharing features of the panel will minimize "stay-alive" heater requirements.

5. Panel temperature control is provided by "noncondensible" gas. Control range can be adjusted by changing the gas charge.

6. The panel, which is a self-contained device, can be used to accommodate add-on equipment with minimum vehicle impact.

Section 7

PROGRAM CONCLUSIONS AND RECOMMENDATIONS

Pertinent conclusions derived from this work are:

1. A transverse header that provides large-capacity, variable-conductance control not previously obtainable with conventional VCHP's has been built and tested. Loads as high as 3,600 w were obtained in the VCHP mode without interference from the noncondensible control gas.

2. The transverse header exhibited only slightly lower capacity in the VCHP mode than in the single-fluid mode.

3. As with conventional gas-loaded pipes, constant, predictable, vapor-temperature control has been obtained.

4. For the conditions tested, shutdown losses averaged about 150 w, yielding a turndown ratio of about 20 to 1. If required, lower losses can be achieved with future design modifications.

5. Two spacecraft applications have been identified using the transverse principle – a VCHP header used in conjunction with a heat-pipe radiator, and a variable-conductance mounting plate for thermal control of electronic boxes.

Having demonstrated the feasibility of the transverse header in a practical configuration, it is suggested that additional effort be applied to better understand and improve its performance:

1. Evaluate means of further controlling shutdown losses, particularly for longer units that would couple to a radiator.

    a. Investigate use of other working fluids and control gases

    b. Redesign evaporator/condenser/baffle regions for minimal losses

2. Investigate the formation and removal of spurious gas pockets that may be present in the active condenser region.

Section 8

REFERENCES

1. "Large Variable-Conductance Heat Pipe, Final Report: Tunnel Artery Heat Pipe", Grumman Aerospace Corporation, March 1973, NASA Contract NAS 8-27793.

2. Kosson, R., Hembach, R., Edelstein, F., and Loose, J., "Development of a High-Capacity, Variable-Conductance Heat Pipe," AIAA Paper No. 73-728, July, 1973.

3. Saaski E. W., "Gas Occlusion in Arterial Heat-Pipes," Progress in Astronautics and Aeronautics, Volume 35, Thermophysics and Spacecraft Thermal Control, pp. 353-370, MIT Press.

4. Edelstein, F., Roukis, J.G., and Loose, J. D., "Development of a 150,000 Watt-Inch Variable-Conductance Heat Pipe for Space Vehicle Thermal Control", ASME Paper No. 72-ENAV-14 (1972).

5. Eninger, J.E., "Menisci Coalesence as a Mechanism for Venting Noncondensible Gas From Heat-Pipe Arteries", AIAA Paper No. 74-748.

6. Marcus, B.D., Edwards, D.K., and Anderson, W.T., "Variable-Conductance Heat-Pipe Technology Research Report No. 4," NASA Space CR-114686, December 1973.

7. Mock, P.R., Marcus, B.D., and Edelman, E.A., "Communications Technology Satellite: A Variable-Conductance Heat-Pipe Application", AIAA Paper No. 74-749.

8. Scallon, T.R. Jr., "Heat-Pipe Thermal Control System Concept for the Space Station", AIAA 7th Thermophysics Conference 72-261, 1972.

9. Tawil, M., et. al., "Heat-Pipe Applications for the Space Shuttle", AIAA 7th Thermophysics Conference, 72-272, 1972.

10. Kays, W., and London, A.L., Compact Heat Exchangers, McGraw-Hill, 1964.

11. Kreith, F. Principles of Heat Transfer, International Textbook Company, 1965.

12. Modular Heat-Pipe Radiator, NASA Contract NAS 9-14100.

Appendix A

SYSTEMS THERMAL MODEL PROGRAM

INPUT DATA-TRANSVERSE HEADER

NSEC =	KVAP =	R =	TAU =						
5	1	55.000	0.200						
D1 =	XL1 =	D2 =	XL2 =	D3 =	XL3 =	D4 =	XL4 =	D5 =	XL5 =
1.108	22.300	1.108	0.100	1.108	22.300	1.108	2.000	4.500	7.480
VRX =	XMRX =	W =	CF =	FLUK =	FLUMU =	FLOWA =	WPER =	AFINR =	XLHX =
118.900	0.018	800.000	1.000	0.353	2.081	0.129	7.775	0.389	22.300
AHEVAP =	AHCOND =	ASPRAY =							
69.120	128.880	144.000							
HHEVAP =	HHCON =	HSPRAY =	HFLU =						
2000.000	3260.000	600.000	-1.000						
TIN =	TSINK =	TRES =							
110.000	55.000	55.000							

FINNED HEAT EXCHANGER

OUTPUT SECTION PERFORMANCE(TEMP=DEGF,Q=WATTS)

TEMP OUT	HTEX EFCT	VAPOR TEMP	INTERFACE LOC	Q TOTAL	PVAP (PSIA)	PRES (PSIA)	TRES
94.178	0.585	82.964	22.300	3709.746	0.1608E 03	0.9808E 02	55.000

TEMPS (DEG F),HFLU(BTU/HR.FT**2.DEGF.)

INLET TEMP	HDR VAPOR	HDR COND	SINK TEMP	HFLU
110.000	82.964	78.626	55.000	2941.315

HEAT EXCH EFFECTIVENESS=   0.585
REYNOLDS NO.=   2373.558

```
C TRANVERSE HEADER PROGRAM                                      TRA00010
      DIMENSION D(10),XL(10),T(10),P(10),PPN(10),A(10)          TRA00020
C READ VCHP HEADER INFO                                         TRA00030
      MR=2                                                      TRA00040
      NR=5                                                      TRA00050
      MW=6                                                      TRA00060
  538 READ(MR,10)NSEC,KVAP                                      TRA00070
      READ(MR,16)R                                              TRA00080
   10 FORMAT(8I2)                                               TRA00090
      READ(MR,16)(D(J),XL(J),J=1,NSEC)                          TRA00100
   16 FORMAT(2F10.4)                                            TRA00110
      READ(MR,16)VRX,XMRX                                       TRA00120
      READ(MR,11)W,CP,FLUK,FLUMU                                TRA00130
C READ FLUID DATA                                               TRA00140
C READ HEAT EXCHANGER DATA                                      TRA00150
      READ(MR,11)FLOWA,WPER,AFINR,XLHX,WPERHX,AFNRHX            TRA00160
C READ AREAS                                                    TRA00170
      READ(MR,11)AHEVAP,AHCOND,ASPRAY                           TRA00180
C READ CONDUCTANES                                              TRA00190
      READ(MR,11)HHEVAP,HHCON,HSPRAY,HFLU                       TRA00200
   11 FORMAT(8E10.4)                                            TRA00210
C READ SYSTEM INPUTS                                            TRA00220
      READ(MR,11)TIN,TSINK,TRES,TAU                             TRA00230
  537 CONTINUE                                                  TRA00240
C WRITE INPUT DATA                                              TRA00250
      WRITE(3,3)                                                TRA00260
    3 FORMAT(1H0,11X,'INPUT DATA-TRANSVERSE HEADER',///)        TRA00270
      WRITE(MW,3)                                               TRA00280
      WRITE(MW,20)W,CP,TIN,TSINK,TRES,TAU                       TRA00290
   20 FORMAT(5X,'W =',F10.3,3X,'CP =',F10.3,3X,'TIN =',F10.3,3X,'TSINK =TRA00300
     A',F10.3,/,5X,'TRES =',F10.3,3X,'TAU =',F10.3)             TRA00310
      WRITE(3,21)                                               TRA00320
   21 FORMAT(4X,'NSEC =',4X,'KVAP =',7X,'R =',5X,'TAU =')       TRA00330
      WRITE(3,9)NSEC,KVAP,R,TAU                                 TRA00340
    9 FORMAT(2I10,2F10.3)                                       TRA00350
      WRITE(3,22)                                               TRA00360
   22 FORMAT(6X,'D1 =',5X,'XL1 =',6X,'D2 =',5X,'XL2 =',6X,'D3 =',5X,'XL3TRA00370
     A =',6X,'D4 =',5X,'XL4 =',6X,'D5 =',5X,'XL5 =')            TRA00380
      WRITE(3,23)(D(J),XL(J),J=1,NSEC)                          TRA00390
   23 FORMAT(10F10.3)                                           TRA00400
      WRITE(3,24)                                               TRA00410
      WRITE(3,23)VRX,XMRX,W,CP,FLUK,FLUMU,FLOWA,WPER,AFINR,XLHX  TRA00420
   24 FORMAT(5X,'VRX =',4X,'XMRX =',7X,'W =',6X,'CP =',4X,'FLUK =',3X,'FTRA00430
     ALUMU =',3X,'FLOWA =',4X,'WPER =',3X,'AFINR =',4X,'XLHX =')  TRA00440
      WRITE(3,25)                                               TRA00450
   25 FORMAT(2X,'AHEVAP =',2X,'AHCOND =',2X,'ASPRAY =',2X,'WPERHX=',2X,'TRA00460
     AAFNRHX =')                                                TRA00470
      WRITE(3,23)AHEVAP,AHCOND,ASPRAY,WPERHX,AFNRHX             TRA00480
      WRITE(3,27)                                               TRA00490
   27 FORMAT(2X,'HHEVAP =',3X,'HHCON =',2X,'HSPRAY =',4X,'HFLU =')  TRA00500
      WRITE(3,23)HHEVAP,HHCON,HSPRAY,HFLU                       TRA00510
      WRITE(3,29)                                               TRA00520
   29 FORMAT(5X,'TIN =',3X,'TSINK =',4X,'TRES =')               TRA00530
      WRITE(3,23)TIN,TSINK,TRES                                 TRA00540
C HEAT EXCHANGER CALCULATIONS                                   TRA00550
```

```
      DHYD=4.*FLOWA/WPER                                    TRA00560
      G=W/FLOWA                                             TRA00570
      RE=DHYD*G*12./FLUMU                                   TRA00580
      PR=FLUMU*CP/FLUK                                      TRA00590
C COLBURN J-FACTOR CURVE FIT FROM KAYS + LONDON DATA        TRA00600
      IF(HFLU)700,701,702                                   TRA00610
  701 WRITE(MW,705)                                         TRA00620
      WRITE(3,705)                                          TRA00630
  705 FORMAT(1H0,20X,'UNFINNED HEAT EXCHANGER',//)          TRA00640
      IF(RE.GE.100..AND.RE.LT.2000.)CJ=.3165/RE**.662       TRA00650
      IF(RE.GE.2000..AND.RE.LE.10000.)GO TO 710             TRA00660
      GO TO 703                                             TRA00670
  710 HFLU=(.023*CP*G)/((RE**.20)*(PR**(2./3.)))            TRA00680
      GO TO 707                                             TRA00690
  703 WRITE(MW,704)                                         TRA00700
      WRITE(3,704)                                          TRA00710
  704 FORMAT(1H0,20X,'FINNED HEAT EXCHANGER',//)            TRA00720
      IF(200..LE.RE.AND.1500..GT.RE)CJ=.230/RE**.391        TRA00730
      IF(RE.GE.1500..AND.RE.LE.10000.)CJ=.2407/RE**.400     TRA00740
  703 HFLU=CJ*G*CP/PR**(2./3.)                              TRA00750
      GO TO 707                                             TRA00760
  702 WRITE(MW,706)                                         TRA00770
      WRITE(3,706)                                          TRA00780
  706 FORMAT(1H0,20X,'INPUTED VALUE FOR HFLU',//)           TRA00790
      IF(AFINR)850,850,851                                  TRA00800
  850 WRITE(MW,852)                                         TRA00810
      WRITE(3,852)                                          TRA00820
  852 FORMAT(1H0,20X,'UNFINNED HEAT EXCHANGER',//)          TRA00830
      GO TO 853                                             TRA00840
  851 WRITE(MW,854)                                         TRA00850
      WRITE(3,854)                                          TRA00860
  854 FORMAT(1H0,20X,'FINNED HEAT EXCHANGER',//)            TRA00870
  853 HFLUF=HFLU                                            TRA00880
      HFLU=HFLUF/144.                                       TRA00890
      GO TO 708                                             TRA00900
  707 HFLUF=HFLU*144.                                       TRA00910
C CALCULATE HX FIN EFFICIENCIES,ALUM FIN,HT.=.10 IN.,DELTA=.006 IN.  TRA00920
  708 XML=.05296*(HFLUF)**.5                                TRA00930
      ETAF=TANH(XML)/XML                                    TRA00940
      ETAO=1.-AFNRHX*(1.-ETAF)                              TRA00950
      UAO=ETAO*HFLU*WPERHX*XLHX                             TRA00960
C INTERMEDIATE CONDUCTANCE CALCULATIONS                     TRA00970
      XKHE=HHEVAP*AHEVAP/144.                               TRA00980
      XKHC=HHCON*AHCOND/144.                                TRA00990
      UAHX=1./(1./UAO + 1./XKHE)                            TRA01000
      ETAHX=1. - EXP(-UAHX/(W*CP))                          TRA01010
      XMR=XMRX                                              TRA01020
      VR=VRX                                                TRA01030
      QTOT=0.                                               TRA01040
      XFOLD=XL(7)/2.                                        TRA01050
  208 CONTINUE                                              TRA01060
      XC=XL(3)/2.                                           TRA01070
  206 Q=0.                                                  TRA01080
C HEAT TRANSFER CALCS                                       TRA01090
C DEFINE SECTION TEMPS                                      TRA01100
```

```
      202 T2=TIN-Q/(W*CP)                                               TRA01110
          TVAP=TIN-(TIN-T2)/ETAHX                                       TRA01120
          IF(XC)90,90,91                                                TRA01130
       90 THC=TVAP                                                      TRA01130
          GO TO 92                                                      TRA01140
       91 THC=TVAP - Q/(XKHC*(XC/XL(3)))                                TRA01150
          IF(THC.LE.TSINK)THC=TVAP                                      TRA01160
       92 T(1)=TVAP                                                     TRA01170
          T(2)=TVAP                                                     TRA01180
          T(3)=(TVAP+TRES)/2.                                           TRA01190
          T(4)=T(3)                                                     TRA01200
          T(5)=TRES                                                     TRA01210
C START DO LOOP FOR VAPOR PRESSURES(PSIA),TEMP = DEG F                  TRA01220
          DO 262  J=1,NSEC                                              TRA01230
          TY=T(J)                                                       TRA01240
          GO TO(251,252,253,254,255,255),KVAP                          TRA01250
C AMMONIA                                                               TRA01260
      251 PY=30.4024+.73634*TY+.007C843*TY**2+3.1669E-5*TY**3+5.273E-8*TY**4  TRA01270
          GO TO 260                                                     TRA01280
C METHAL ALCOHOL                                                        TRA01290
      252 PY=.17346+7.0203E-03*TY+1.1645E-04*TY**2+1.0408E-06*TY**3+8.734E-0  TRA01300
         A3*TY**4+8.8291E-11*TY**5+2.4425E-13*TY**6-3.8962E-15*TY**7-1.7009E  TRA01310
         8-17*TY**8+4.8223E-20*TY**9                                    TRA01320
          GO TO 260                                                     TRA01330
C FREON-21                                                              TRA01340
      253 PY=4.5763+.12483*TY+1.3944E-03*TY**2+7.5128E-06*TY**3+1.5607E-08*T  TRA01350
         AY**4-4.6709E-12*TY**5                                         TRA01360
          GO TO 260                                                     TRA01370
C ACETONE                                                               TRA01380
      254 PY=.46263+1.6375E-02*TY+2.5953E-04*TY**2+2.0810E-06*TY**3+2.8619E-  TRA01390
         A03*TY**4-4.7071E-11*TY**5+2.5721E-13*TY**6+3.4843E-15*TY**7    TRA01400
          GO TO 260                                                     TRA01410
      255 CONTINUE                                                      TRA01420
      260 P(J)=PY                                                       TRA01430
      262 CONTINUE                                                      TRA01440
C CALCULATES(PV/T) OF NITROGEN FOR EACH SECTION                        TRA01450
          CONT=3.14159/(4.*1728.)*144.                                 TRA01460
          DO 50  N=2,NSEC                                              TRA01470
          PPN(N)=P(1)-P(N)                                             TRA01480
       50 A(N)=PPN(N)*CONT*(D(N)**2)*XL(N)/(T(N)+460.)                 TRA01490
          NNS=NSEC-1                                                   TRA01500
          G=0.                                                         TRA01510
C SUM OF COLD GAS INVENTORY                                            TRA01520
          DO 65  I=2,NNS                                               TRA01530
       65 G=G+A(I)                                                     TRA01540
C MASS OF NITROGEN LESS SECTION 2                                      TRA01550
          HT1=G-A(2)                                                   TRA01560
          XLFT2=XL(2)                                                  TRA01570
C MASS OF NITROGEN LESS SECT 2 + 3                                     TRA01580
          HC=G-A(2)-A(3)                                               TRA01590
          I=NSEC                                                       TRA01600
C CHECK IF INTERFACE IN SECT 2                                         TRA01610
          IF(T(1)-T(2))180,180,96                                      TRA01620
       96 X1=XLFT2-(4.*12.*(T(2)+460.)*(XMR*R*(T(I)+460.)-HT1*(T(I)+460.)-    TRA01630
         A(P(1)-P(I))*VR/12.))/((P(1)-P(2))*3.14159*D(2)**2*(T(I)+460.))  TRA01640
                                                                       TRA01650
```

```
      IF(X1-XL(2))170,170,180                                    TRA01660
170   XC=T.                                                      TRA01670
      GO TO 120                                                  TRA01680
C INTERFACE IN CONDENSER                                         TRA01690
190   X2=XL(3)+XL(2)-(4.*12.*(T(3)+460.)*(XMR*R*(T(I)+460.)-HC*  TRA01700
     A(T(I)+460.)-(P(1)-P(I))*VR/12.))/((P(1)-P(3))*3.14159*D(3)**2*(T( TRA01710
     BI)+460.))                                                  TRA01720
      X2=(1.-TAU)*X2OLD+TAU*X2                                   TRA01720
      X2OLD=X2                                                   TRA01730
      IF(X2-XL(2)-XL(3))195,205,205                              TRA01740
195   XC=X2-XL(2)                                                TRA01750
      IF(XC)642,642,120                                          TRA01760
642   XC=0.                                                      TRA01770
      GO TO 120                                                  TRA01780
205   XC=XL(3)                                                   TRA01790
120   CONTINUE                                                   TRA01800
      QNEW=(HSPRAY/144.)*AHCOND*(XC/XL(3))*(THC-TSINK)           TRA01810
      IF(ABS(Q-QNEW)-30.)203,203,201                             TRA01820
201   Q=(1.-TAU)*Q+TAU*QNEW                                      TRA01830
      IF(ABS(Q)-150000.)202,202,204                              TRA01840
204   TAU=TAU/2.                                                 TRA01850
      GO TO 208                                                  TRA01860
203   QTOT=QTOT+Q                                                TRA01870
      QTOT=QTOT/3.412                                            TRA01880
      WRITE(3,7)                                                 TRA01890
      WRITE(MW,7)                                                TRA01900
7     FORMAT(1H0,21X,'OUTPUT SECTION PERFORMANCE(TEMP=DEGF,Q=WATTS)',//)TRA01910
      WRITE(3,19)                                                TRA01920
      WRITE(MW,19)                                               TRA01930
19    FORMAT(5X,'TEMP',6X,'HTEX',5X,'VAPOR',3X,'INTERFACE',7X,  TRA01940
     A'0',5X,'PVAP',9X,'PRES',/6X,'OUT',6X,'EFCT',6X,'TEMP',5X,'LOC',9X TRA01950
     B,'TOTAL',3X,'(PSIA)',7X,'(PSIA)',7X,'TRES',//)            TRA01960
      WRITE(3,60)T2,ETAHX,TVAP,XC,QTOT,P(1),P(5),TRES           TRA01970
      WRITE(MW,60)T2,ETAHX,TVAP,XC,QTOT,P(1),P(5),TRES          TRA01980
60    FORMAT(4F10.3,F13.3,2E12.4,F10.3/)                        TRA01990
      WRITE(3,61)                                                TRA02000
      WRITE(MW,61)                                               TRA02010
61    FORMAT(1H0,21X,'TEMPS (DEG F),HFLU(BTU/HR,FT**2,DEGF,)',//)TRA02020
      WRITE(3,62)                                                TRA02030
      WRITE(MW,62)                                               TRA02040
62    FORMAT(5X,'INLET',7X,'HDR',7X,'HDR',6                     TRA02050
     AX,'SINK',/6X,'TEMP',5X,'VAPOR',6X,'COND',6X,'TEMP',6X,'HFLU',/)  TRA02060
      WRITE(3,63)TIN,TVAP,THC,TSINK,HFLUF                        TRA02070
      WRITE(MW,63)TIN,TVAP,THC,TSINK,HFLUF                       TRA02080
63    FORMAT(5F10.3/)                                            TRA02090
      WRITE(3,64)ETAHX,RE                                        TRA02100
      WRITE(MW,64)ETAHX,RE                                       TRA02110
64    FORMAT(2X,'HEAT EXCH EFFECTIVENESS=',F10.3,/2X,'REYNOLDS NO.=',F10TRA02120
     A.3,/)                                                      TRA02130
1000  WRITE(MW,1030)                                             TRA02140
1030  FORMAT(' INPUT DATA PARAMETRIC CHANGES')                   TRA02150
499   READ(NR,500)NPAR                                           TRA02160
500   FORMAT(I3)                                                 TRA02170
      GO TO(501,502,503,504,505,506,507,508,509,510,511,512,513,514,515,TRA02180
     A 516,517,518,519,520,521,522,523,524,525,526,527,528,529,530,    TRA02190
                                                                  TRA02200
```

```
      B  531,532,533,534,535,536,537,538,539),NPAR        TRA02210
  511 READ(NR,600)NSEC                                    TRA02220
  600 FORMAT(I2)                                          TRA02230
      GO TO 499                                           TRA02240
  502 READ(NR,600)KVAP                                    TRA02250
      GO TO 499                                           TRA02260
  503 READ(NR,601)R                                       TRA02270
  601 FORMAT(F10.4)                                       TRA02280
      GO TO 499                                           TRA02290
  504 READ(NR,601) D(1)                                   TRA02300
      GO TO 499                                           TRA02310
  505 READ(NR,601)XL(1)                                   TRA02320
      GO TO 499                                           TRA02330
  506 READ(NR,601) D(2)                                   TRA02340
      GO TO 499                                           TRA02350
  507 READ(NR,601)XL(2)                                   TRA02360
      GO TO 499                                           TRA02370
  508 READ(NR,601) D(3)                                   TRA02380
      GO TO 499                                           TRA02390
  509 READ(NR,601)XL(3)                                   TRA02400
      GO TO 499                                           TRA02410
  510 READ(NR,601) D(4)                                   TRA02420
      GO TO 499                                           TRA02430
  511 READ(NR,601)XL(4)                                   TRA02440
      GO TO 499                                           TRA02450
  512 READ(NR,601) D(5)                                   TRA02460
      GO TO 499                                           TRA02470
  513 READ(NR,601)XL(5)                                   TRA02480
      GO TO 499                                           TRA02490
  514 READ(NR,601)VRX                                     TRA02500
      GO TO 499                                           TRA02510
  515 READ(NR,601)XMRX                                    TRA02520
      GO TO 499                                           TRA02530
  516 READ(NR,601)W                                       TRA02540
      GO TO 499                                           TRA02550
  517 READ(NR,601)CP                                      TRA02560
      GO TO 499                                           TRA02570
  518 READ(NR,601)FLUK                                    TRA02580
      GO TO 499                                           TRA02590
  519 READ(NR,601)FLUMU                                   TRA02600
      GO TO 499                                           TRA02610
  520 READ(NR,601)FLOWA                                   TRA02620
      GO TO 499                                           TRA02630
  521 READ(NR,601)WPEP                                    TRA02640
      GO TO 499                                           TRA02650
  522 READ(NR,601)AFINP                                   TRA02660
      GO TO 499                                           TRA02670
  523 READ(NR,601)XLHX                                    TRA02680
      GO TO 499                                           TRA02690
  524 READ(NR,601)WPEPHX                                  TRA02700
      GO TO 499                                           TRA02710
  525 READ(NR,601)AFNPHX                                  TRA02720
      GO TO 499                                           TRA02730
  526 READ(NR,601)AHFVAP                                  TRA02740
      GO TO 499                                           TRA02750
```

```
527 READ(NR,601)AHCOND                              TRAC2760
    GO TO 499                                       TRAC2770
528 READ(NR,601)ASPRAY                              TRAC2780
    GO TO 499                                       TRAC2790
529 READ(NR,601)HHEVAP                              TRAC2800
    GO TO 499                                       TRAC2810
530 READ(NR,601)HHCON                               TRAC2820
    GO TO 499                                       TRAC2830
531 READ(NR,601)HSPRAY                              TRAC2840
    GO TO 499                                       TRAC2850
532 READ(NR,601)HFLU                                TRAC2860
    GO TO 499                                       TRAC2870
533 READ(NR,601)TIN                                 TRAC2880
    GO TO 499                                       TRAC2890
534 READ(NR,601)TSINK                               TRAC2900
    GO TO 499                                       TRAC2910
535 READ(NR,601)TRES                                TRAC2920
    GO TO 499                                       TRAC2930
536 READ(NR,601)TAU                                 TRAC2940
    GO TO 499                                       TRAC2950
539 CONTINUE                                        TRAC2960
    CALL EXIT                                       TRAC2970
    END                                             TRAC2980
```

Appendix B

ANALYSIS OF LOSSES IN CYLINDRICAL TRANSVERSE HEADER

Test data presented in paragraph 5.2.2, Figure 5-6, indicates losses of about 400 w when the pipe is shut down by virtue of the noncondensible gas completely filling the condenser vapor space. The temperature difference between the water data source (80°F) and spray sink (55°F) is 25°F. The conductance between the evaporator and condenser surfaces necessary to support such a loss would have to be

$$\frac{kA}{L} = \frac{Q}{\Delta T} = \frac{400}{25} = 16 \frac{w}{°F}$$

These losses are made up of conduction through the webs and end walls, convection through gas/vapor space, and ammonia diffusion through gas. The magnitude of these losses is estimated below to determine which ones are significant. Suggested modifications can then be made to reduce losses and improve the turndown ratio.

CONDUCTION THROUGH WEBS AND END-WALLS

Each of the six stainless steel webs is made up of eight layers of 170-mesh screen whose wire diameter is 0.0024 in. The web is 22.3 in. long. It is assumed that the evaporator space contains only ammonia and that the baffle is therefore at the evaporator temperature. Thus, the conduction length is the distance between the baffle and the inside of the condenser, which is 0.1825 in. The conductance is

$$\frac{kA}{L}_{\text{web wire}} = \frac{\overset{\displaystyle\ulcorner k_{\text{stst}}}{\big\downarrow}(10)(6)(8)(170)(22.3)(\pi/4)(0.0024)^2}{\left[(0.1825)(12)\right]}$$

$$= 3.75 \text{ Btu/hr-°F} = 1.1 \text{ w/°F}$$

The conductance through the ammonia ($k_{NH_3} = 0.29$ Btu/hr-°F-ft) within the web is estimated to be

$$\left(\frac{kA}{L}\right)_{NH_3} = 0.6 \text{ Btu/hr-°F} = 0.18 \text{ w/°F}$$

B-1

Thus, the total web conductance is

$$\left(\frac{kA}{L}\right)_{web} = 1.1 + 0.18 = 1.3 \ w/^{\circ}F$$

The ends of the pipe have relatively thick aluminum paths between the evaporator and condenser tubes, as shown in the sketch below.
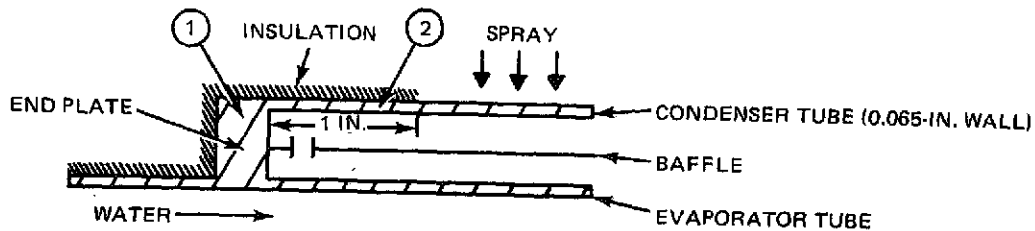
However, the conductance into just a 1-in. length of the thin condenser tube is

$$\left(\frac{kA}{L}\right)_{1-2} = \frac{\overset{k}{(100)}\overset{AL}{} \overset{wall}{(0.065)} \overset{diam}{\pi(2)}}{(1)(12)}$$

$$\approx 3.4 \ Btu/hr-^{\circ}F = 1.0 \ w/^{\circ}F$$

For both ends,

$$\left(\frac{kA}{L}\right)_{end\ walls} = 2.0 \ w/^{\circ}F$$

To maintain this value of end-wall conductance, the outside surface, including the 1-in. condenser strip, must be insulated from the spray coolant. Although during testing this portion of the pipe was not insulated, it also was not spray-cooled. End losses were therefore not excessive.

The total conductive losses are estimated to be approximately

$$\left(\frac{kA}{L}\right) = 1.3 + 2.0 = 3.3 \ w/^{\circ}F$$

B-2

CONVECTION LOSSES

Natural convection will occur between the hot baffle and the colder condenser. Assuming nitrogen at a total pressure of 140 psia (ammonia pressure at 75°F), the heat-transfer coefficient at the baffle and condenser surface is estimated to be

$$h = 3 \text{ Btu/hr-}^\circ\text{F-ft}^{2*}$$

Using a mean diameter of 1.68 in. between the baffle and condenser, the area is

$$(\pi) \frac{(1.68)\ (22.3)}{144} = 0.818 \text{ ft}^2$$

The conductance is

$$UA = \frac{1}{1/3(0.818) + 1/3(0.818)} = 1.23 \text{ Btu/hr-}^\circ\text{F} = 0.4 \text{ w/}^\circ\text{F}$$

The sum of the conductive and convective losses is far below the value of 16 w/°F required to explain the observed losses. This is illustrated graphically in Figure B-1.

DIFFUSION LOSSES

If it is assumed that the entire baffle outer surface is wet with ammonia, diffusion from this surface to the condenser wall can be estimated from the following:

$$\dot{m}_A = \frac{2\pi L D_{AN} P}{RTP_N \ln \frac{r_C}{r_B}} (P_{AB} - P_{AC})$$

The resulting heat loss is

$$Q = \dot{m}_A \lambda \text{ (MW)}$$

where

$\dot{m}_A$ = moles of ammonia/hr diffusing from baffle to condenser

L = length = 22.3 in.

D_{AN} = diffusivity of ammonia in nitrogen (at 10 atm) = 0.077 ft^2/hr**

P = total pressure = 140.5 psia

R = gas constant

T = absolute temperature = 65 + 460 = 525°F

- - - - - - -

*Kreith, "Principles of Heat Transfer", International Textbook Co., 2nd Edition, 1965, pp 333-335.

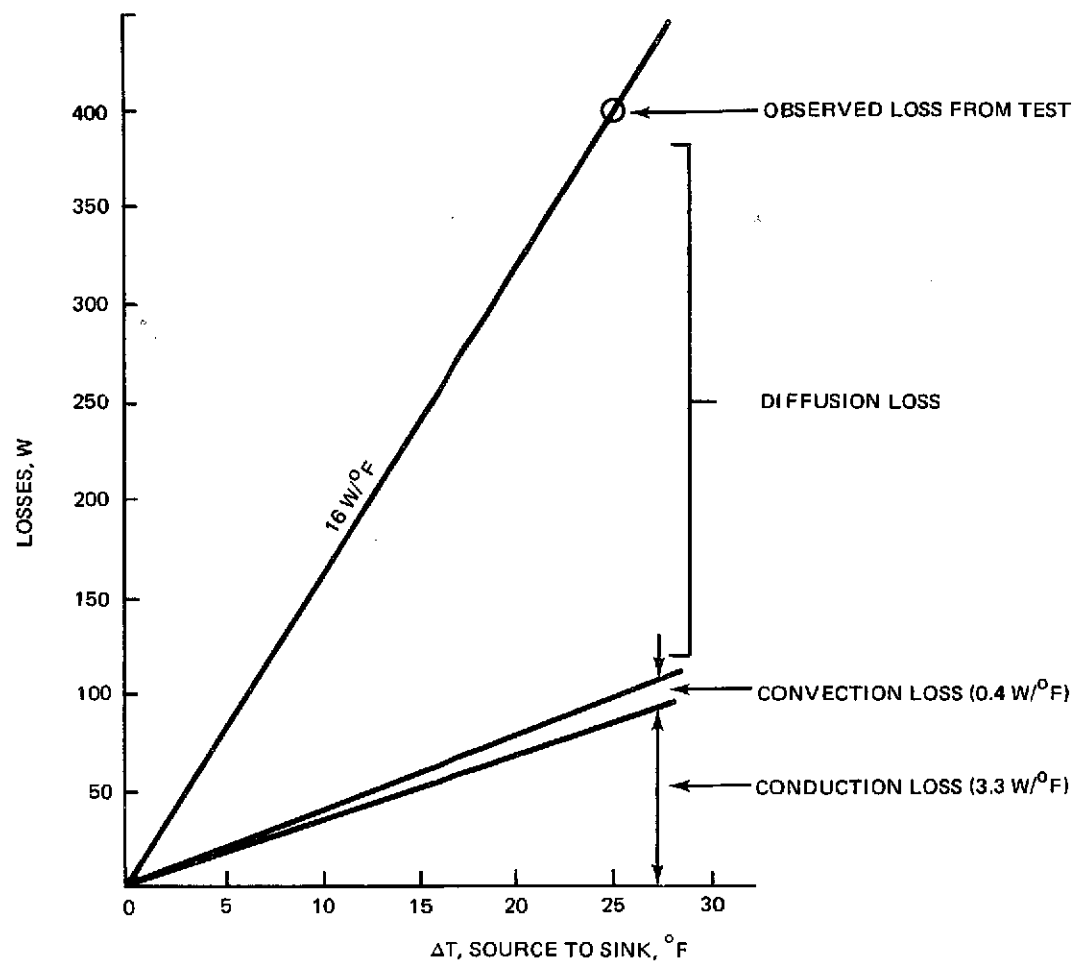**Treybal, R.E., "Mass-Transfer Operations", McGraw-Hill, 1955, p 21.

Figure B-1. Transverse Header Losses

P_N = mean nitrogen pressure = 21.2 psia

P_{AB} = ammonia partial pressure at baffle = 140.5 psia (75°F)

P_{AC} = ammonia partial pressure at condenser = 98.1 psia (55°F)

r_C = condenser radius = 0.9325 in.

r_B = baffle radius = 0.75 in.

λ = heat of vaporization of ammonia = 503 Btu/lb

MW = ammonia molecular wt = 17 lb/lb-mole

Substitution yields a value of diffusional heat transfer of

$$Q = 520 \text{ w}$$

This value is larger than required to explain the difference between the observed loss of 400 w and the calculated conduction/convection loss of 93 w. However, it points out that ammonia diffusion represents a significant loss and that perhaps only a portion of the baffle surface is wet with ammonia.

CONCLUSIONS AND RECOMMENDATIONS

1. Major losses in the shutoff mode are probably due to diffusion of ammonia through nitrogen. Possible modifications of the transverse header to reduce these losses include:

    a. Shielding and sealing webs and baffle on condenser side to minimize wetting with ammonia

    b. Reducing number of webs

    c. Using a noncondensible gas that has a lower value of diffusivity with ammonia, e.g., methane

    d. Increasing distance between baffle and condenser

2. Insulate the end walls of the pipe to insure low conduction losses.